ANKARA YILDIRIM BEYAZIT UNIVERSITY

GRADUATE SCHOOL OF NATURAL AND APPLIED SCIENCES

DEVELOPMENT AND PERFORMANCE ANALYSIS OF TRANSMITTER RECEIVER STRUCTURES FOR HIGH DATA RATE COMMUNICATION SYSTEMS AT 240 GHZ

M.Sc. Thesis by

Özgün ERSOY

Department of Electronics and Communication Engineering

June, 2017

ANKARA

DEVELOPMENT AND PERFORMANCE ANALYSIS OF TRANSMITTER RECEIVER STRUCTURES FOR HIGH DATA RATE COMMUNICATION SYSTEMS AT 240 GHZ

A Thesis Submitted to

the Graduate School of Natural and Applied Sciences of

Ankara Yıldırım Beyazıt University

In Partial Fulfillment of the Requirements for the Degree of Master of Science in Electrical and Electronics Engineering, Department of Electrical and Electronics Engineering

by

Özgün ERSOY

June, 2017

ANKARA

M.Sc. THESIS EXAMINATION RESULT FORM

We have read the thesis entitled **"DEVELOPMENT AND PERFORMANCE ANALYSIS OF TRANSMITTER RECEIVER STRUCTURES FOR HIGH DATA RATE COMMUNICATION SYSTEMS AT 240 GHZ"** completed by **ÖZGÜN ERSOY** under the supervision of **ASSOC. PROF. DR. ASAF BEHZAT ŞAHİN** and we certify that in our opinion it is fully adequate, in scope and in quality, as a thesis for the degree of Master of Science.

Assoc. Prof. Dr. Asaf Behzat ŞAHİN

(Supervisor)

Jury Member

Jury Member

Prof. Dr. Fatih V. ÇELEBİ

Director

Graduate School of Natural and Applied Sciences

ETHICAL DECLARATION

I hereby declare that, in this thesis which has been prepared in accordance with the Thesis Writing Manual of Graduate School of Natural and Applied Sciences,

- All data, information and documents are obtained in the framework of academic and ethical rules,
- All information, documents and assessments are presented in accordance with scientific ethics and morals,
- All the materials that have been utilized are fully cited and referenced,
- No change has been made on the utilized materials,
- All the works presented are original,

and in any contrary case of above statements, I accept to renounce all my legal rights.

Date: .../.../2017 **Signature:**

Name&Surname: Özgün ERSOY

ACKNOWLEDGMENTS

I would like to express my sincere gratitude to my supervisors Assoc. Prof. Dr. Asaf Behzat ŞAHİN and for his support and guidance.

I would also like to express my gratitude to Assist. Prof. Dr. Enver ÇAVUŞ and Assist. Prof. Dr. Serdar ÖZYURT for their support and guidance.

Finally, I would like to thank my mother, father, sister for being and supporting me all the way.

2017, … June **Özgün ERSOY**

DEVELOPMENT AND PERFORMANCE ANALYSIS OF TRANSMITTER RECEIVER STRUCTURES FOR HIGH DATA RATE COMMUNICATION SYSTEMS AT 240 GHZ

ABSTRACT

The terahertz band are located in the communication spectrum between the microwave band and the infrared wave band. The use of the terahertz band allows for increased capacity and data communication rates for indoor communication systems. The frequency multiplication method is used for signal generation in THz frequencies. Frequency multiplication can be performed using active circuit elements such as transistors, or passive circuit elements such as Schottky diodes.

In this thesis, firstly Schottky diode technology and Schottky diode based frequency multiplier and subharmonic mixer structures have been investigated. In the next step, the design and modelling of the frequency upconverter and frequency downconverter for 240 GHz communication systems are carried out using frequency multiplier and subharmonic mixer structures. The effect of noise and conversion losses of nonlinear frequency multipliers and subharmonic mixers on THz signal power are investigated. Finally, indoor communication transmitter receiver models with high data rates at 240 GHz are designed in Simulink and performance analysis is performed for different types of modulation.

Keywords: THz Communication, Schottky Diode Based Frequency Multiplication, Frequency Upconverter, Frequency Downconverter, Simulink

240 GHZ'DE YÜKSEK VERİ HIZI HABERLEME SİSTEMLERİ İÇİN VERİCİ ALICI YAPILARININ GELİŞTİRİLMESİ VE PERFORMANS ANALİZİ

ÖZ

Terahertz frekans bandı, haberleşme spektrumunda mikrodalga bandı ile kızılötesi bandı arasında yer almaktadır. Terahertz bandının kullanımı, bina içi haberleşme sistemlerinin kapasite ve veri iletişim hızlarının artırılmasına olanak sağlamaktadır. THz frekanslarında sinyal üretimi için frekans çoklama yöntemi kullanılmaktadır. Frekans çoklama, transistor ve ampfilikatör gibi aktif devre elemanları kullanılarak ya da Schottky diyot gibi pasif devre elemanları kullanılarak gerçekleştirilebilmektedir.

Bu çalışmada, ilk olarak Schottky diyot teknolojisi ve Schottky diyot temelli frekans çarpıcı ve alt harmonik karıştırıcı yapıları incelenmiştir. Sonraki adımda, frekans katlayıcı ve alt harmonik karıştırıcı yapıları kullanılarak, 240 GHz haberleşme sistemleri için frekans yükseltici ve frekans alçaltıcı tasarımı ve modellemesi yapılmıştır. Lineer olmayan frekans çarpıcı ve alt harmonik karıştırıcı yapılarının sahip olduğu gürültü ve dönüşüm kayıplarının, üretilen THz sinyal gücü üzerindeki etkisi incelenmiştir. Son olarak, 240 GHz bandında, yüksek veri hızlarına sahip bina içi haberleşme verici alıcı modelleri Simulink ortamında tasarlanarak farklı modulasyon türleri için performans analizi yapılmıştır.

Anahtar kelimeler: THz Haberleşme, Schottky Diyot Temelli Frekans Çoklama, Frekans Yükseltici, Frekans Alçaltıcı, Simulink

CONTENTS

NOMENCLATURE

Roman Letter Symbols

A_c	:	Amplitude of carries signal, V
C_j	:	Nonlinear junction capacitance, F
C_{j0}	:	Nonlinear junction capacitance at 0 V
E_b	:	Transmitted signal energy per bit
E_s	:	Transmitted signal energy per symbol
f_c	:	Carrier frequency, Hz
I_{SAT}	:	Saturation current, A
I_d	:	Current of diode, A
M	:	Set size
θ_c	:	Phase of carrier signal, rad
r_j	:	Nonlinear junction resistance, ohm
R_s	:	Parasitic resistance, ohm
T_b	:	Bit duration time
T_s	:	Symbol duration time
V_j	:	Barrier height
V_{bi}	:	Built in voltage
V_p	:	Peak voltage, V

Acronyms

AWGN	:	Additive White Gaussian Noide
BASK	:	Binary Amplitude Shift Keying
BER	:	Bit Error Rate
BPF	:	Bandpass Filter
BPSK	:	Binary Phase Shift Keying
BW	:	Bandwidth
CDR	:	Clock Data Recovery
F	:	Noise Factor
FM	:	Frequency Modulation
FPGA	:	Field Programmable Gate Array

GHz	:	Gigahertz
Gbps	:	Giga bit per second
IEEE	:	Institute of Electrical and Electronics Engineers
IF	:	Intermediate Frequency
ISI	:	Inter-Symbol Interference
LDPC	:	Low Density Parity Check
LO	:	Local Oscillator
LPF	:	Lowpass Filter
MATLAB	:	Matrix Laboratory
MHz	:	Megahertz
MMIC	:	Monolithic Microwave Integrated Cicuits
mW	:	Miliwatt
NF	:	Noise Figure
NRZ	:	Non-Return to Zero
OFDM	:	Orthogonal Frequency Division Multiplex
OOK	:	On-Off Keying
QAM	:	Quadrature Amplitude Modulation
QPSK	:	Quadrature Phase Shift Keying
PAN	:	Personal Area Network
RF	:	Radio Frequency
SFDR	:	Spurious Free Dynamic Range
SHM	:	Sub-Harmonic Mixer
SiGe	:	Silicium-Germanium
SNR	:	Signal to Noise Ratio
THz	:	Terahertz
WLAN	:	Wireless Local Area Network
UWB	:	Ultra Wide Band

LIST OF TABLES

LIST OF FIGURES

CHAPTER 1

INTRODUCTION

The widespread use of mobile communications and the increasing number of users and the amount of data in proportion to this necessitate the need for quality and rapid communication especially in environments such as home and office, and the need for increased the capacity and data communication speed of indoor wireless communication systems. This requirement for data transmission speeds is not seemed possible from the existing microwave band because of density data traffic. In this regard, the use of the terahertz frequency band, which is located between the microwave and the infrared wave band in the communication spectrum, offers an important solution for wireless communication applications that require high data rates. The use of this frequency band allows the data rates in wireless networks to reach speeds of 10-100 gbps.

1.1 Objective of Thesis

In this study, communication receiver/transmitter systems with high data rates using different modulation types in the 240 GHz band for indoor applications are designed and the performance of this system is examined in Simulink. The modulation process to be performed is carried out in a relatively low frequency band and is transported to the targeted high frequency band using Schottky diode based frequency multiplication technique in nonlinear construction, using a mixer and frequency multipliers. Therefore, modulated signals are upconverted to higher frequencies. On the receiver side, the frequency downconversion is achieved by multiplying the local oscillator signal generated by using the mixer and frequency multiplier chain with the modulated signal from the communication channel and the performance analysis is performed after the demodulation. Different modulation techniques are examined and by making adjustments depend on modulation type, transmitter and receiver structures for THz communication systems are modelled.

1.2 Scheme of Thesis

The following sections of the presented thesis are organized as follows:

In chapter 2, information about mm-wave and THz communication systems are given and studies related to the communication systems using THz frequency bands in the literature are mentioned.

In chapter 3, Schottky diode technology is introduced and information about Schottky diode based frequency multipliers and mixers is given therotically. Characteristic features of these components that affect system configuration and operation are examined. At the end of this part, up-converter and down-converter structures simulated in Chapter 5 for a 240 GHz communication systems are explained.

In chapter 4, offers an information about the techniques of digital modulation. Modulator and demodulator structures used in simulation are explained.

In chapter 5, transmitter and receiver systems at 0.24 THz are designed and modeled in Simulink. In this context, each step is simulated by using Simulink blocks in the SimRF and communication system toolboxes. The simulation results obtained are shown as a plot and performance analysis of the models are examined.

Chapter 6 is the final chapter of thesis includes the conclusions.

CHAPTER 2

MM-WAVE AND TERAHERTZ COMMUNICATION SYSTEMS

The millimeter and terahertz band are located in the communication spectrum between the microwave band and the infrared wave band. The widespread use of Internet and the development of new technologies in mobile communication reveal the need to the enhanced of data transmission capabilities. In addition, the need for quality and fast communication in indoor environments such as the home and office reveals the need to increase the capacity and data rate of communication systems. In this scope, the high-capacity communication applications and systems shifting to millimeter and terahertz frequency band in terms of providing capacity increase and channel efficiency offers solutions. The frequencies of millimeter wave signals are between 30 and 300 GHz, and the wavelength varies between 1 millimeter and 1 centimeter. These signals show both radio waves and optic waves characteristics. Because different gases and humidity in the atmosphere show absorption alteration depending on the frequency, the millimeter wave band is divided into wide band channels centered at 70 GHz, 140 GHz and 240 GHz. In recent years, several studies have been made related to the communication systems using these frequency bands. In these studies, frequencies of 60 GHz, 120 GHz, 200 GHz and above were mostly preferred.

Since 2000's, the studies for 60 GHz have been started and a lot of theoretical and experimental studies have been carried out.

An analytical model for assessing link stability of 60 GHz radio for indoor wireless network has been defined and a ray based model which is calculate the shadowing loss result from the presence of people around the communication link has been developed by Wang, Prasad and Niemegeers [1]. The channel capacity performance of a 60 GHz wireless communication system over Ricean fading channels is observed and compared with the capacity in Rayleigh channel and an additive white Gaussian noise channel by Zhang, Wang, Lu and Gulliver [2].

In Jie, J. Wang, Zhang and G. Wang conducted a research is calculated the channel capacity of 60 GHz wireless communication systems over indoor line of sight and non-line of sight channels and investigated relationship between capacity and communication distance [3].

In M. Marinkovic and colleagues' study, comparison of LDPC and convolutional codes performance of 60 GHz OFDM based wireless communication systems are shown [4]. The algorithms in the 60 GHz physical layer consisting of modulation, equalization, and space-time processing are described by Daniels and Heath [5].

In C. Park and T.S. Rappaport's work, standardizations and regulations corresponding to short range wireless techonologies for next generation personal area networks (PAN) are described. In addition to this, short range broadband wireless communication and multigigabit wireless networks that use ultra-wideband (UWB) and 60 GHz millimeter-wave communication technologies are presented [6].

In A. Maltsey and collegues' study, the experimental setup with highly directional antennas and 800 MHz bandwidth for 60 GHz Wireless Local Area Network (WLAN) systems was improved. As a result of the experiments performed for conference room, the intra cluster statistical parameters of the propagation channel were evaluated and statistical model for reflected clusters has been suggested [7].

The experimental study of an indoor environment related to Multiple Input Multiple Output Orthogonal Frequency Division Multiplexing (MIMO-OFDM) millimeter wave system using standard IEEE 802.15.3c was performed in Martinez-Ingles and colleques' experimental work. According to study, channel matrices have been obtained. After that, intrinsic propagation characteristics such as path loss, capacity have been observed and analysis of performance with different space-time coding schemes has been performed [8].

60 GHz multi-Gbps wireless systems consisting of SiGe radio components implemented in FPGA by using noncohorent detection techniques in the study of Katayama. In this study, modulation type for multi-Gbps wireless systems is bandwidth efficient frequency shift keying method, therefore, noncohorent detection

is carried out by using FM discriminator and clock data recovery (CDR) at the receiver [9].

The studies in 60 GHz frequency band have reached to certain level and high data rate requirement has increased the interest to over 100 GHz bands. 10 Gbps data transmission with a bit error rate (BER) below 10^{-12} over distance of 250 meter at 120 GHz was implemented by using photonic millimeter wave generator and transmitter by Hirata and collegues [10].

In C. Wang and collegues' work, 16 QAM modulated data stream has high data rate, such as 10 gbps and 2 gbps, has been transmitted at 0.14 THz band over 1.5 kilometer with bit error rate below $1e^{-6}$ and $1.7e^{-7}$, respectively [11].

RF and baseband integrated circuits in 120 GHz band and QPSK modulation have been used to demonstrate a 10 Gbps LOS wireless communication system at a distance of 170 meters in Takahashi and collegues study [12].

When communication systems developed for over 200 GHz bands are investigated, it is seen that various experimental studies have been conducted on this area. In these experiments, frequency multi-milimeter wave sources are used as signal sources. In the study conducted by Kallfass and collegues, wireless data link providing high data rates up to 25 gbps is suggested. In this scope of study, design and performance of the system consisting of MMICs transmit and receive frontends have been investigated and wireless data link operating at 220 GHz with OOK modulated data experiments have been performed [13]. In the other study, Antes and collegue have implemented wireless communication system measurements with data rates up to 30 gbps for distance up to 20 meter at 220 GHz. According to study, while transmission distance of system of 10 meter and 20 meters separately, data rate of 25 gbps and 15 gbps can be transmitted [14].

Design of the receiver and transmitter used subharmonic LO signal for 240 GHz wireless transmission experiments supporting data rates of up to 40 gbps has been developed by Lopez-Diaz and collegues [15]. In H-J. Song and collegues' work, 8

gbps data transmission at 250 GHz using photonic techonologies based modulator and schottky barrier diode based dedector is carried out [16].

300 GHz transmission system consist of schottky diode mixer technology based transmitter and receiver units is developed to model THz communication channel by Jastrow, Münter, Piesiewicz, Kürner, Koch and Kleine-Ostmann [17].

In the study of C. Wang and collegues, wireless communication link WLAN prototype based on IEEE 802.11b/g protocol is suggested. In this scope of the study, 0.34 THz subharmonic mixer, 0.34 THz waveguide bandpass filter and 0.17 THz multiplier chain are used to transmit 3 gbps data with 16 QAM modulator and demodulator and BER performance is analyzed [18].

L. Moeller, J. Federici and K. Su suggest a THz wireless communications system to increase the capacity on 625 GHz carrier frequency. In this study, transmission distance, error-free detection, power, bit error rate (BER), signal to noise ratio (SNR) are analyzed for 2.5 gbps data signal and to obtain a 625 GHz carriers frequency multiplier chain is used [19].

Schottky diode based mixer technology providing to develop to THz communication channel model is shown and the performance of the digital signal transmission system using this model is analyzed depend on phase noise and modulation errors at 300 Ghz by Castrow and collgues [20].

In the scope of J. Antes and J. Reichart' work, a 220 GHz wireless communication system over a distance of one kilometer with data rates up to 40 gbps has been presented. As a result of experimental studies, 25 gbps data transmission over a distance of 0.6 meter has been succeeded [21].

In Liu, Wang and Cao's study, to enhance the bit error rate performance of the wireless communication systems that is used OOK modulated THz signals against atmospheric absorption and scattering, LDPC codes are implemented [22].

The use of the terahertz frequency band, offers an important solution for wireless communication applications that require high data rates. The use of this frequency

band allows the data rates in wireless networks to reach speeds of 10-100 gbps. In this study, communication receiver/transmitter systems with high data rates using different modulation types in the 240 GHz band for indoor applications are simulated and the performance of this system is examined. The modulation process to be performed is carried out in a relatively low frequency band and transported to the targeted high frequency band using Schottky diode based frequency multiplication technique, using a mixer and multiplier chain.

CHAPTER 3

SCHOTTKY DIODE FREQUENCY MULTIPLIERS AND MIXERS

Developments in radio communication and broadcasting lead to technical problems in signal generation [23]. High frequency signals are generated either by up-converting the low frequency signals with frequency multipliers or by directly applying oscillator to signal at carrier frequency.

In millimeter and microwave communication systems, modulation, pulse shaping and filtering are first done in lower frequency bands and then moved to higher frequency bands. In this study, 0.24 THz band millimeter wave carrier signal source is used. However, there are no transistors or oscillator that can provide more than 1 mW power at this frequency band Then, in order to generate 200 GHz and higher frequency signals, frequency multiplier method is used. In frequency multiplier method, a system with nonlinear response produces the harmonics of the input signal and after filtering the desired multiplier coefficient is obtained. For this purpose, while active frequency multiplier such as nonlinear transistor and amplifiers are used in RF band; because of their efficiency, Schottky diode based passive frequency multiplier structures are used in the millimeter wave band.

3.1 Schottky Diode Technology

Schottky diode structures are very important in THz frequency signal generation and detection and are widely used in many applications such as radio astronomy and molecular spectroscopy [24].

Schottky diode structure are commonly used for frequency multiplying and matched with active elements such as oscillators and transistor amplifiers [25]. Schottky diode based components are used for either up-converting these active components to THz band or for down-converting THz signals. THz band up-conversion is one of the most

important advantages Schottky diodes provide. Schottky diodes are analyzed using below I-V and C-V characteristics.

$$I_d = I_{SAT}\left(e^{\left(\frac{V_j - I_d R_S}{V_0}\right)} - 1\right) \quad \textbf{(3.1)}$$

$$C_j = \frac{C_{j0}}{\sqrt{1 - \frac{V_j}{V_{bi}}}} \quad \textbf{(3.2)}$$

where r_j, is nonlinear junction resistance parameter caused by carrier emissions on metal semiconductor barrier whereas C_j is nonlinear capacitance parameter caused by variable depletion depth. R_S resistance is a parasitic component representing ohmic losses in diode structure. Furthermore, skin effect, diode heating and velocity saturation can affect diode performance in THz frequencies [26].

Nonlinear characteristics of Schottky diodes allow for conversion of the incident signal and multiplying its frequency. RF performances can be obtained using I-V and C-V characteristics of the nonlinear diode [27].

3.2 Schottky Diode Based Components

Schottky diode structures are used in frequency multipliers, mixers, amplifiers and detectors. In this thesis study, simulations for a 0.24 THz band communication system are done. The simulated system can be experimentally realized in this frequency band using Schottky diode based components. Therefore, during the simulations, nonlinear effects caused by Schottky based structures such as frequency doubler, frequency tripler and mixer are taken into account. In this chapter, Schottky diode based components, frequency up-converter and down-converter structures of the communication system are explained.

3.2.1 Frequency Multipliers

Schottky diodes' nonlinear characteristics can be used for generating harmonics of the incident signal [27]. Thus, exact multiple harmonics of the incident signal can be obtained at the output of the nonlinear circuit. Using a band-pass filter, the desired

harmonic can be chosen among the others. Figure 3.1 shows block diagram of the frequency multiplier.

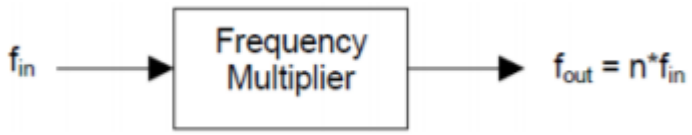

Figure 3.1 Frequency multiplier block diagram

Frequency multiplication is realized using nonlinear I-V and C-V characteristics. Diode's Q-V characteristic can be defined in terms of power series [28].

$$Q\big(V(t)\big) = A_0 + A_1V(t) + A_2V(t)^2 + A_3V(t)^3 + \cdots \quad \textbf{(3.3)}$$

Taking the derivative of Equation 3.3, current equation can be derived.

$$I(t) = \frac{dQ(t)}{dt} = [A_1 + 2A_2V(t) + 3A_3V(t)^2 + \ \ldots\ ]\frac{dV(t)}{dt} \quad \textbf{(3.4)}$$

When the incident signal is a sinusoidal one, it can be observed that current and voltage equations are formed of its harmonics.

Conversion efficiency is the ratio of power transmitted to the load and incident signal power. Conversion efficiency parameter of frequency multiplier is defined either as conversion loss or gain. The aim of the frequency multiplier design is to increase the efficiency by minimizing the conversion loss. Otherwise, transmitted power to the load will suffer as incident power will be used more in the nonlinear structure. In addition, noise effect of frequency multipliers has to be considered [29].

3.2.1.1 Frequency Doublers

Frequency doublers are the most sought multiplier structures as the unwanted harmonics are well above the desired output frequency. Using planar and integrated diodes allows for Schottky anode to distribute input power. Hence, power consumption increases, which solves the main disadvantage of the frequency doubler [30]. Consequently, increasing the bandwidth and doubling efficiency of the frequency doubler can be focused more. Frequency doubler output RF frequency is double the

input RF frequency and as the component's frequency ranges increases efficiency and output power decreases. Low frequency source signal can be up-converted to THz band using many cascaded frequency multipliers [31]. Frequency multiplier circuits are expected to generate enough power for a couple hundred GHz bandwidth as Schottky diode technology develops more [30].

Since frequency doublers are used for broadening microwave and millimeter wave sources' frequency range, specific frequency doublers are produced for different frequency bands. Table 3.1 shows VDI brand frequency doublers' input-output frequency range, input power range and efficiency.

Table 3.1 VDI product specifications for frequency doublers [32].

VDI Part Number	RF Output Frequency (GHz)	RF Input Frequency (GHz)	Typical Efficiency (%)	RF Input Power Range (mW)
WR15x2	50-75	25-37.5	9.0	250-1000
WR12x2	60-90	30-45	8.0	500-1000
WR10x2	75-110	37.5-55	9.0	250-500
WR8.0x2	90-140	45-70	9.0	50-200
WR6.5x2	110-170	55-85	8.0	50-200
WR5.1x2	140-220	70-110	7.5	20-50
WR4.3x2	170-260	85-130	6.0	20-50
WR3.4x2	220-330	110-165	6.0	20-50
WR2.8x2	260-400	130-200	4.0	10-35
WR2.2x2	325-500	162.5-250	3.0	5-20
WR1.9x2	400-600	200-300	2.5	10-30

Configuration and dimensions of WR4.3x2 doubler model in Table 3.1 are shown in Figure 3.2.

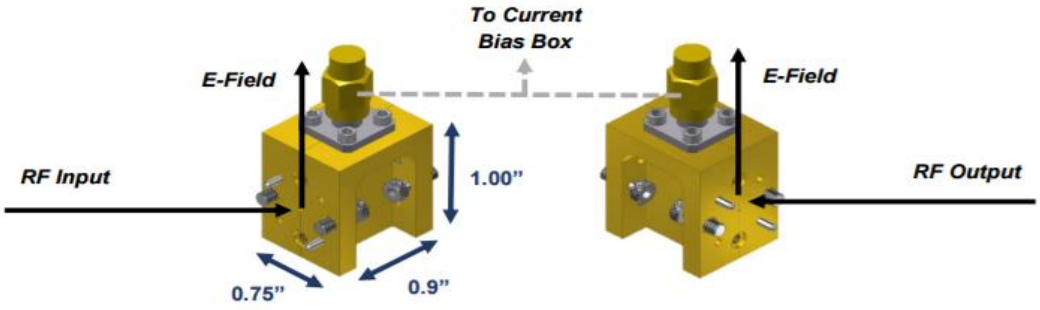

Figure 3.2 VDI WR4.3x2 frequency doubler structure [16]

3.2.1.2 Frequency Triplers

Frequency tripler structures are used for generating three times the RF input frequency at the output. As the multiplication order increases, number of undesired harmonics in input-output frequency range increases as well. Hence, the circuit becomes more complex to counteract this [30]. Since, at the output frequency tripler, second harmonic of the input signal will be generated, this harmonic should be optimized. Accordingly, nowadays, Virginia Diodes Company produces planar Schottky diode based frequency triplers for millimeter wavelengths with this in mind. Tripler structures are sturdy and reliable as they have only rectangular waveguide input and output ports. Frequency tripler structures, as frequency doublers, are specifically produced for different frequency bands. Table 3.2 shows input-output frequency range, input power range and efficiency of VDI brand frequency triplers. Configuration and dimensions of WR3.4x3 tripler model in Table 3.2 is shown in Figure 3.3.

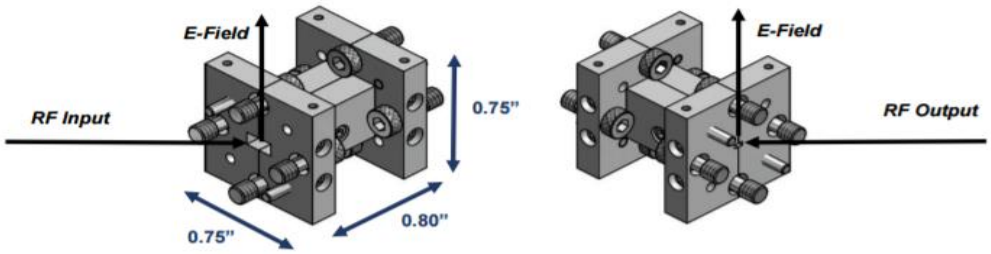

Figure 3.3 VDI WR3.4x3 frequency tripler structure [33]

Table 3.2 VDI product specifications for frequency triplers [33]

VDI Part Number	RF Output Frequency (GHz)	RF Input Frequency (GHz)	Typical Efficiency (%)	RF Input Power Range (mW)
WR15x3	50-75	16.67-25	3.5	HP (100-500)
WR12x3	60-90	20-30	3.5	HP (75-400)
WR10x3	75-110	25-36.7	3.5	MP (40-180), HP (75-360)
WR9.0x3	82-125	27.3-41.7	3.5	HP (60-315)
WR8.0x3	90-140	30-46.7	3	MP (20-120), HP (40-220)
WR6.5x3	110-170	36.7-56.7	3	S (20-120), HP (40-180)
WR5.1x3	140-220	46.7-73.3	3	S (10-40), HP (20-120)
WR4.3x3	170-260	56.7-86.7	3	S (10-40), HP (20-120)
WR3.4x3	220-330	73.3-110	3	S (5-40), HP (20-120), UHP (50-150)
WR2.8x3	260-400	86.7-133.3	3	S (5-40), HP (20-120)
WR2.2x3	325-500	108.3-166.7	2	S (10-25), HP (15-100), UHP (30-150)
WR1.9x3	400-600	133.3-200	1.5	S (10-25), HP (15-100), UHP (30-150)
WR1.5x3	500-750	166.7-250	1.5	S (5-30), HP (20-60)
WR1.2x3	600-900	200-300	1	S (5-25), HP (20-50)
WR1.0x3	750-1100	250-366.7	0.5	S (5-25), HP (20-50)
WR0.8x3	900-1400	300-466.7	0.2	S (5-25)
WR0.65x3	1100-1700	366.7-566.7	0.2	LP (0.3-8), S (5-25)
WR0.51x3	1400-2200	466.7-733.3	0.1	LP (0.3-8)

3.2.2 Mixers

Mixers are active or passive components with two inputs and one output port that are used for frequency conversion [34]. The two input ports are respectively named as radio frequency (RF) and local oscillator (LO), while output port is named as intermediate frequency (IF). Frequency conversion is realized by modulating f_{RF} frequency RF signal with f_{LO} frequency LO signal. IF signal at the output of mixer has harmonics of both RF and LO signal frequencies sum and difference. In frequency conversion, generating output frequency lower than input RF signal frequency is called down-conversion while generating output frequency higher than input RF signal frequency is called up-conversion. In other words, during frequency conversion, input RF signal is shifted towards desired frequency band. Mixers, different from frequency multipliers, do not alter the phase and amplitude of the input signal at the output [29]. Mixers cause distortions such as intermodulation distortion and spurious responses as they have nonlinear response. Furthermore, undesired harmonics at the output of the mixer can be suppressed using proper filters. Since noise sources might prove difficulties during nonlinear simulations, mixer structures are designed to have best conversion gain rather than having best noise performance [35]. First of all, conversion gain parameter is approximated without noise sources. Then, to achieve full performance of mixer, noise sources are added while required minimum LO power is conserved. Doing so, conversion gain is maximized [35].

Submilimeter wave Schottky mixers are designed in two different ways. These are fundamental planar Schottky diode mixers and sub-harmonically pumped planar Schottky diode mixers. In the first one, IF signal has only the frequency is containing LO and RF frequencies difference. In the latter, LO signal at *1/N* times the RF signal, with integer $N \geq 2$, that is, RF signal is modulated by the N^{th} harmonic of the LO signal.

Even though sub-harmonically pumped mixers (SHM) have higher conversion loss, the difficulties of generating high frequency LO signal with other mixers and SHM's low phase noise and lower LO signal compatibility make them much more preferred. Since the communication system designed in this study works with LO frequencies above 200 GHz, SHM blocks are utilized. SHM structures, like other Schottky diode based components, are specifically produced for different frequency bands. Table 3.3

shows RF and LO frequency ranges, maximum IF frequencies and conversion losses for VDI brand SHM structures. Configuration and dimensions of WR3.4 SHM in Table 3.3 are shown in Figure 3.4.

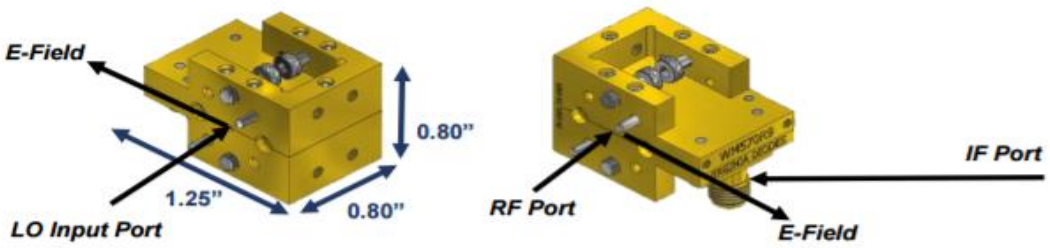

Figure 3.4 VDI WR3.4 SHM structure [36]

Table 3.3 VDI product specifications for subharmonic mixers [36].

VDI Part Number	RF Frequency (GHz)	LO Frequency (GHz)	Maximum IF Frequency (GHz)	Conversion Loss (dB)	Noise Temperature (K)
WR15SHM	50-75	25-37.5	10	7	400-800
WR12SHM	60-90	30-45	12	7	400-800
WR10SHM	75-110	37.5-55	15	7	400-800
WR8.0SHM	90-140	45-70	19	7	400-800
WR6.5SHM	110-170	55-85	24	7	400-800
WR5.1SHM	140-220	70-110	31	7.5	500-1000
WR4.3SHM	170-260	85-130	36	8	600-1200
WR3.4SHM	220-330	110-165	40	8.5	700-1400
WR2.8SHM	260-400	130-200	40	9	800-1500
WR2.2SHM	325-500	162.5-250	40	9.5	1000-2000

Schottky diode based mixer and frequency multiplier structures have characteristics such as noise figure, noise factor, conversion loss, intermodulation and spurious free dynamic range.

3.2.2.1 Noise Figure

Noise Figure (NF) represents distortion in signal to noise ratio (SNR). Each component produce noise and these are added to present white noise. The amount of added noise is named as Noise Figure and defined as below.

$$NF = 10\log\frac{P_{noise\ out}}{P_{noise\ in}.G} \quad \textbf{(3.5)}$$

where *G* is the gain in devices.

Noise figure is used for determining how much amplifiers, mixers or frequency multipliers lower SNR. Noise factor (F), on the other hand, is the ratio of input SNR to output SNR. Noise factor can be derived using the SNR formula.

$$SNR_{in} = \frac{P_{in}}{P_{noise\ in}}\ \frac{[W]}{[W]} \quad \textbf{(3.6)}$$

$$SNR_{out} = \frac{P_{out}}{P_{noise\ out}}\ \frac{[W]}{[W]} \quad \textbf{(3.7)}$$

$$F = \frac{SNR_{in}}{SNR_{out}} \quad \textbf{(3.8)}$$

$$NF_{dB} = 10\log\frac{P_{noise\ out}}{P_{noise\ in}.G} = 10\log F \quad \textbf{(3.9)}$$

SNR_{out} value is expected to be lower than SNR_{in} since components in equation 3.8 add noise to the system.

3.2.2.2 Conversion Loss

Since nonlinear diodes, like Schottky, used in mixer and frequency multiplier are lossy, such components' outputs suffer losses, which in turn lowers conversion efficiency. Low conversion efficiency value means that input power is spent on

nonlinear component. Conversion loss is used for characterizing conversion efficiency. The conversion loss is defined as

$$Conversion\ Loss = \frac{P_{in}}{P_{out}} \quad \frac{[W]}{[W]} \tag{3.10}$$

When conversion loss is observed for a mixer with minimum loss, below equations are obtained,

$$V_{IF}(t) = V_{RF}.\sin(2\pi f_{RF}t).V_{LO}.\sin(2\pi f_{LO}t)$$

$$= V_{RF}.V_{LO}.\frac{1}{2}.[\cos(2\pi(f_{LO} - f_{RF})t) - \cos(2\pi(f_{LO} + f_{RF})t)] \tag{3.11}$$

If in equation 3.11, V_{LO} = 1, the amplitude of V_{IF} can be defined as below.

$$V_{IF} = V_{RF}.\frac{1}{2} \tag{3.12}$$

$$Conversion\ Loss = 20\log\frac{V_{RF}}{V_{IF}} = 6.02\ dB \tag{3.13}$$

When equation 3.12 is inserted into equation 3.10, minimum conversion loss at the mixer output is calculated as 6.02 dB. This value increases once diode losses are taken into account [34].

3.2.2.3 Intermodulation

The undesired signals that result from the interaction of more than one signal cause intermodulation distortions at the output of the nonlinear amplifier and mixer devices. Intermodulation sonucunda oluşan frekans bileşenleri spurious frequencies olarak adlandırılır.

Intermodulation components are produced by two signals at the output are expressed as:

$$\mathrm{m}f_1 \pm \mathrm{n}f_2 \tag{3.14}$$

where m and n are integers.

All the harmonics, except the third harmonics, of the spectrum are suppressed. The reason for this is that third order intermodulation outputs are very close to desired signal frequency. Spurious free dynamic range (SFDR) measurement is done to suppress two tones third order intermodulation outputs. SFDR analysis determines the power range at which the signal can be detected without undesired harmonics.

3.3 Frequency Upconversion and Downconversion

In this section, up-converter and down-converter structures, simulated in Chapter 5, for a 240 GHz communication system are explained.

Generating output frequency lower than input RF signal frequency is defined as down-conversion, whereas generating output frequency higher than input RF signal frequency is defined as up-conversion. Since the designed system is working in 240 GHz, aforementioned Schottky diode based frequency multipliers and SHM structures are used for generating LO signal and carrying modulated signal into desired frequency band. Schematic for 240 GHz frequency up-converter structure is given in Figure 3.5.

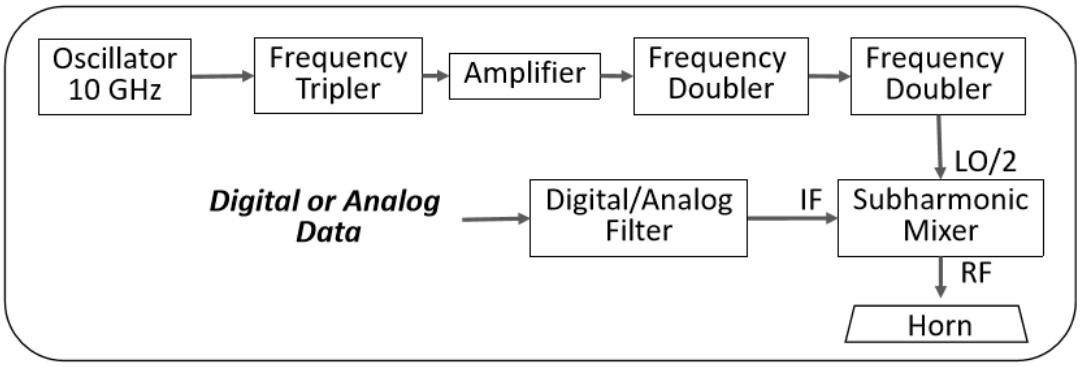

Figure 3.5 240 GHz frequency upconverter

As Figure 3.5 shows, 10 GHz LO signal is shifted to 30 GHz, 60 GHz and 120 GHz respectively using frequency tripler and doublers while weakened signal is amplified with an amplifier. Doing so, LO signal required for frequency up-conversion is obtained. Lastly, filtered digital or analog data signal is up-converted to 240 GHz using LO signal at the output of SHM. Figure 3.6 shows schematics for frequency down-converter at the receiver end.

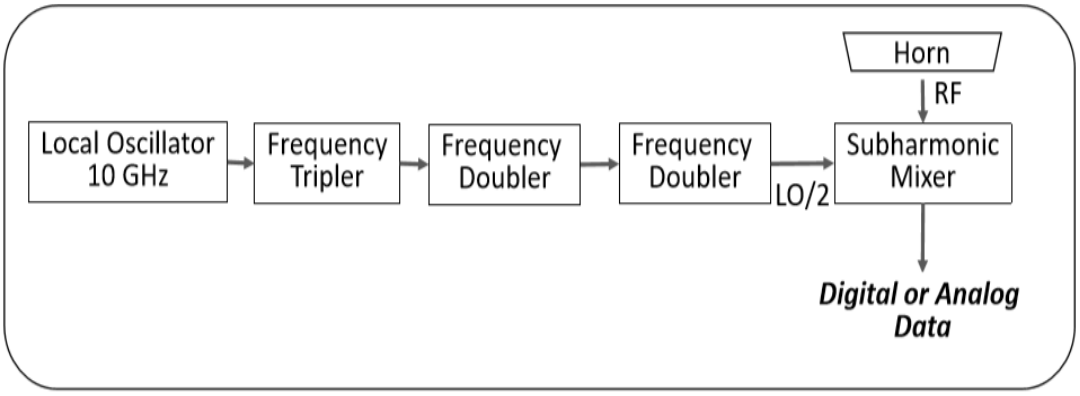

Figure 3.6 240 GHz frequency downconverter

At the receiver end, first of all, required LO signal is produced. Same as frequency up-converter, 10 GHz LO signal is shifted to 30 GHz, 60 GHz and 120 GHz frequencies respectively using frequency tripler and doublers. Lastly, SHM is used for down-converting upconverted 240 GHz data signal. Frequency down-conversion is completed as transmitted data signal is recovered at the output of SHM.

CHAPTER 4

DIGITAL MODULATION TECHNIQUES

Modulation is the technique that alters characteristics, such as amplitude, phase and frequency of the signal with respect to data signal. The main aim of modulation is to minimize the possibility of distortions at high speed transmission of the digital signal [37]. Digital modulation offers much more advantages compared to analog modulation. Some of these advantages are; better noise immunity, robustness against to channel distortions and easier reproduction of data [38]. Moreover, digital systems possess control mechanisms that can detect and correct transmission errors and they support encryption and source coding to improve transmission performance [38].

Since contemporary communication systems are based on high frequency bands, the data signal frequency spectrum has to be shifted towards higher bands. Data signal can be shifted towards RF or THz bands after modulation with a carrier signal. Being able to change the amplitude, frequency and phase of the carrier signal with respect to data signal allows for producing different modulation techniques. Amplitude shift keying is the modulation technique where amplitude of the carrier signal is changed, whereas modulation techniques where frequency or phase of carrier signal changes are called Frequency Shift Keying and Phase Shift Keying respectively.

The carrier signal is defined by

$$c(t) = A_c \cos(2\pi f_c t + \theta_c) \quad \textbf{(4.1)}$$

where A_c is the carrier amplitude, f_c is the carrier frequency, and θ_c is the carrier phase.

In digital communication, the carrier amplitude is

$$A_c = \sqrt{\frac{2}{T_b}} \quad \textbf{(4.2)}$$

where T_b is the bit duration. Thus, the carrier signal can be written as [39]:

$$c(t) = \sqrt{\frac{2}{T_b}}\cos(2\pi f_c t + \theta_c) \quad \textbf{(4.3)}$$

4.1 Binary Amplitude Shift Keying (BASK)

In amplitude shift keying method, amplitude of the carrier signal is modulated. BASK modulation uses two different amplitude values of carrier signal to represent data signal with 0 and 1 symbols. Frequency and phase of the carrier are fixed, while amplitude is keyed in between 0 and 1 symbol values [39]. On-Off keying (OOK) modulation is realized by choosing one of the 0, 1 symbol amplitude values as 0. Choosing 0 as one of the symbol values provides lesser power consumption as at this level there is no need for carrier transmission.

4.1.1 Generation of OOK modulated signals

OOK signals are obtained by multiply carrier signal with message signal. Message signal, *m(t)* is defined by

$$m(t) = \begin{cases} \sqrt{E_b}, & \text{for binary symbol 1} \\ 0, & \text{for binary symbol 0} \end{cases} \quad \textbf{(4.4)}$$

where E_b is named transmitted signal energy per bit, and is calculated using equation given below.

$$E_b = \int_0^{T_b} |s(t)|^2 \, dt \quad \textbf{(4.5)}$$

The modulation equation is:

$$s(t) = m(t).c(t) \quad \textbf{(4.6)}$$

where *s(t)* denotes a modulated signal, and can be written as, [39];

$$s(t) = \begin{cases} \sqrt{\frac{2E_b}{T_b}}\cos(2\pi f_c t + \theta_c), & \text{for symbol 1} \\ 0, & \text{for symbol 0} \end{cases} \quad \textbf{(4.7)}$$

The waveform of OOK modulated signal depending on binary data sequence is shown in Figure 4.1

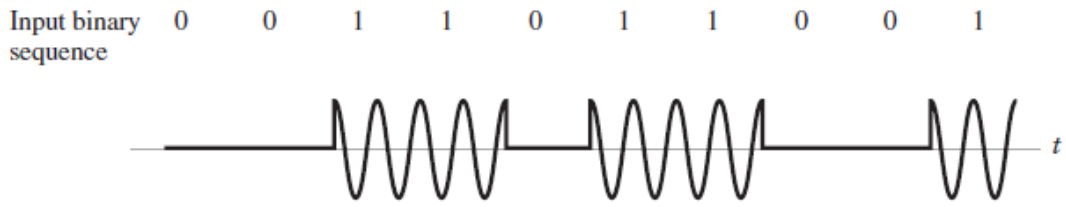

Figure 4.1 OOK modulated signal [4]

In OOK modulation, as the carrier signal is multiplied by the data signal, the frequency spectrum of the data signal is shifted to carrier frequency. As a result, the bandwidth required for transmission equals two times the bandwidth of the baseband data signal.

4.1.2 Demodulation of OOK signals

There are various methods for recovering the data signal at the receiver end. These can be classified as either coherent or non-coherent demodulation methods.

In coherent demodulation, a sinusoidal signal with the same frequency as carrier signal is used. The transmitted OOK signal is first sent to a BPF with center frequency of f_c and bandwidth of OOK signal bandwidth. The applied BPF, only passes the transmission frequency interval, while preventing inter symbol interference (ISI) and reducing noise effect. Then, BPF output signal is multiplied with the carrier signal and integrated using an integrator. In Integrator, correlation of the carrier signal and received signal is done. Demodulation is completed after a proper decision maker circuit is applied with respect to correlation. Figure 4.2 shows the block diagram of coherent OOK demodulator used for OOK demodulation.

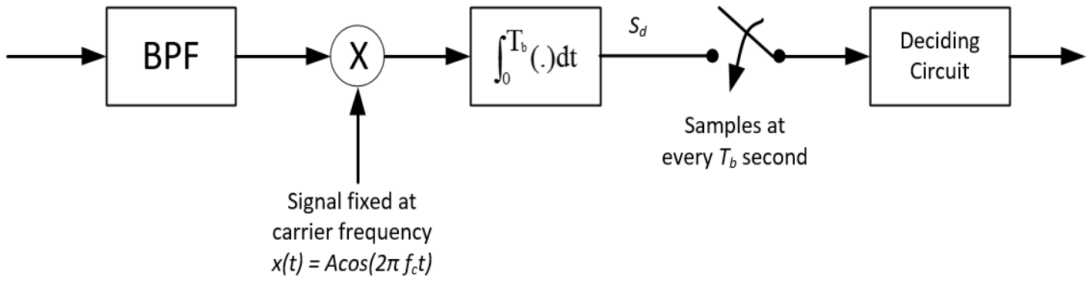

Figure 4.2 Coherent OOK demodulator

Non-coherent demodulation on the other hand, do not require a sinusoidal signal with carrier frequency. Instead, Envelope detector consisting of rectifier and LPF is used. Firstly, as in coherent case, BPF filter with center frequency of f_c and OOK signal bandwidth is applied. Then, using envelope detector, envelope of filtered BASK signal is obtained. Finally, using the sampler and decision maker circuit, the sampled envelope detector output is compared with threshold values at each T_b to recover the original data signal. Figure 4.2 shows the block diagram of non-coherent OOK demodulator used for OOK demodulation.

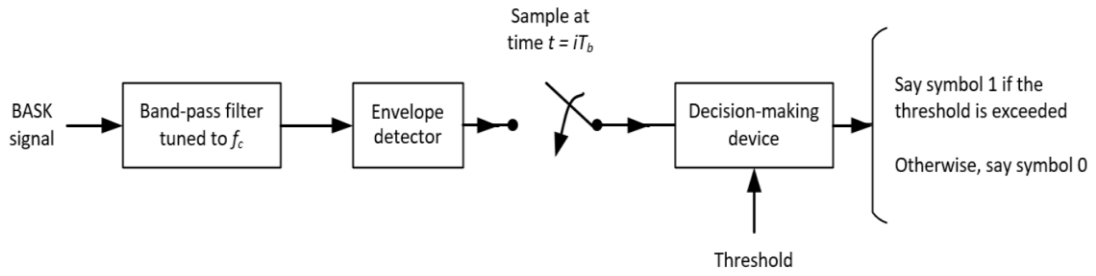

Figure 4.3 Noncoherent OOK demodulator

4.2 Binary Phase Shift Keying (BPSK)

In binary phase shift keying (BPSK), carrier signal's phase is modulated. BPSK modulation uses two phase levels of carrier to represent 0 and 1 digital symbols. $s_1(t)$ and $s_2(t)$, represent symbols 1 and 0 are defined by

$$s_1(t) = \sqrt{\frac{2E_b}{T_b}}\cos(2\pi f_c t), \quad \text{for symbol 1} \tag{4.8}$$

$$s_2(t) = \sqrt{\frac{2E_b}{T_b}}\cos(2\pi f_c t + \pi), \quad \text{for symbol 0} \tag{4.9}$$

where T_b denoting the bit duration and E_b denoting the transmitted signal energy per bit. These signals are named as antipodal signals due to phase shift.

4.2.1 BPSK modulation

Non-return-to zero encoder (NRZ) and product modulator are used for realizing BPSK modulation. Message signal is encoded using NRZ. Thus, symbol 1 is represented with positive amplitude of $\sqrt{E_b}$ while symbol 0 is represented with negative amplitude of $-\sqrt{E_b}$. Then, using Product modulator, NRZ encoded binary signal is multiplied with carrier signal at amplitude of $\sqrt{\frac{2}{T_b}}$ to obtain BPSK modulated signal. Figure 4.4 shows the block diagram of BPSK modulator.

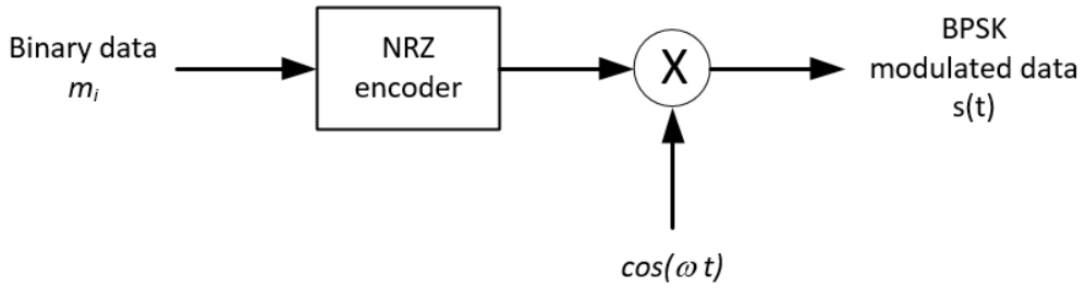

Figure 4.4 BPSK modulator

Since the BPSK signal is obtained as multiply of carrier and message signal in the time domain, its spectrum can be found as the convolution of message and carrier signal spectrum. After convolution, the BPSK signal bandwidth can be defined as;

$$BW_{BPSK} = \frac{2}{T_b} \tag{4.10}$$

4.2.2 BPSK demodulation

In BPSK demodulation, non-coherent demodulators are not used as the carrier amplitudes are same and amplitude changes cannot be detected with envelope

detectors. Thus, coherent demodulator is preferred in BPSK demodulators. Figure 4.5 shows the block diagram of Coherent demodulator.

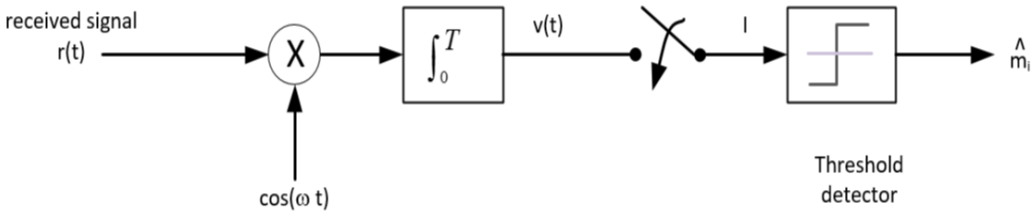

Figure 4.5 Coherent BPSK demodulator

BPSK signal is multiplied with a sinusoidal signal with carrier frequency and phase using product modulator. Then the output of product modulator is integrated over one bit period with an integrator. Integrator, takes the correlation of carrier signal and received signal. Symbol 0, s_0 and symbol 1, s_1 at the output of the integrator are calculated as;

$$s_0 = \int_0^{T_b} s_2(t).c(t)$$

$$= \int_0^{T_b} \sqrt{\frac{2E_b}{T_b}}\cos(2\pi f_c t + \pi) \times \sqrt{\frac{2}{T_b}}\cos(2\pi f_c t)$$

$$= \int_0^{T_b} -\sqrt{\frac{2E_b}{T_b}}\cos(2\pi f_c t) \times \sqrt{\frac{2}{T_b}}\cos(2\pi f_c t)$$

$$= -\int_0^{T_b} \sqrt{\frac{4E_b}{T_b^2}} cos^2(2\pi f_c t) \quad = -\sqrt{\frac{4E_b}{T_b^2}} \int_0^{T_b} \frac{1}{2} + \frac{1}{2}\cos(4\pi f_c t)$$

$$= -\sqrt{\frac{4E_b}{T_b^2}} \frac{T_b}{2} = -\sqrt{E_b}, \quad \text{for symbol 0,} \qquad \textbf{(4.11)}$$

$$s_1 = \int_0^{T_b} s_1(t).c(t)$$

$$= \int_0^{T_b} \sqrt{\frac{2E_b}{T_b}}\cos(2\pi f_c t) \times \sqrt{\frac{2}{T_b}}\cos(2\pi f_c t)$$

$$= \int_0^{T_b} \sqrt{\frac{4E_b}{T_b^2}} cos^2(2\pi f_c t) \quad = \sqrt{\frac{4E_b}{T_b^2}} \int_0^{T_b} \frac{1}{2} + \frac{1}{2}\cos(4\pi f_c t)$$

$$= \sqrt{\frac{4E_b}{T_b^2}} \frac{T_b}{2} = \sqrt{E_b}\,, \quad \text{for symbol 1,} \qquad \textbf{(4.12)}$$

The sampled integrator output is compared to threshold values at each T_b second using a decision maker circuit and a sampler. In decision maker circuit, the best threshold is taken as 0 which is the average of integrator output s_0 and s_1. During comparison, being above the threshold means symbol 1 is detected, while the opposite means symbol 0 is detected. Consequently, the original data signal is transmitted from the channel is recovered at the output of decision maker circuit.

4.3 Quadrature Phase Shift Keying (QPSK)

In digital communications, there are different modulation techniques for efficiently utilizing bandwidth of the allocated channel. One of such techniques is symbol based QPSK modulation. In QPSK modulation technique, each symbol consists of two bits and four carriers with equally distributed phases are used. QPSK modulated signal is defined by [40]

$$s_{QPSK}(t) = \sqrt{\frac{2E_s}{T_s}} \cos(2\pi f_c t + (i-1)\frac{\pi}{2}) \quad i = 1,2,3,4 \qquad \textbf{(4.13)}$$

where E_s is the transmitted signal energy per symbol and T_s is the symbol duration which is twice the bit duration. QPSK modulated signal is written by using trigonometric formulae in the interval of $0 \leq t \leq T_s$.

$$s_{QPSK}(t) = \sqrt{\frac{2E_s}{T_s}} \cos(2\pi f_c t)\cos[(i-1)\frac{\pi}{2}]$$

$$- \sqrt{\frac{2E_s}{T_s}} \sin(2\pi f_c t)\sin[(i-1)\frac{\pi}{2}] \qquad \textbf{(4.14)}$$

In equation 4.14, the first and second terms correspond to BPSK modulation. In other words, the QPSK signal can be considered as sum of two BPSK signals. In QPSK modulation, the first of the transmitted bits modulates the cosines carrier whereas the

other one modulates sinusoidal carrier. Consequently, four carriers of QPSK transmit the 10, 00, 01 and 11 data respectively.

4.3.1 QPSK modulation

For QPSK modulation, firstly, the message signal is transformed into polar form using non-return-to-zero-level encoder. This conversion is necessary, as in BPSK modulation, to represent symbol 1 as positive amplitude of $\sqrt{E_b}$ and symbol 0 as negative amplitude of $-\sqrt{E_b}$. Secondly, NRZ encoded message signal is split into even and odd bits using a serial to parallel converter. Even and odd bits are used to modulate sine and cosine carriers in in-phase and quadrature phase channels. Modulated signals are BPSK signals. Finally, QPSK signal is obtained as the sum of two BPSK signals modulated in in-phase and quadrature phase channels. Figure 4.6 shows the block diagram of QPSK modulation.

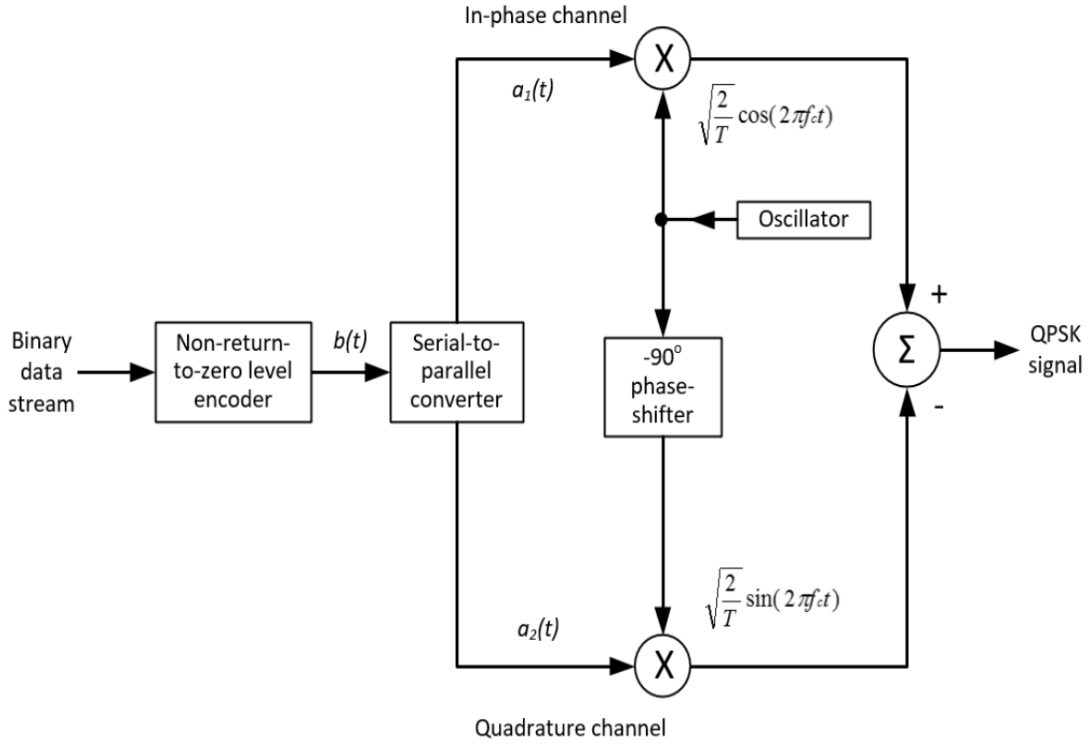

Figure 4.6 QPSK modulation block diagram

4.3.2 QPSK demodulation

For QPSK demodulation, coherent demodulator is used as in BPSK demodulation. In order to recover even and odd bit series at the output of serial-to-parallel converter, the QPSK signal is multiplied with coherent carriers in in-phase and quadrature channels and the signals obtained are integrated using integrator. hen, integrator output signals are run through decision maker circuits to recover even bit sequences in in-phase channel and odd bit sequences in quadrature phase channel. Finally, using the parallel to serial converter in receiver, the original message signal is recovered. Figure 4.7 shows the block diagram of QPSK demodulation steps.

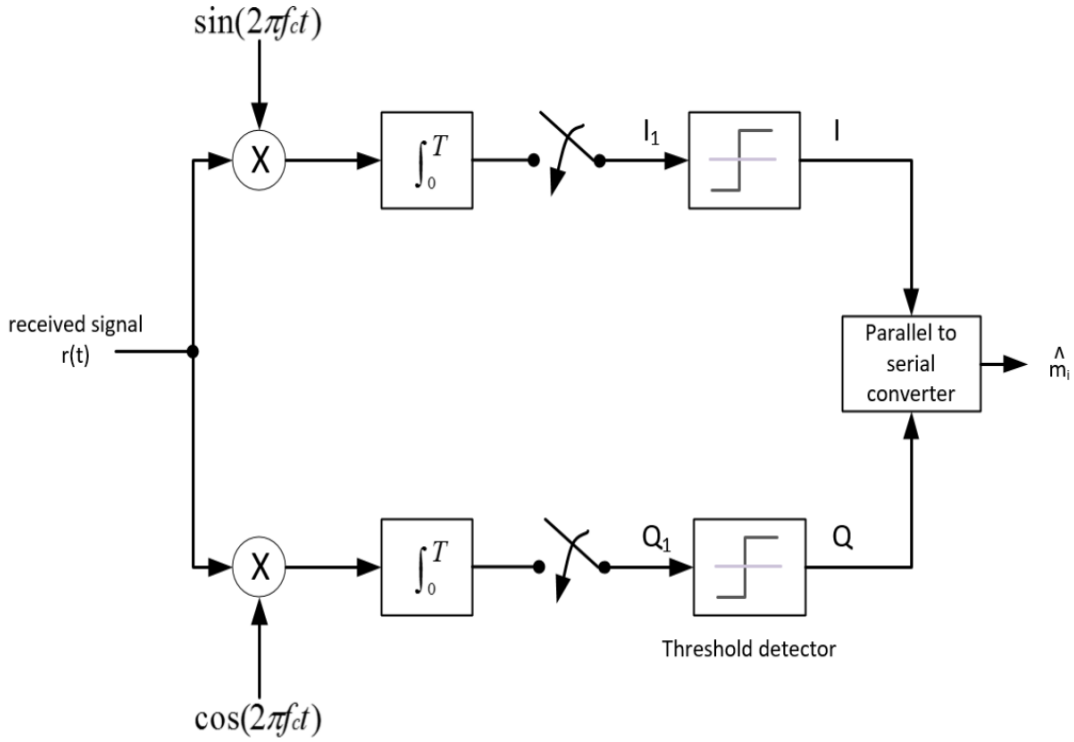

Figure 4.7 QPSK demodulation block diagram

4.4 M-ary Phase Shift Keying (M-PSK)

MPSK modulation keys carrier signal phase in more than two levels. MPSK modulation uses M carrier signals and each have different phase values. There phase values are obtained dividing the phase domain into M parts. M transmitted signals are expressed by

$$s_i(t) = \sqrt{\frac{2E_s}{T_s}}\cos\left(2\pi f_c t + \frac{2\pi}{M} i\right), \quad i = 0,1,\dots,M-1 \qquad 0 \le t \le T_s \qquad \textbf{(4.15)}$$

where E_s is the transmitted signal energy per symbol and f_c is the carrier frequency. This expression can be write as;

$$s_i(t) = \left[\sqrt{E_s}\cos(\frac{2\pi}{M} i)\right]\left[\sqrt{\frac{2}{T_s}}\cos(2\pi f_c t)\right]$$

$$-\left[\sqrt{E_s}\sin(\frac{2\pi}{M} i)\right]\left[\sqrt{\frac{2}{T_s}}\sin(2\pi f_c t)\right], \quad \begin{matrix} i = 0,1,\dots,M-1 \\ 0 \le t \le T_s \end{matrix} \qquad \textbf{(4.16)}$$

If $\phi_1(t)$ and $\phi_2(t)$ are determined as, respectively, $\sqrt{\frac{2}{T_s}}\cos(2\pi f_c t)$ and $\sqrt{\frac{2}{T_s}}\sin(2\pi f_c t)$ over the time interval $0 \le t \le T_s$, MPSK signal is rewritten by;

$$s_{MPSK}(t) = \left[\sqrt{E_s}\cos\left(\frac{2\pi}{M} i\right)\right]\phi_1(t) - \left[\sqrt{E_s}\sin\left(\frac{2\pi}{M} i\right)\right]\phi_2(t) \qquad \textbf{(4.17)}$$

$$i = 0,1,\dots,M-1$$

In equation 4.17, $\cos\left(\frac{2\pi}{M} i\right)$ and $\sin\left(\frac{2\pi}{M} i\right)$ are orthogonal carriers; $\phi_1(t)$ and $\phi_2(t)$ are in-phase and quadrature phase components. In-phase and quadrature phase components are used for constellation diagram that shows the amplitude and phase values of carrier signals [38]. Figure 4.8 shows a constellation diagram of 8-PSK modulation with M=8 carriers.

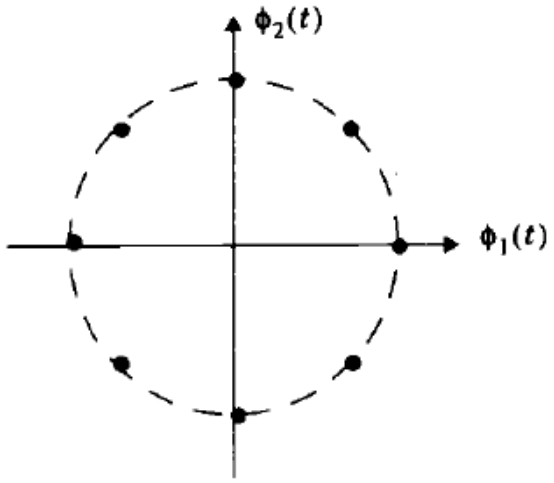

Figure 4.8 Constellation diagram of 8-PSK modulation [38]

For MPSK demodulation, same demodulator structures as BPSK and QPSK demodulations are used. The received MPSK signal, after being split into in-phase and quadrature phase components, is correlated with carriers using integrator. Demodulation is completed after deciding which carrier is transmitted with respect to correlation results.

In MPSK modulation, bandwidth decreases as the symbol duration, T_s increases. Therefore, although the frequency band allocated for communication system is utilized much more efficiently, the increasing number of carriers make the system suffer more from noise.

CHAPTER 5

SIMULATIONS

The simulations for designed system are conducted on Matlab Simulink. First of all, the following simulations are run in Simulink;

- Modelling of various modulation types such as OOK, BPSK and QPSK,
- OFDM system modelling,
- Frequency downconverter and frequency up-converter modelling.

During the simulation of these models, the blocks on SimRF and communication System toolbox under Simulink library are used. Then using these Simulink models, high data rate communication transmitter/receiver systems working on 0.24 THz band are made. Finally, performance analysis is done for the created systems and analysis results are observed.

5.1 Modelling and Design of 0.24 THz Band OOK Communication Transmitter/Receiver System

In Simulink, a 0.24 THz band communication system utilizing OOK modulation with 10 gbps data rate is designed. In this model, the digital data incident on frequency up-converter is up-converted to 0.24 THz band using a mixers and multiplier chain. In the receiver end, on the other hand, the received data is down-converted to base band using the mixer and multiplier chain in frequency downconverter. The transmitter and receiver models for 0.24 THz band are acquired after below steps are accomplished:

- Generating 10 GHz carrier signal,
- Upconversion of the carrier signal frequency to 30 GHz using frequency multiplier,
- Generating data signal with high data rate,
- Applying OOK modulation to the data signal with the carrier signal generated,

- Gradually upconversion of the frequency of the OOK modulated signal to 60 GHz, 120 GHz and 240 GHz using frequency doublers and suitable band-pass filters
- In the receiver end, producing a 11GHz frequency local oscillator signal,
- Increasing the frequency of the local oscillator signal to 33GHz using frequency multiplier,
- Gradually increasing the frequency of the local oscillator signal to 66 GHz, 132 GHz and 264 GHz using frequency doublers and suitable band-pass filters,
- Down-converting and demodulating the transmitted 240 GHz band OOK modulated signal using the local oscillator signal,

5.1.1 Generating the Carrier Signal

The Simulink model in figure 5.1 is used for generating the carrier signal. The Configuration block is used for adjusting the system options such as Fundamental tones, Harmonic order, Step Size, Simulation noise and Solver. For each SimRF sub system a new Configuration block must be defined [41].

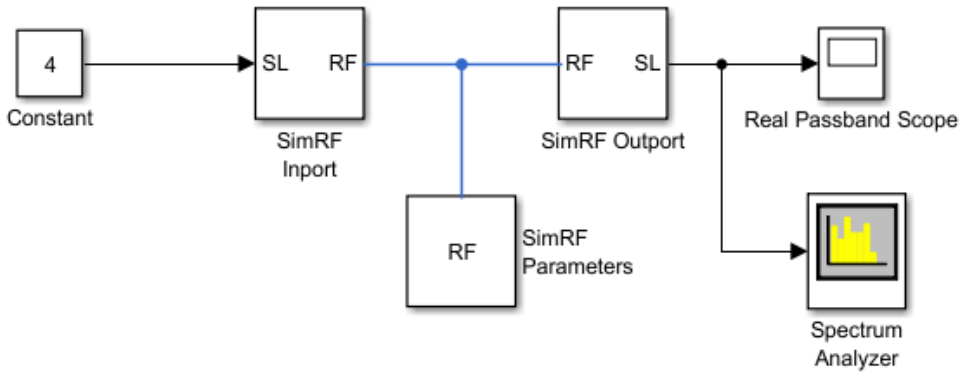

Figure 5.1 Generation of carrier signal

Inport block allows for converting the Simulink signal to SimRF voltage or current while the Outport block provides the reverse conversion [41]. The generated carrier signal has 4 V peak voltage and 10 GHz frequency. The time and frequency domain plots of the carrier signal are shown in Figure 5.2 and Figure 5.3 respectively.

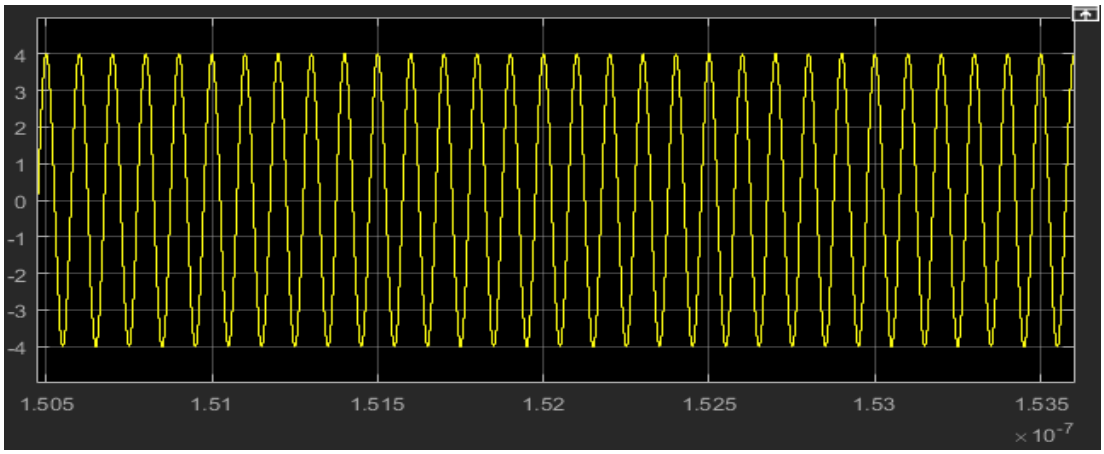

Figure 5.2 10 GHz carrier signal in time domain

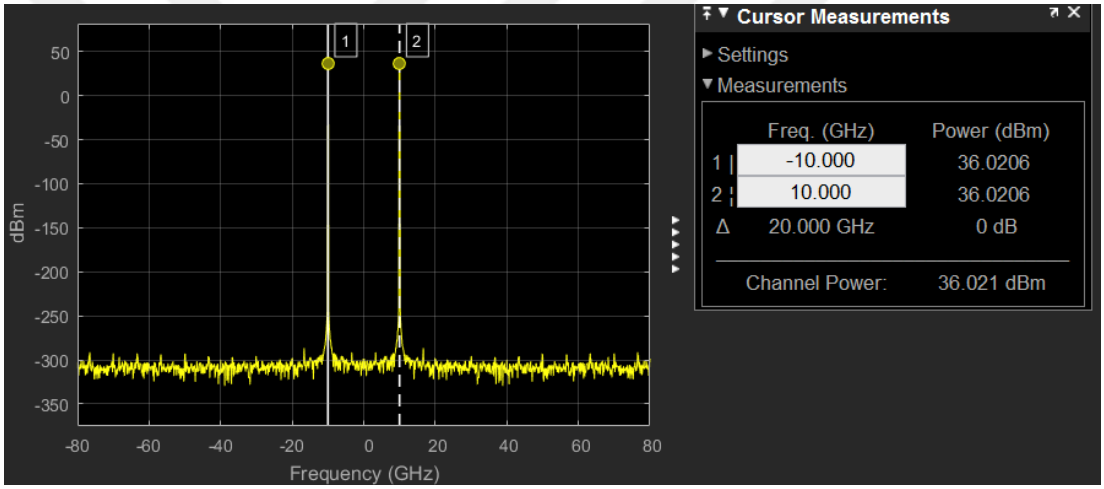

Figure 5.3 10 GHz carrier signal in frequency domain

5.1.2 Upconverting the Carrier Signal Frequency to 30 GHz

The communication system being modelled is required to work in 0.24 THz band. Hence, THz band millimeter signal is used as carrier signal source. For these frequency intervals, there are no transistors or dielectric oscillators that can generate more than 1mW power. That's why it is preferred to use frequency multiplication to generate 200 GHz or more frequency signals. Frequency multiplication is realized by generating the harmonics of the input signal frequency with a nonlinear response system and by selecting the desired harmonic via corresponding filters.

Figure 5.4 shows the Simulink model for the frequency multiplication method used for upconverting the carrier signal frequency from 10 GHz to 30 GHz.

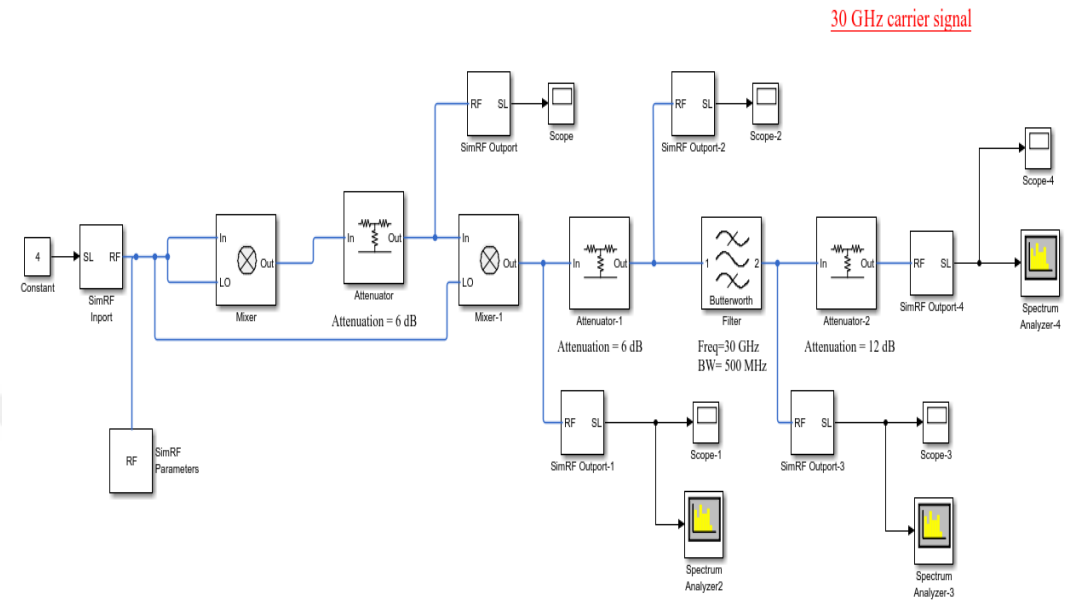

Figure 5.4 Simulink model showing that 30 GHz carrier signal is obtained from a 10 GHz carrier signal

Observing this model, it can be seen that the frequency multiplication procedure is obtained using Mixer, Attenuator and Filter blocks in SimRF library. The mixer block with the settings shown in Figure 5.5, multiplies the RF input signal with LO input signal given below to generate the output signal.

$$V_{RF} = A_{RF}.\cos(w_{RF}t) \quad \textbf{(5.2a)}$$

$$V_{LO} = A_{LO}.\cos(w_{LO}t) \quad \textbf{(5.2b)}$$

$$V_{in}.V_{LO} = A_{in}.\cos(w_{in}t).A_{LO}.\cos(w_{LO}t)$$

$$= \frac{A_{in}A_{LO}}{2}\cos[(w_{in} + w_{LO})t] + \frac{A_{in}A_{LO}}{2}\cos[(w_{in} - w_{LO})t] \quad \textbf{(5.2c)}$$

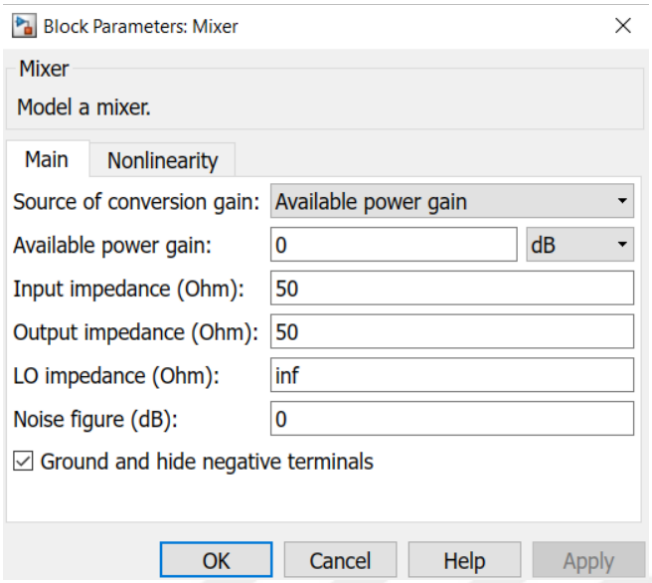

Figure 5.5 Mixer block parameters

Additionally, noise effect can be modelled adjusting the Noise Figure (NF) parameter of Amplifier block in the Mixer block. However, to do so Simulate Noise option of Configuration block must be activated [41]. The Attenuator block with the parameters given in Figure 5.6, is used for halving the amplitude of the Mixer block output signal. Therefore, Attenuation parameters of Attenuator and Attenuator-1 are chosen as 6dB.

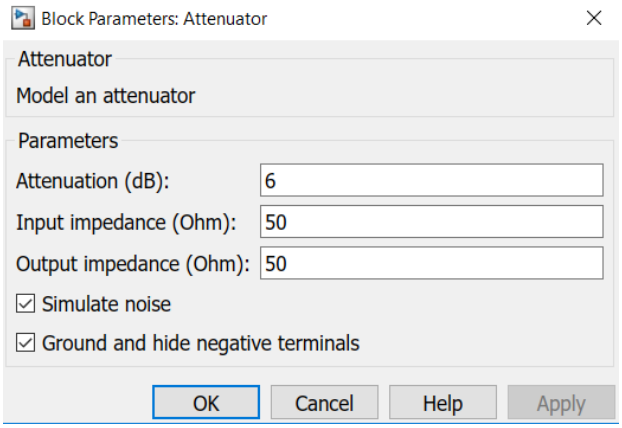

Figure 5.6 Attenuator block parameters

In this model, 20 GHz carrier signal is generated at the output of the Mixer block. At the output of the Mixer-1 block, 10 GHz and 30 GHz harmonics are generated by multiplying the 20 GHz carrier signal of Mixer block with a 10 GHz carrier signal.

The frequency spectrum for the harmonics generated at output of Mixer-1 is shown in Figure 5.7.

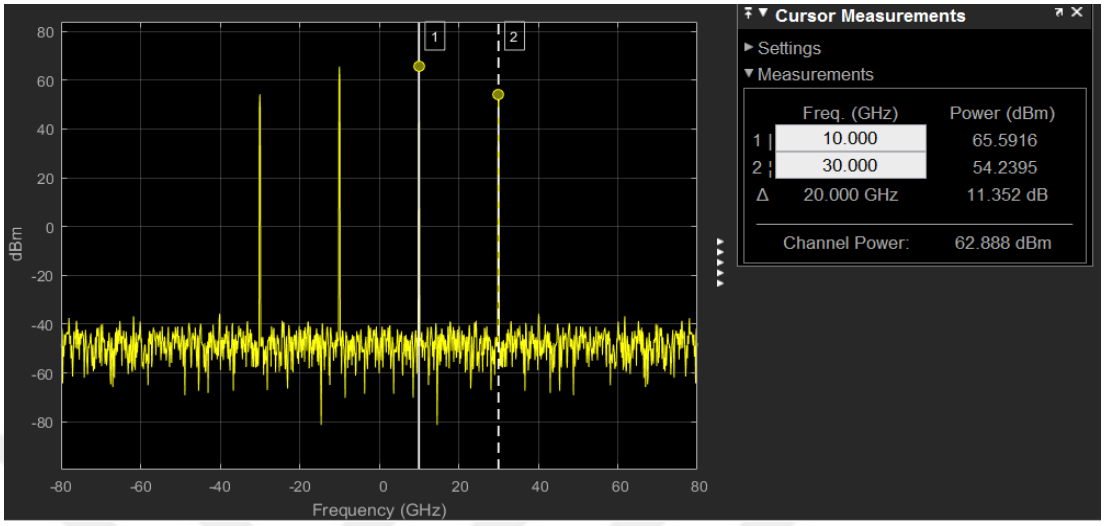

Figure 5.7 Spectrum of Mixer-1 block output

The desired harmonic among the others is chosen with filtering. For filtering, the Filter block in SimRF library is used. Filter block parameters are shown in Figure 5.8.

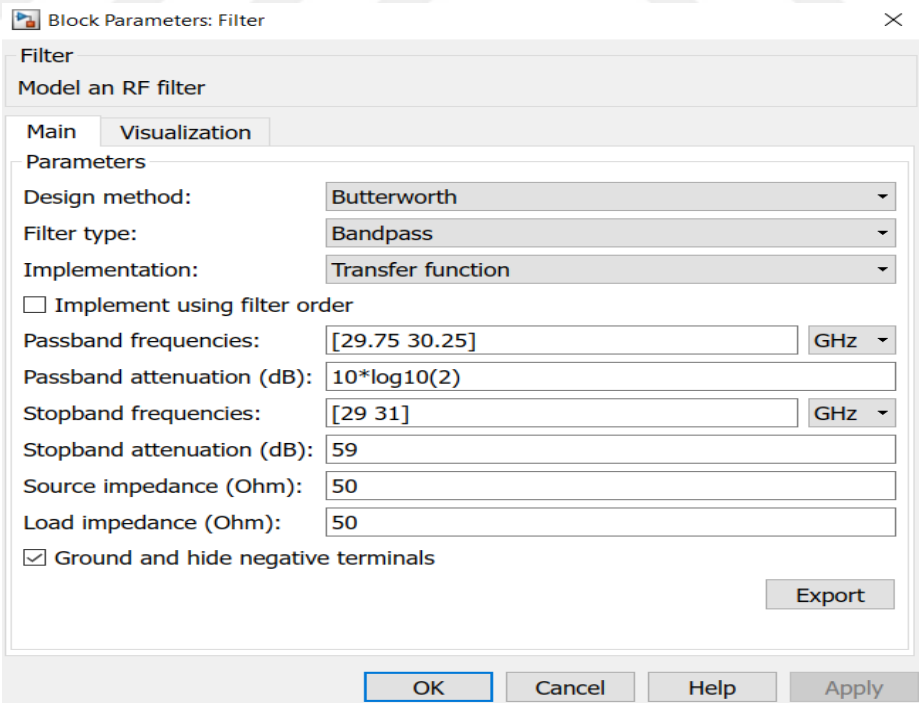

Figure 5.8 Filter block parameters

The generated filter is of type Butterworth BPF with passband frequencies; 29.75 GHz, 30.25 GHz and stopband frequencies; 29 GHz and 31 GHz. The carrier signal frequency is successfully upconverted to 30 GHz after the filtering. Time and frequency domain plots for filter block output carrier signal are shown in Figure 5.9 and Figure 5.10 respectively.

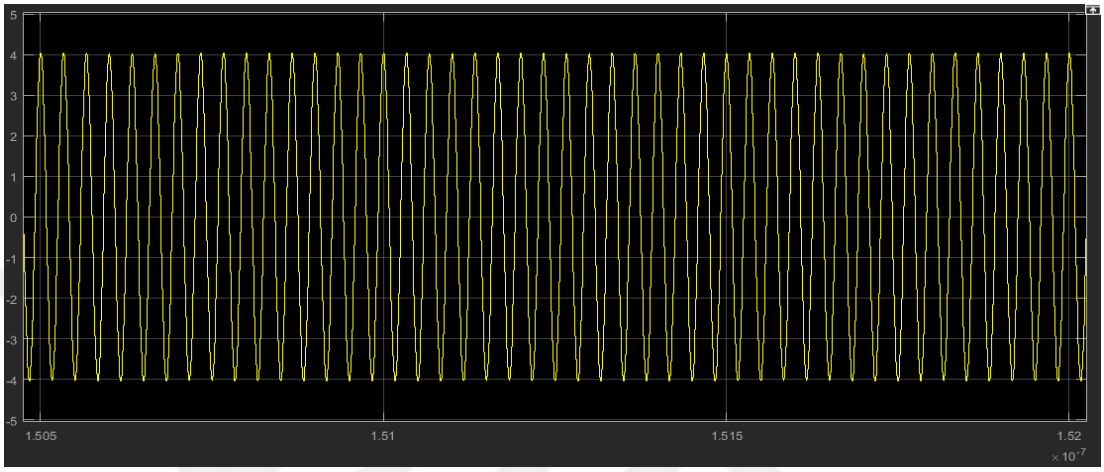

Figure 5.9 30 GHz carrier signal in time domain

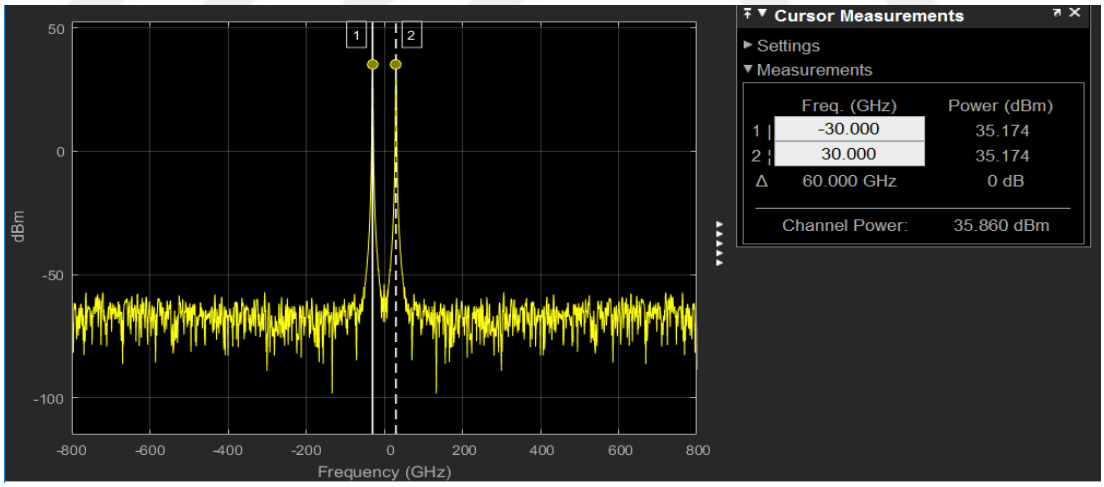

Figure 5.10 30 GHz carrier signal in frequency domain

5.1.3 Generating Data Signal with High Data Rates

The data signal with high data rates is generated using the Random Integer Generator block with parameters given in Figure 5.11. Using M parameter, uniformly distributed

random number sequence in [0, M-1] interval is generated [41]. Here the M parameter is defined as Set size.

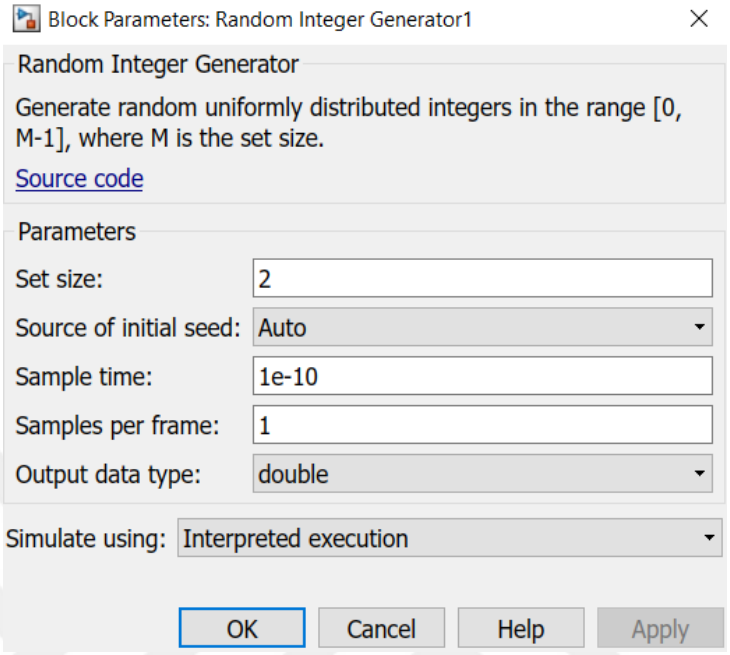

Figure 5.11 Random Integer Generator block parameter

The Simulink model for generating data signal with high data rates is shown in Figure 5.12. The resulting data signal has 10 gbps data rate.

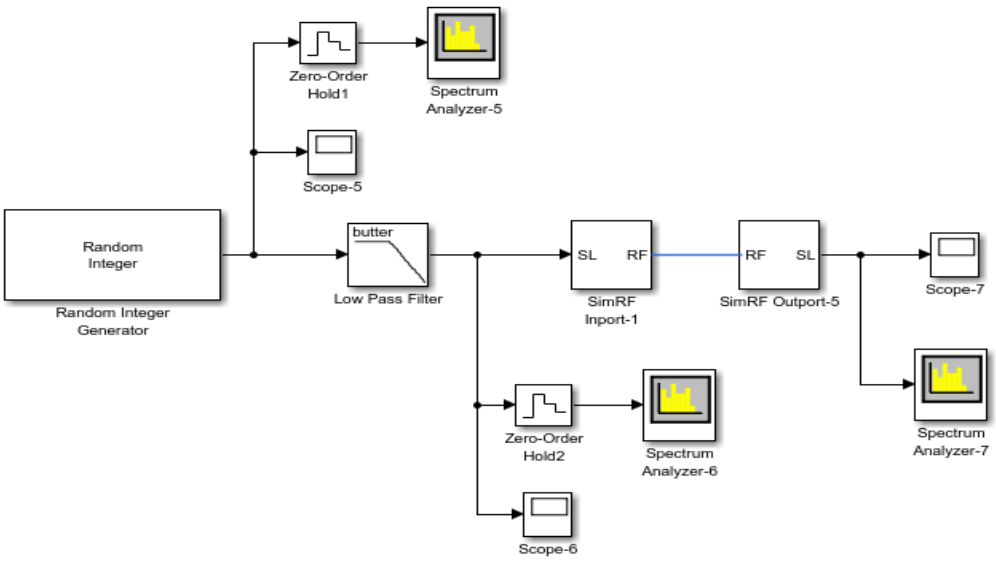

Figure 5.12 Generation of data signal with high data rate

Time and frequency domain plots for the data signal are shown in Figure 5.13 and Figure 5.14 respectively.

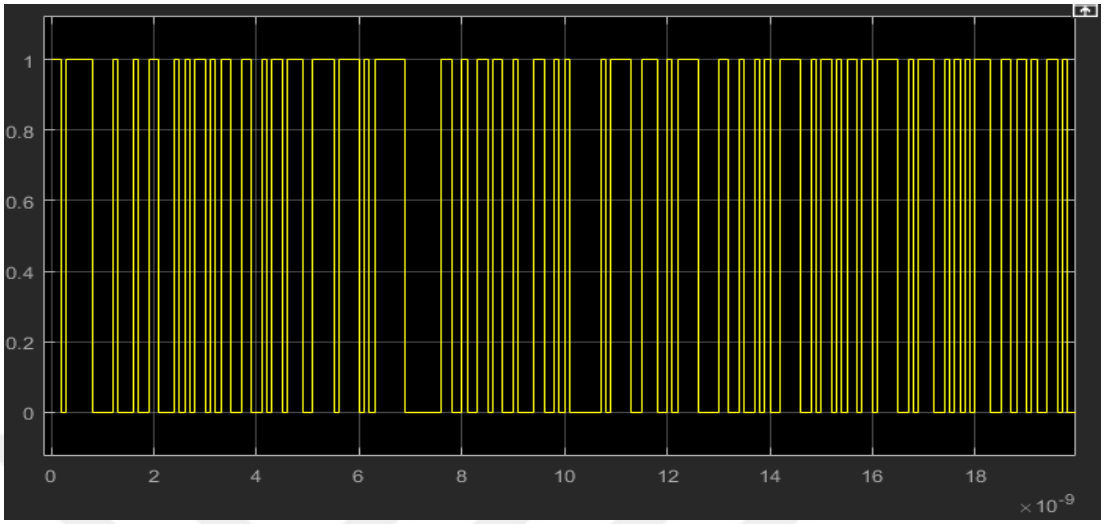

Figure 5.13 10 gbps data signal in time domain

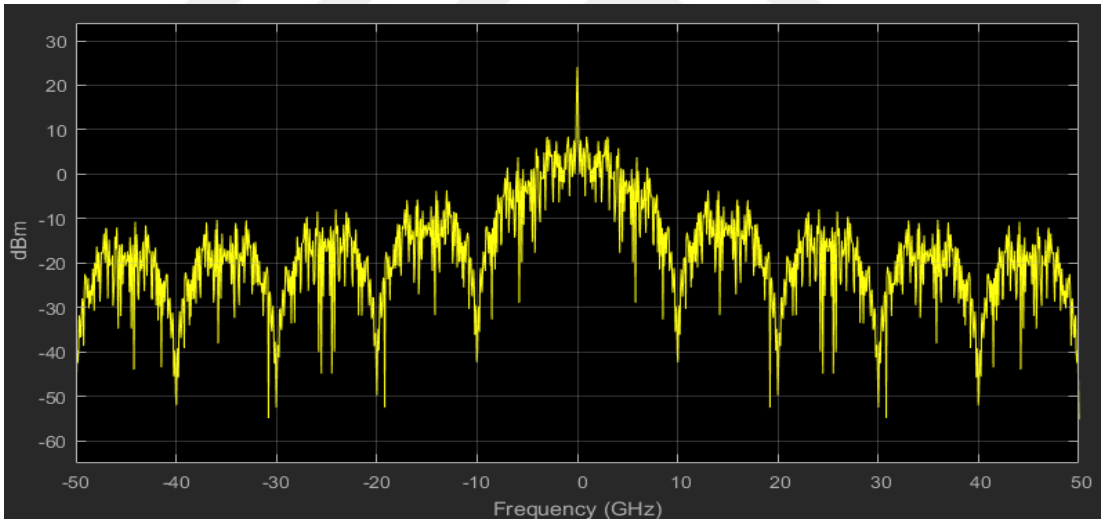

Figure 5.14 10 gbps data signal in frequency domain

The 10 gbps data signal at the output of the Random Integer Generator block is sent to a Low Pass Filter. This is because, the bandwidth of the experimental data signal is approximately 0.7-0.8-fold of theoretically calculated bandwidth. The filter is an 8^{th} order, low-pass Butterworth filter with cut-off frequency of 7 GHz. Time and

frequency domain plots for the LPF output data signal are shown in Figure 5.15 and Figure 5.16 respectively.

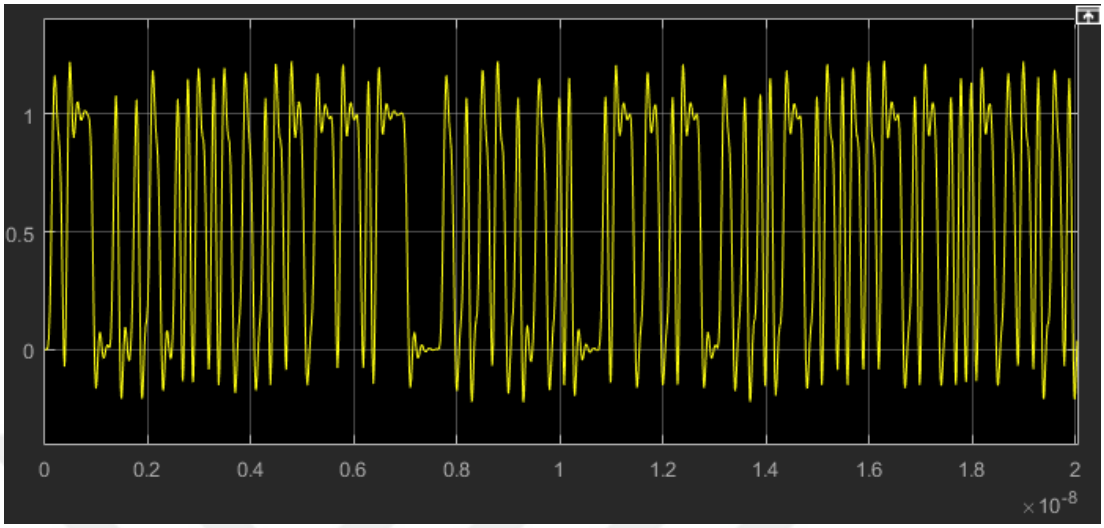

Figure 5.15 LPF output in time domain

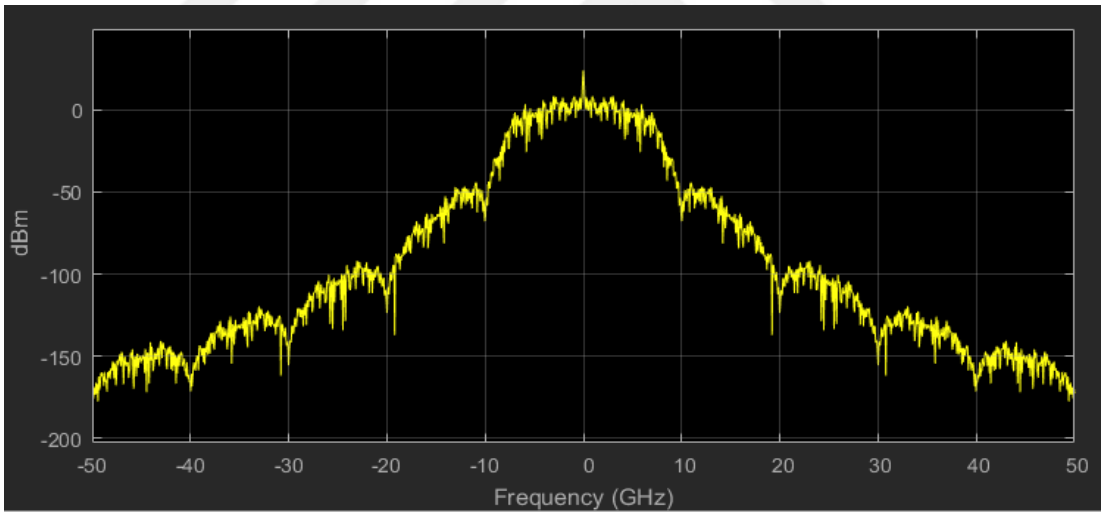

Figure 5.16 LPF output in frequency domain

5.1.4 OOK Modulation

In this stage, OOK Modulation of data signal generated in Figure 5.15 is done using the 30 GHz carrier signal generated in Figure 5.9. The Simulink model of this stage is shown in Figure 5.17.

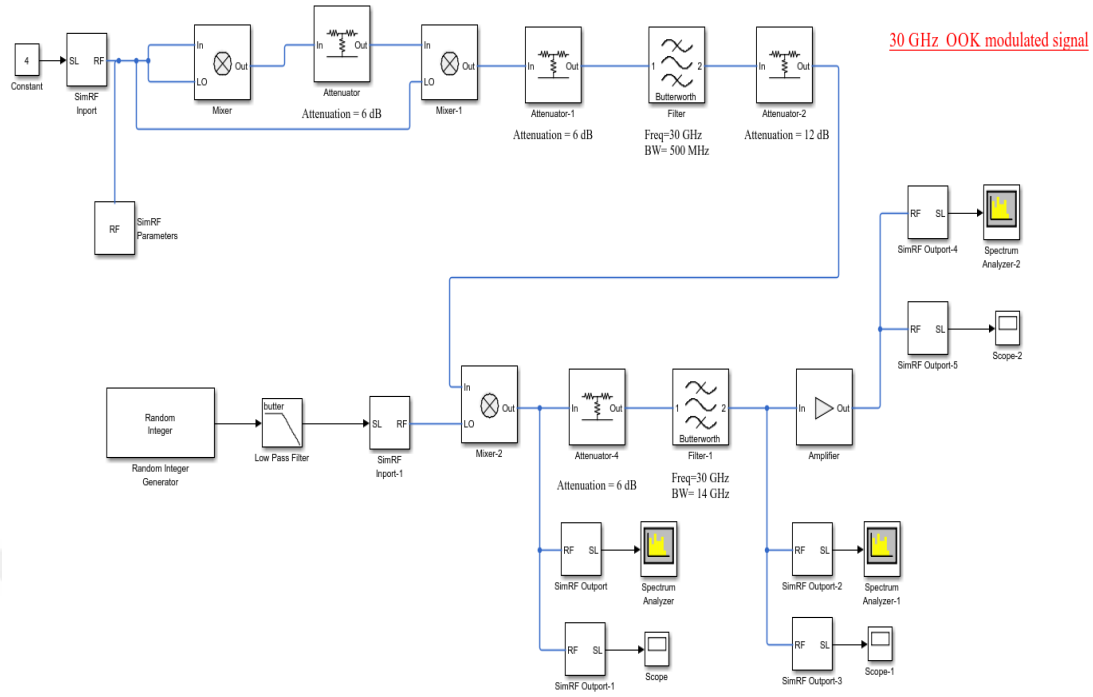

Figure 5.17 OOK simulation model

OOK modulated signal, is considered as the result of data signal being multiplied with the carrier signal in time domain. Therefore, The OOK modulated signal's spectrum can be obtained as the convolution of data signal and carrier signal's spectrum. The time and frequency domain plots for the OOK modulated data signal at the output of the Mixer-2 block are shown in Figure 5.18 and Figure 5.19 respectively.

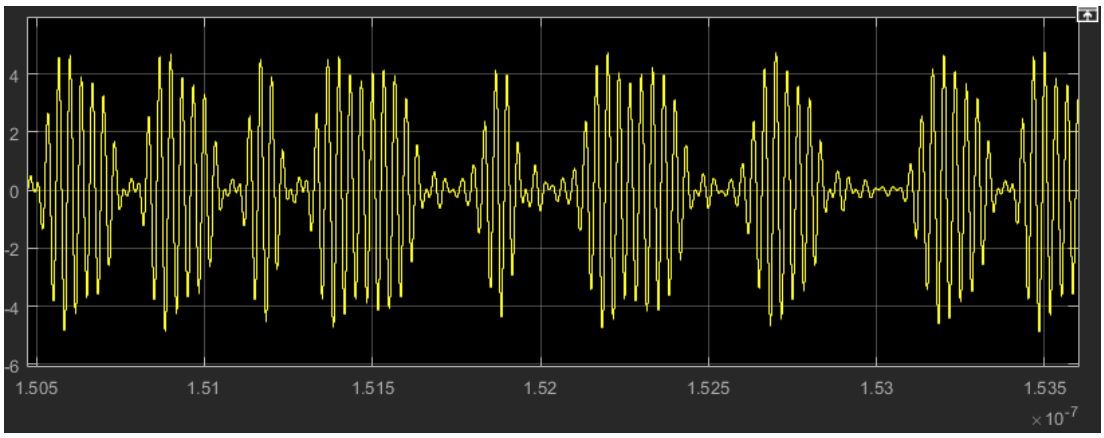

Figure 5.18 30 GHz OOK modulated signal in time domain

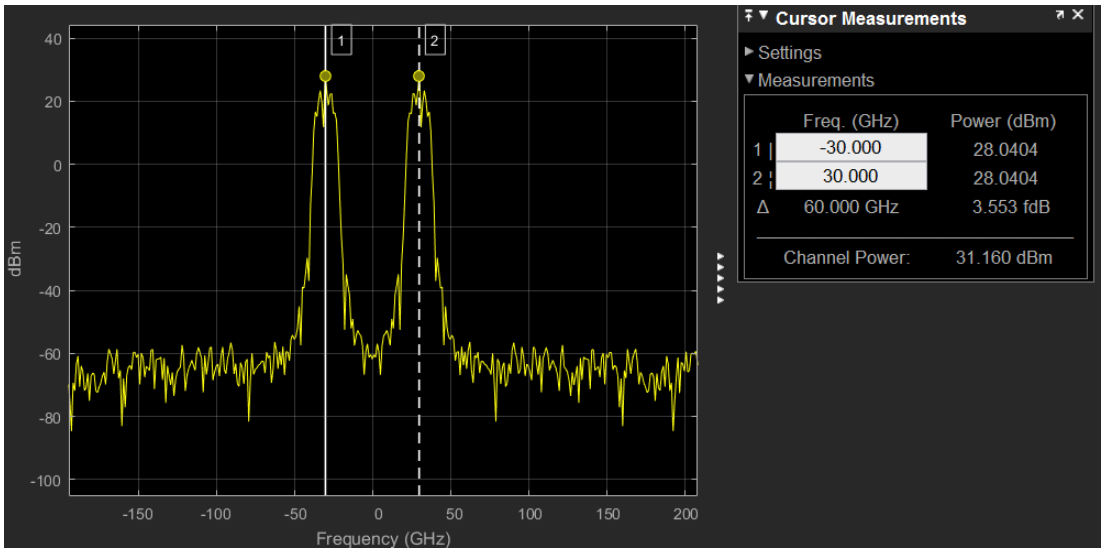

Figure 5.19 30 GHz OOK modulated signal in frequency domain

In amplitude modulation, the baseband data signal is directly multiplexed with the carrier signal. As a result, the spectrum of baseband data signal is shifted towards carrier signal frequency and the required bandwidth for transmission is double of data signal bandwidth. Therefore, 6 dB attenuated signal at the Attenuator-4 block is sent to Filter-1 block with double bandwidth compared to data signal and parameters given in Figure 5.20.

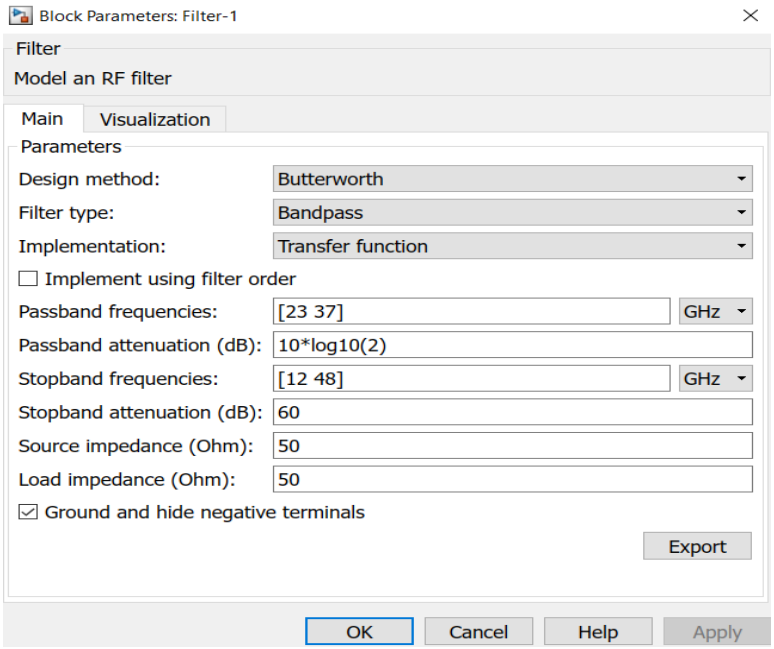

Figure 5.20 Filter-1 block parameters

Filter-1 block filter is of Butterworth BPF type with passband frequencies; 23 GHz and 37 GHz; stopband frequencies 12 GHz and 48 GHz respectively. The obtained modulated signal at the output of Filter-1 block suffers from the losses of Mixer and filter. In order to counteract these losses, the signal is amplified in an Amplifier block with 8 dB gain. The time and frequency domain plots for the Amplifier block output signal are shown in Figure 5.21 and Figure 5.22 respectively.

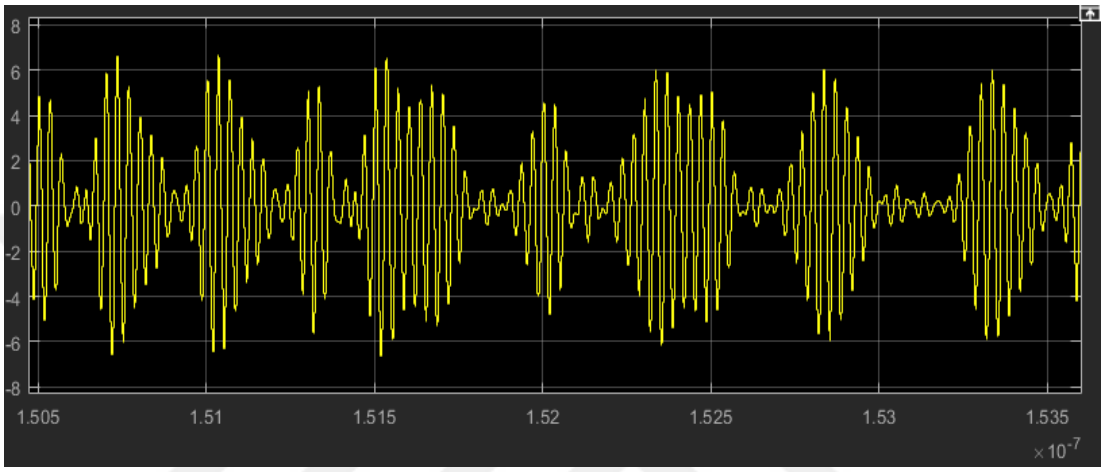

Figure 5.21 Output of amplifier block in time domain

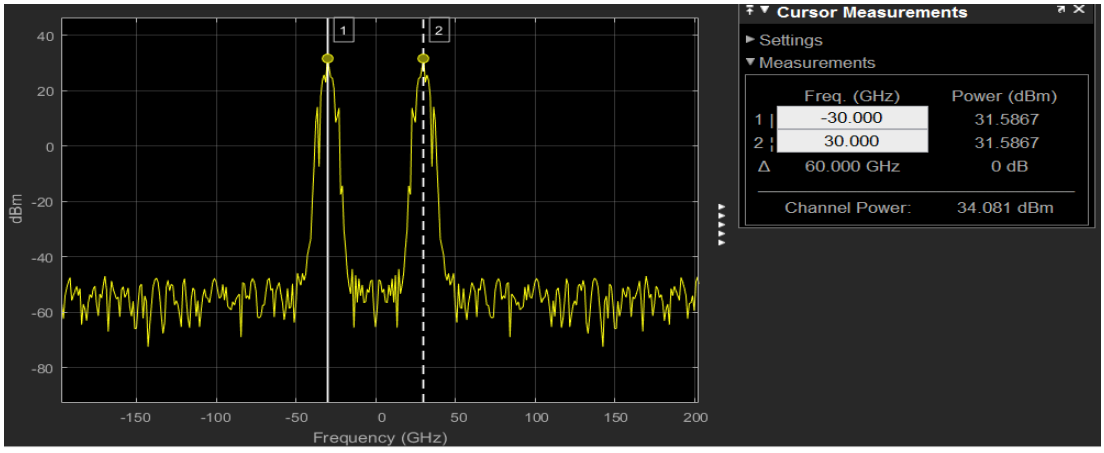

Figure 5.22 Output of amplifier block in frequency domain

5.1.5 Upconversion of the OOK Modulated Signal to 240 GHz Band

The main approach in microwave and millimeter wave communication systems has always been to make modulation, pulse shaping and narrow baseband filtering on lower frequencies and then to bring results into higher frequency bands. Frequency upconversion for modulated signal, which has frequency spectrum centered at the carrier frequency, can be done using Mixer blocks. Mixer blocks consist of multiplier modulator and band-pass filter. Nonlinear Schottky diodes are used for this as they provide efficiency in millimeter wave band.

Accordingly, 30 GHz frequency of the OOK modulated signal is up-converted to 60 GHz, 120 GHz and 240 GHz respectively, using frequency doublers and a suitable band pass filters. Freqeuncy doubler is realized using the Mixer block in SimRF library of Simulink is used with given parameters in Figure 5.5. Mixer block incident signal is multiplexed with itself, so the output signal of the block has double the frequency. Among the harmonics generated with up-conversion, the one with the desired frequency multiplier constant is chosen using proper band-pass filters. The Simulink model for the designed frequency up-converter that utilizes frequency multiplication method to up-convert the OOK modulated signal into 240 GHz band is given in Figure 5.23.

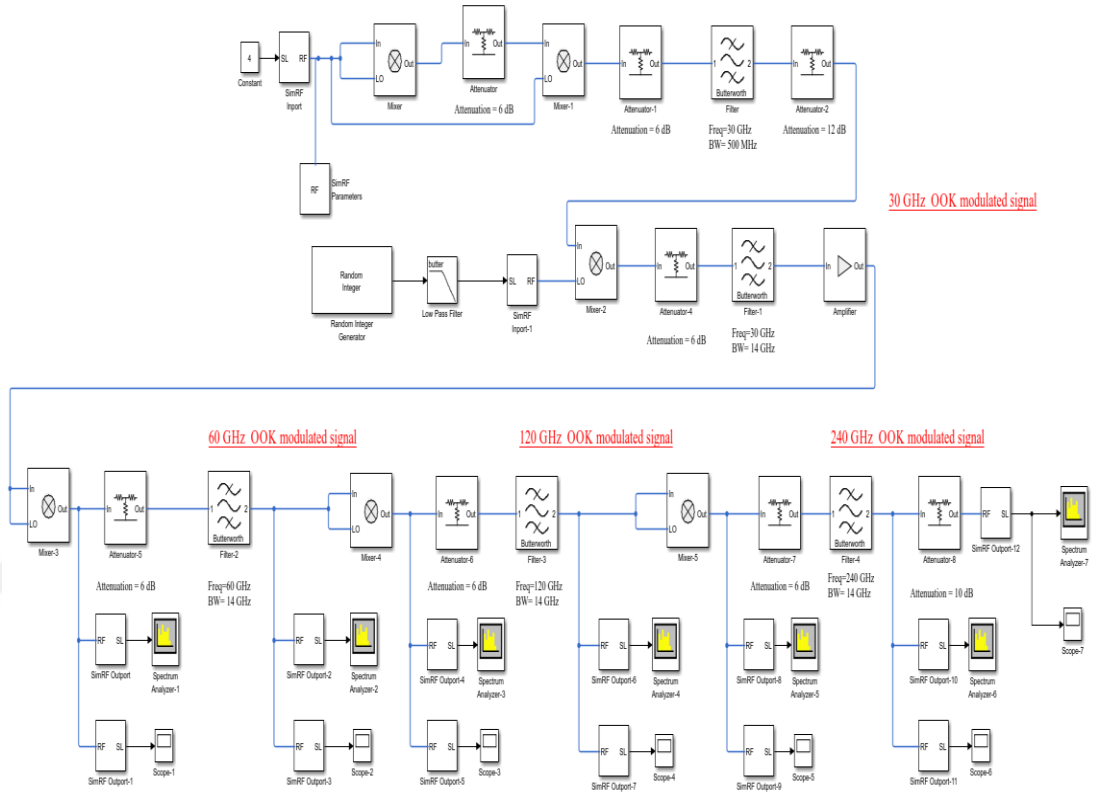

Figure 5.23 Design of frequency upconversion blocks

As figure 5.23 shows, the frequency up-converter consists of Mixer, Attenuator and Filters blocks. Firstly, at the output of Mixer-3 block, baseband and 60 GHz frequency OOK modulated signal is generated. The time and frequency domain plots for obtained signal are shown in Figure 5.24 and Figure 5.25 respectively.

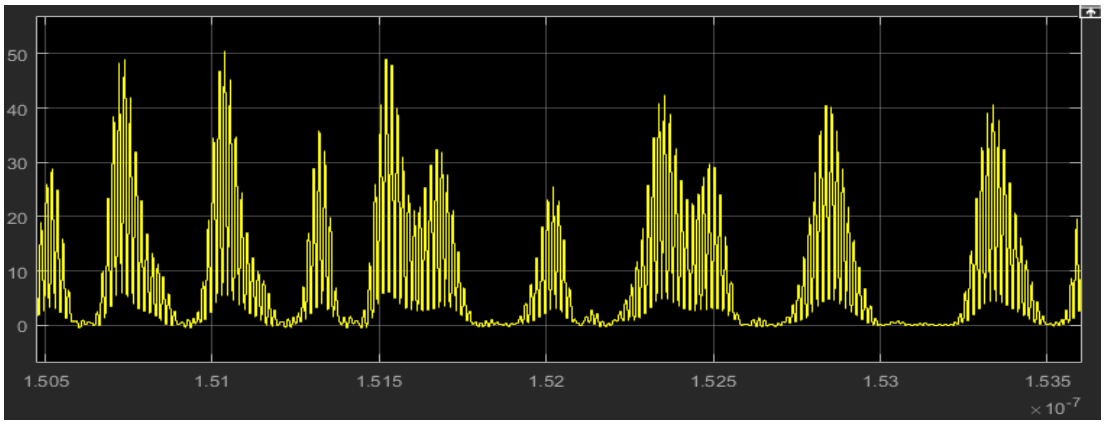

Figure 5.24 Output of Mixer-3 in time domain

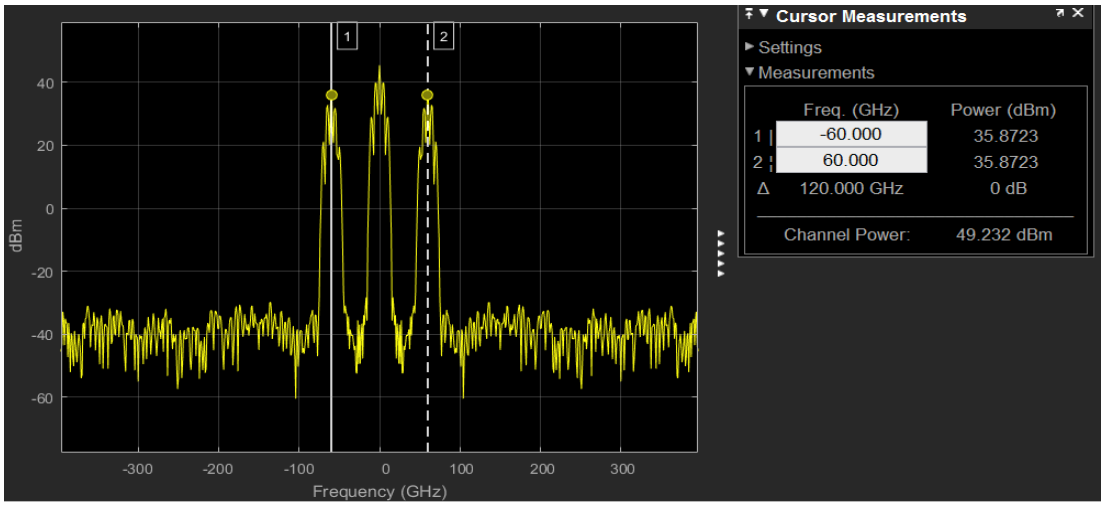

Figure 5.25 Output of Mixer-3 in frequency domain

The amplitude of the Mixer-3 block output signal is halved using Attenuator-5 block. This is due to the fact that, the ½ factor of trigonometric inverse transform formulas cannot be realized using Mixer blocks. Filter-2 block with given parameters in Figure 5.26 is used for obtaining only the 60 GHz up-converted OOK modulated signal and negating the effects of other harmonics shown in Figure 5.25.

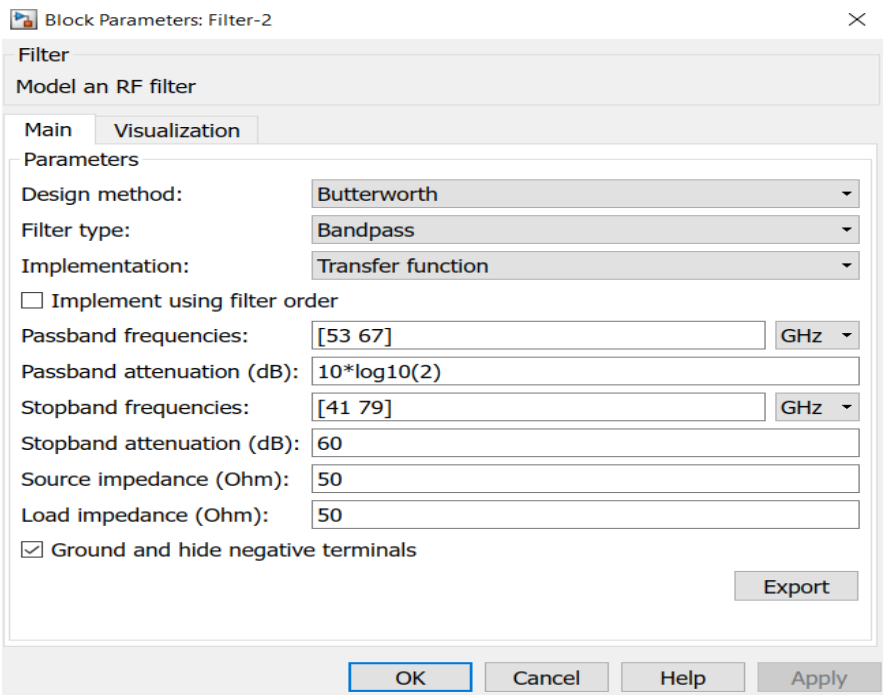

Figure 5.26 Filter-2 block parameters

For Filter-2 block, Butterworth BPF type with passband frequencies; 53 GHz, 67 GHz and stopband frequencies; 41 GHz, 79 GHz is chosen. OOK modulated signal is successfully up-converted to 60 GHz using the filter. The time and frequency domain plots for Filter-2 block output signal are given in Figure 5.27 and Figure 5.28.

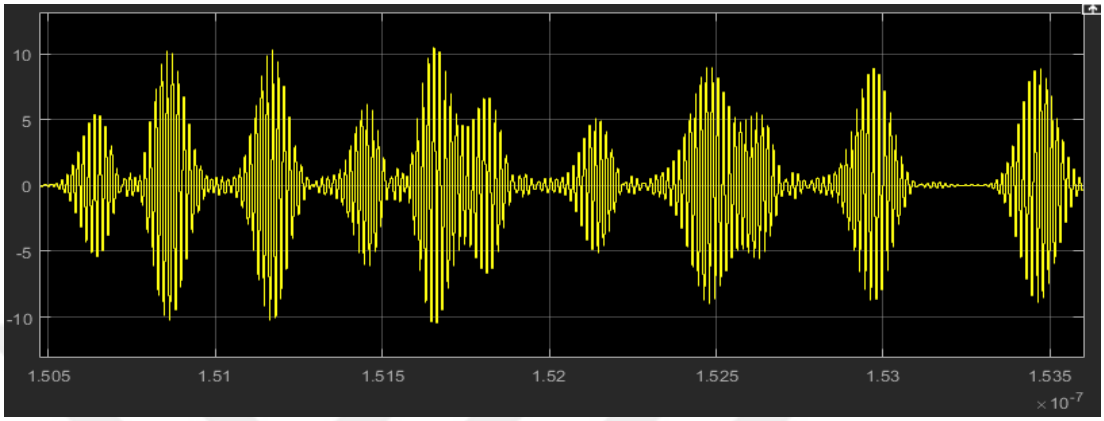

Figure 5.27 60 GHz OOK modulated signal in time domain

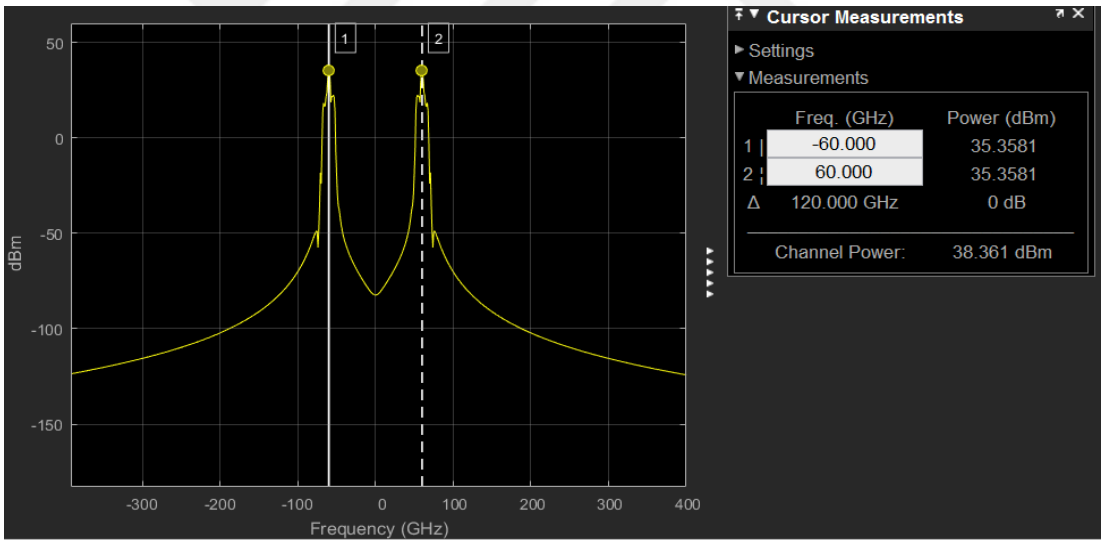

Figure 5.28 60 GHz OOK modulated signal in frequency domain

The same steps used in up-converting 30 GHz OOK modulated signal into 60GHz are applied for up-conversions from 60 GHz to 120 GHz and from 120 GHz to 240 GHz. In Figure 5.23 the 60 GHz OOK modulated signal is squared using the Mixer-4 block. As a result, baseband and 120 GHz frequency OOK modulated signals are obtained. The frequency domain plot of the output signals is shown in Figure 5.29.

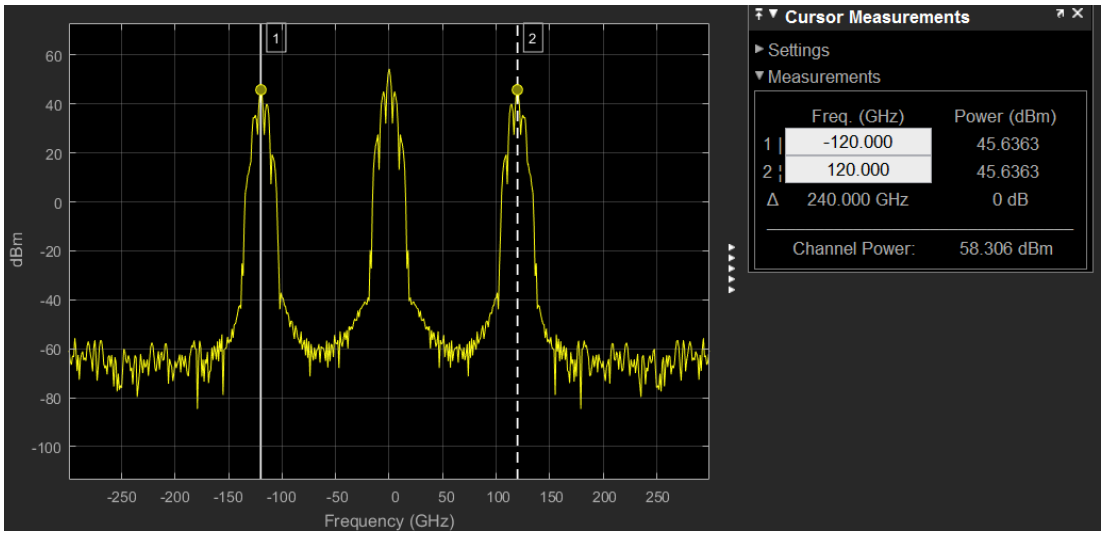

Figure 5.29 Output of Mixer-4 in frequency domain

Amplitude of Mixer-4 block output signal is halved using Attenuator-6 block. Filter-3 block with parameters given in Figure 5.30, is used to obtain only the 120 GHz up-converted OOK modulated signal shown in Figure 5.29 and to negate the effects of other harmonics.

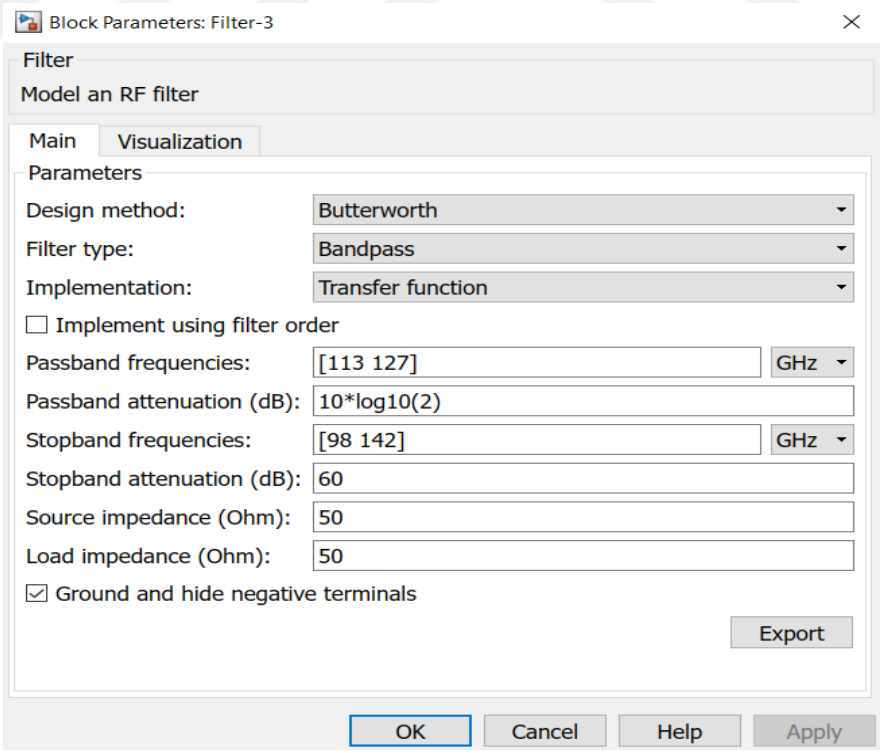

Figure 5.30 Filter-3 block parameters

Filter-3 block is a Butterworth BPF with passband frequencies; 113 GHz, 127 GHz and stopband frequencies; 98 GHz, 42 GHz. OOK modulated signal is successfully up-converted to 120 GHz thanks to filtering. The time and frequency domain plots for Filter-3 block output signal are shown in Figure 5.31 and Figure 5.32.

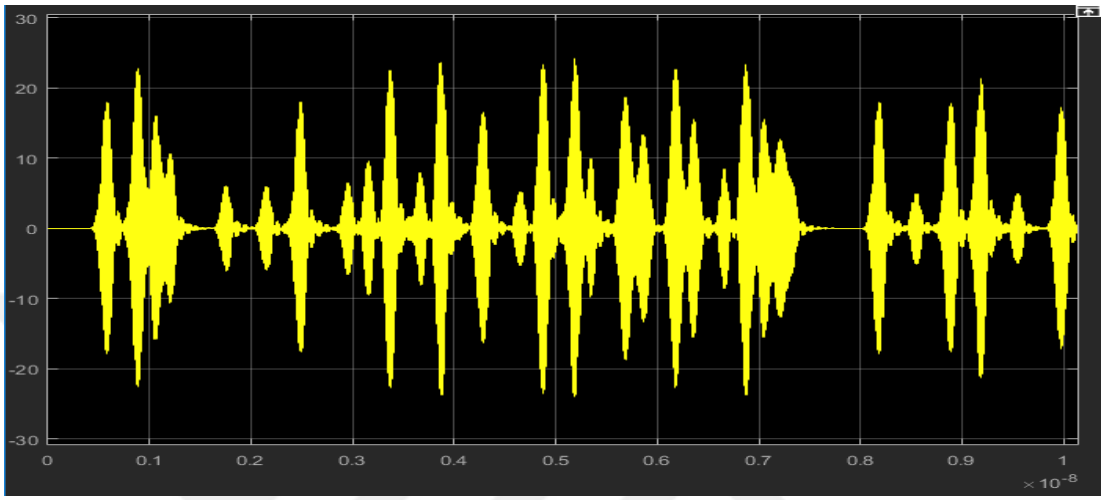

Figure 5.31 120 GHz OOK modulated signal in time domain

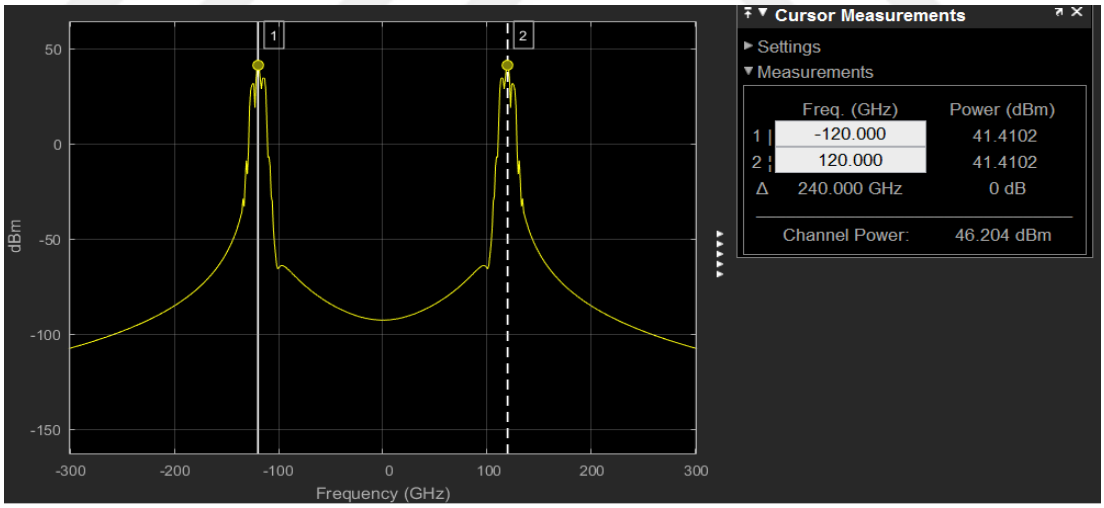

Figure 5.32 120 GHz OOK modulated signal in frequency domain

Likewise, Mixer-5 block is used for squaring 120 GHz OOK modulated signal to obtain baseband and 240 GHz frequency OOK modulated signals. The frequency domain plot of the resulting signals is shown in Figure 5.33.

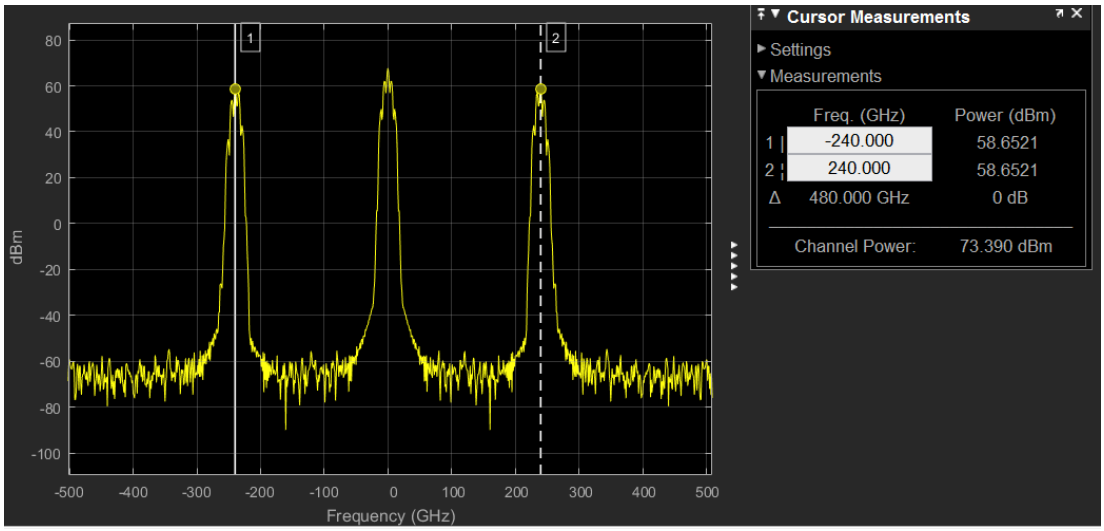

Figure 5.33 Output of Mixer-5 in frequency domain

Amplitude of the Mixer-4 block output signal is halved using Attenuator-7 block with 6 dB attenuation parameter. Filter-4 block with parameters given in Figure 5.34 is used for getting only the 240 GHz up-converted OOK modulated signal.

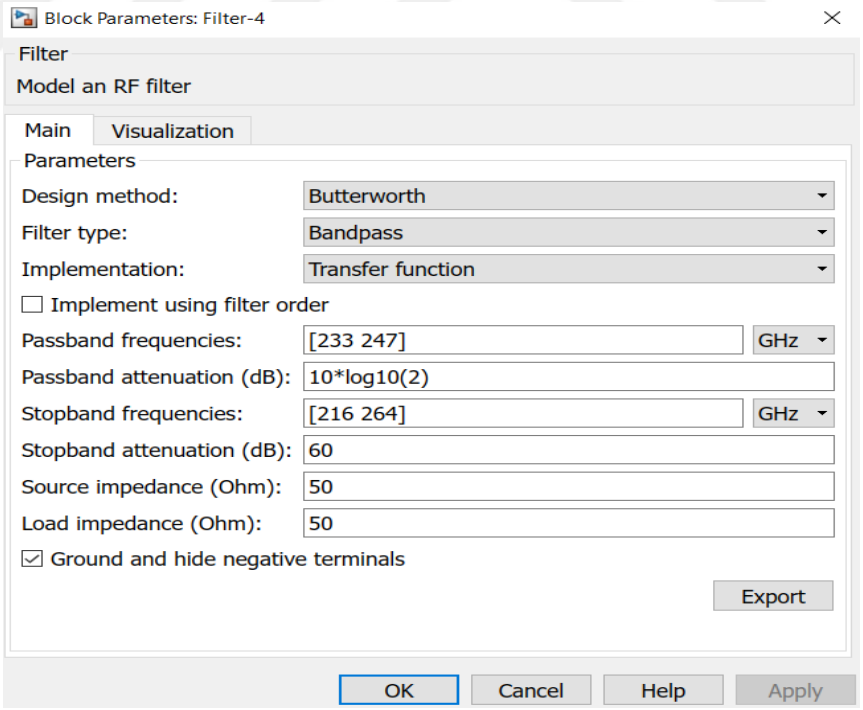

Figure 5.34 Filter-4 block parameters

Filter-4 block is a Butterworth BPF with passband frequencies; 233 GHz, 247 GHz and stopband frequencies; 216 GHz, 264 GHz. OOK modulated signal is successfully up-converted to 240 GHz thanks to filter. The time and frequency domain plots of Filter-4 block output signal are shown in Figure 5.35 and Figure 5.36.

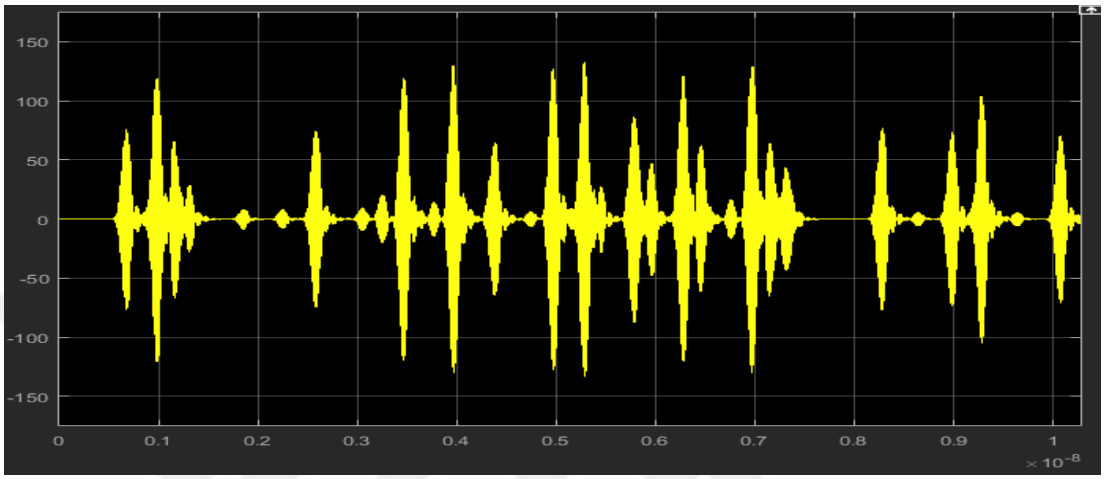

Figure 5.35 240 GHz OOK modulated signal in time domain

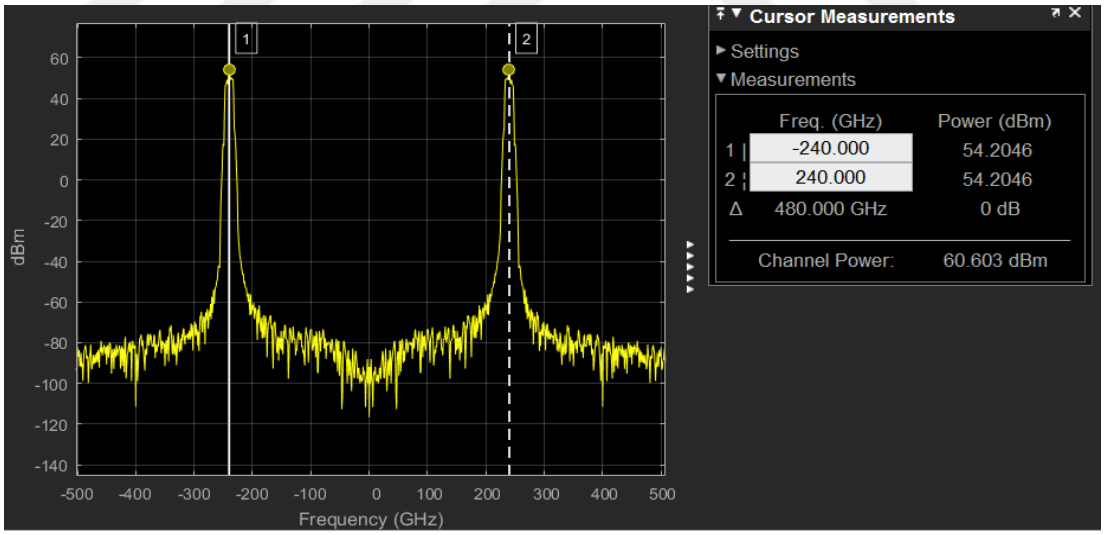

Figure 5.36 240 GHz OOK modulated signal in frequency domain

The 240 GHz OOK modulated signal is attenuated as desired using the Attenuator-8 block. Attenuation is done in simulation study to account for the loss factors of nonlinear Schottky diode based frequency doublers, frequency triplers and mixers that

will be used during the experimental stage. In Figure 5.23 Attenuator-8 block attenuation parameter is set as 10 dB. Finally, the frequency up-converter block designs are completed and 240 GHz up-converted OOK modulated output signal is obtained. The time and frequency domain plots of this signal are shown in Figure 5.37 and Figure 5.38.

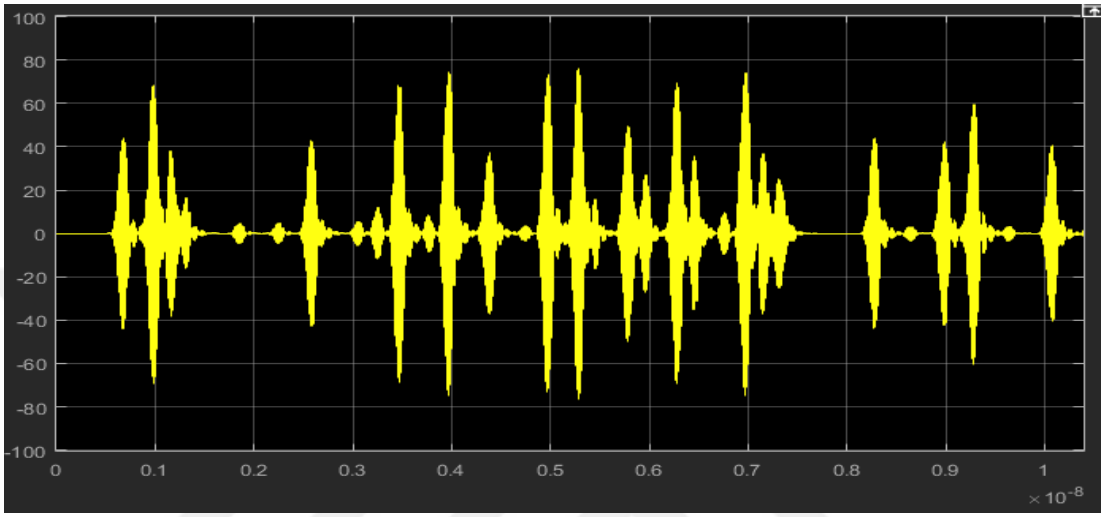

Figure 5.37 Output of Attenuator-8 in time domain

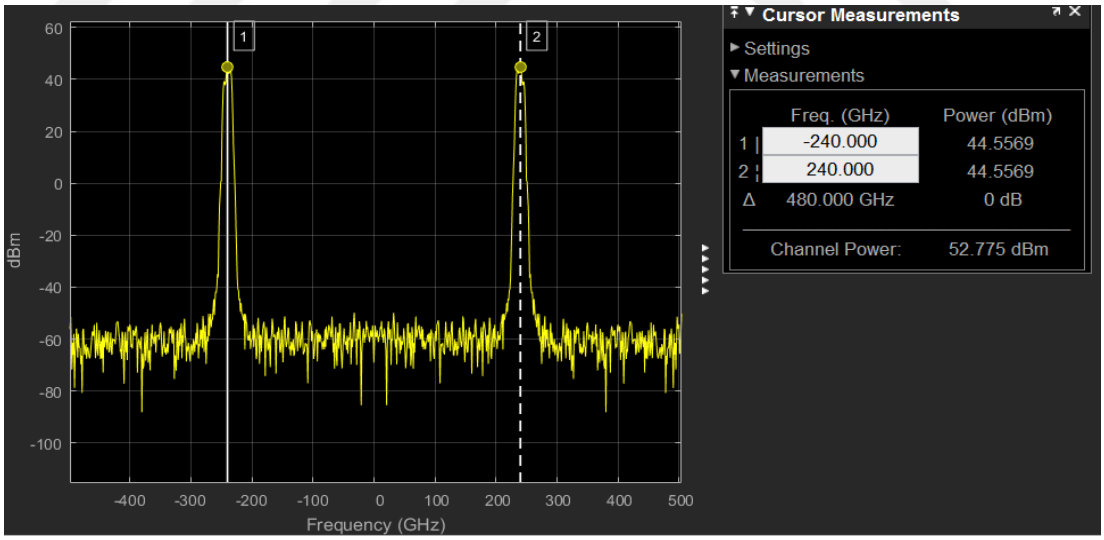

Figure 5.38 Output of Attenuator-8 in frequency domain

5.1.6 Modelling Frequency Down-Converter Blocks

With the modelling of frequency up-converter blocks in Simulink, the transmitter of 240 GHz OOK modulated communication system is complete. In this section, the 240 GHz OOK modulated signal will be down-converted with a frequency down-converter model. Frequency down-conversion will be realized by multiplexing the OOK modulated signal with the generated local oscillator (LO) signal. Finally, the down-converted OOK modulated signal at the output of frequency down-converter block will be demodulated with a non-coherent Envelope Detector demodulator.

Frequency down-converter will be designed using the same Simulink blocks of frequency up-converter. Only the block parameters will be different. Frequency down-converter design will start with generating LO signal necessary for down-converting the 240 GHz OOK modulated signal. Since there are no oscillators with 200 GHz or more frequency output, a relatively small frequency LO signal will be generated and its frequency will be increased to desired band using frequency multiplication method. Accordingly, 3 V peak voltage and 11 GHz frequency LO signal is obtained with the Simulink model given in Figure 5.39.

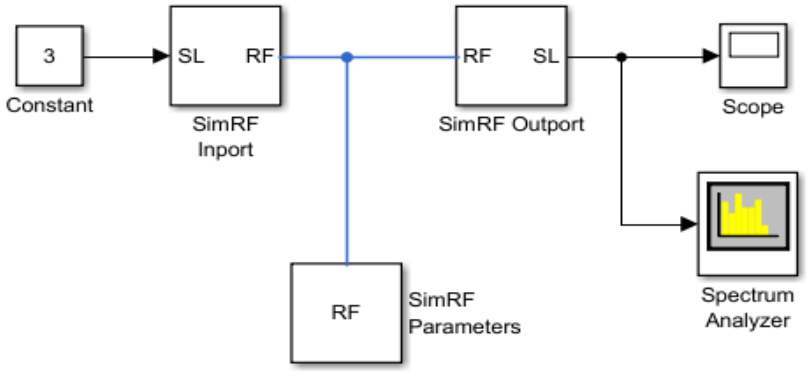

Figure 5.39 Generation of LO signal

The time and frequency domain plots for LO signal are shown in Figure 5.40 and Figure 5.41.

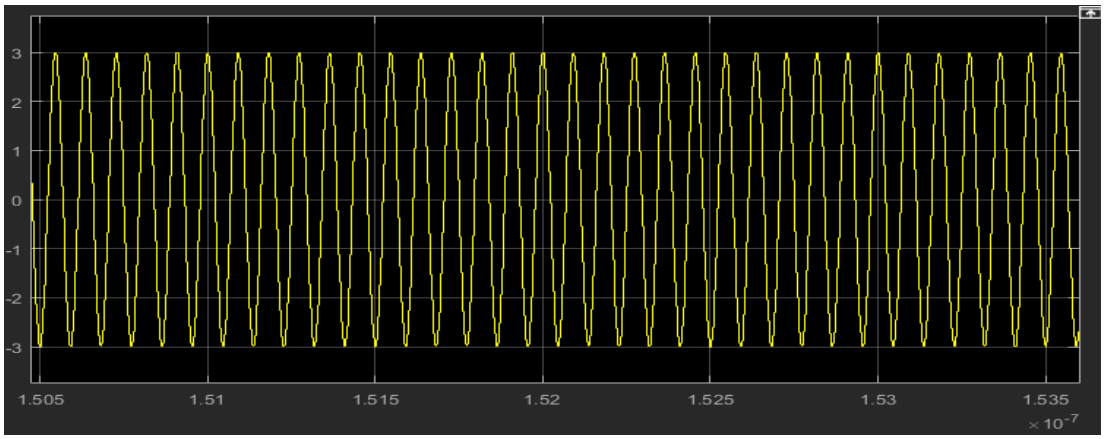

Figure 5.40 11 GHz LO signal in time domain

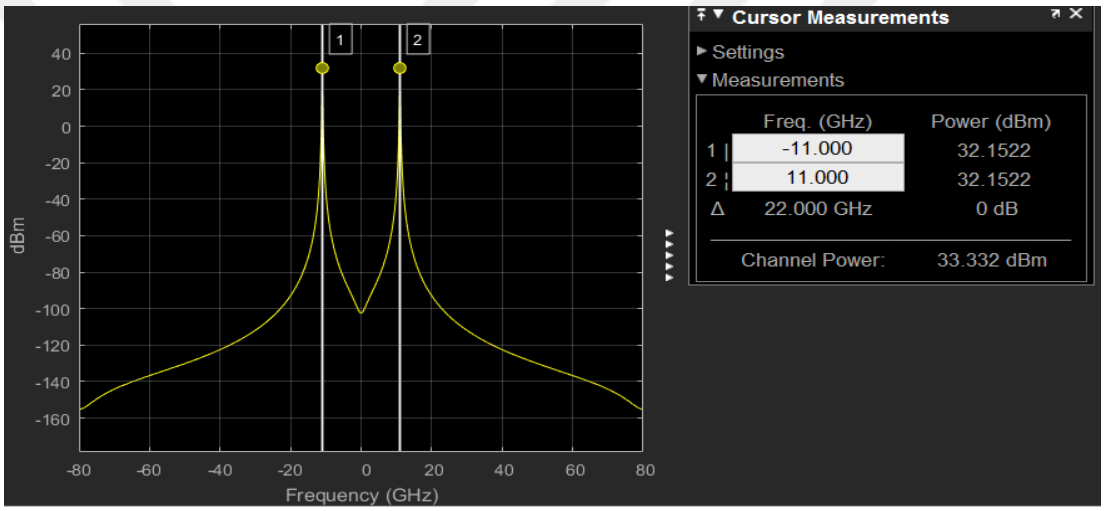

Figure 5.41 11 GHz LO signal in frequency domain

After this step, the LO signal will first be up-converted to 33GHz using frequency tripler. Then, using frequency doublers, it will be up-converted to 66 GHz, 132 GHz and 264 GHz respectively. Figure 5.42 shows the Simulink model with frequency tripler that up-converts LO signal to 33 GHz.

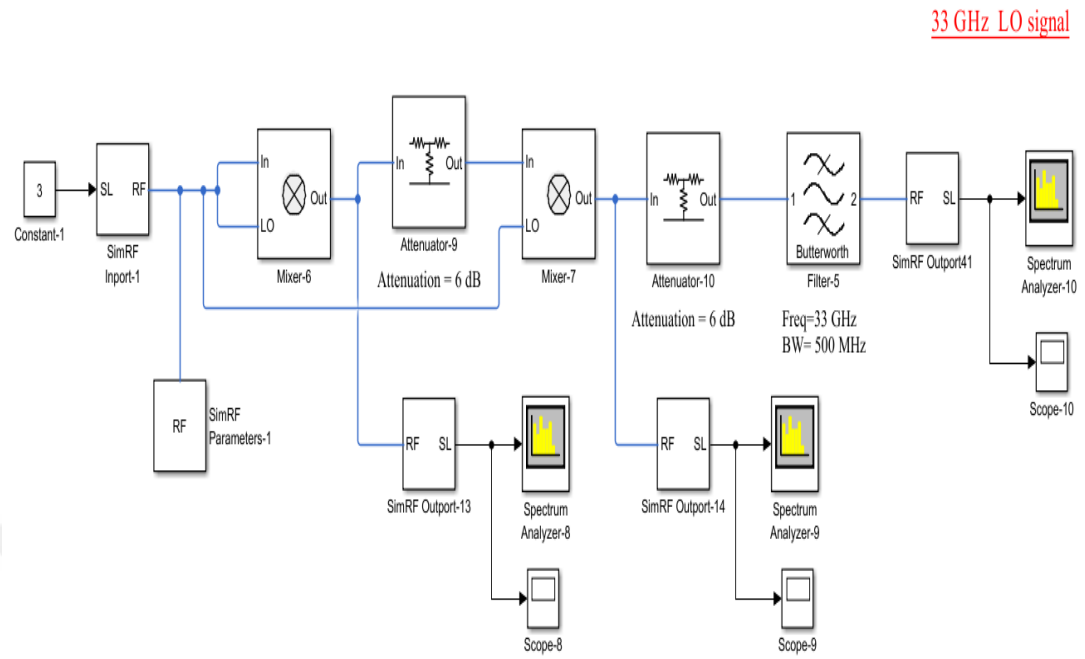

Figure 5.42 Simulink model showing that 33 GHz LO signal is obtained

Observing this model, it can be seen that frequency tripler is modelled using Mixer, Attenuator and Filter blocks are presented in SimRF library. Attenuator blocks, as before, are used for halving the amplitude of Mixer block outputs. That is why, Attenuator-9 and Attenuator-10 blocks have 6 dB Attenuation parameter.

In this model, 22 GHz LO signal is obtained at the output of Mixer-6 block. Then, in Mixer-7 block, 22 GHz LO signal is multiplied with 11 GHz LO signal to obtain 11 GHz and 33 GHz harmonics at the output. The frequency domain plot for Mixer-7 block output is shown in Figure 5.43.

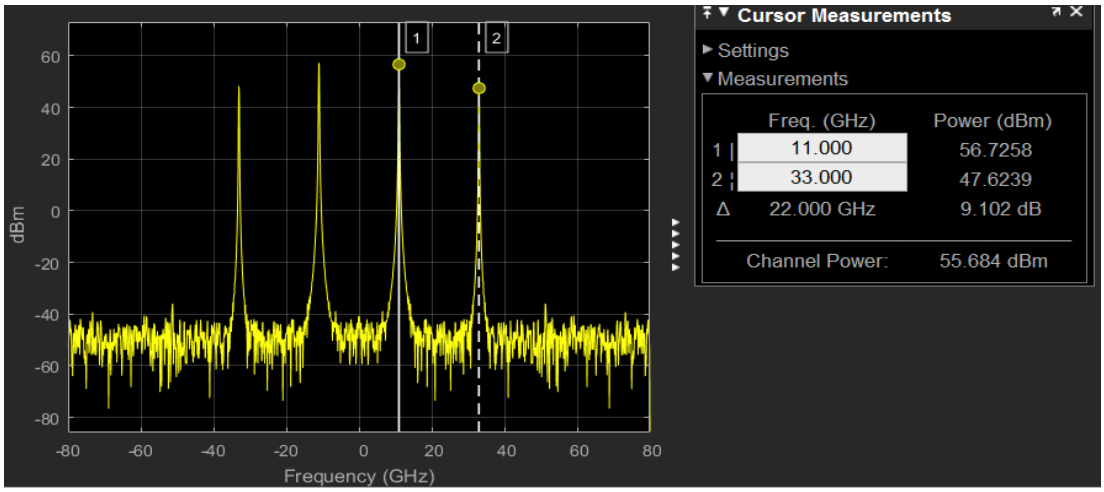

Figure 5.43 Spectrum of Mixer-7 output

Filtering is applied in order to select the desired harmonic among others. Filter-5 block with parameters given in Figure 5.44 is used as filter.

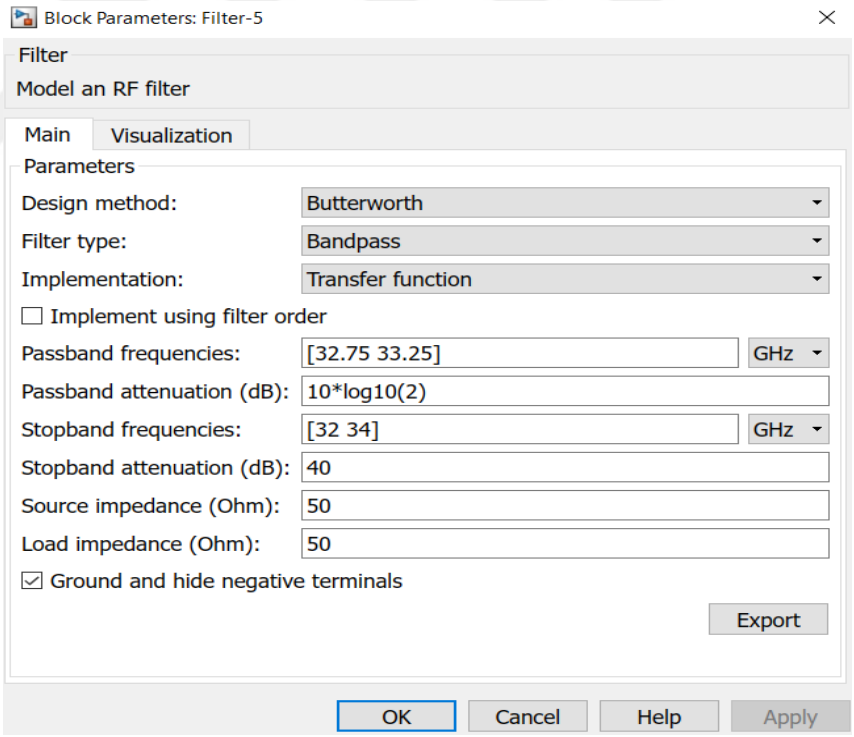

Figure 5.44 Filter-5 block parameters

Filter-5 block is of Butterworth BPF type with passband frequencies; 32.75 GHz, 33.25 GHz and stopband frequencies; 32 GHz, 34 GHz. LO signal is successfully up-

converted to 33 GHz after filtering. The time and frequency domain plots for Filter-5 block output LO signal is shown in Figure 5.45 and Figure 5.46.

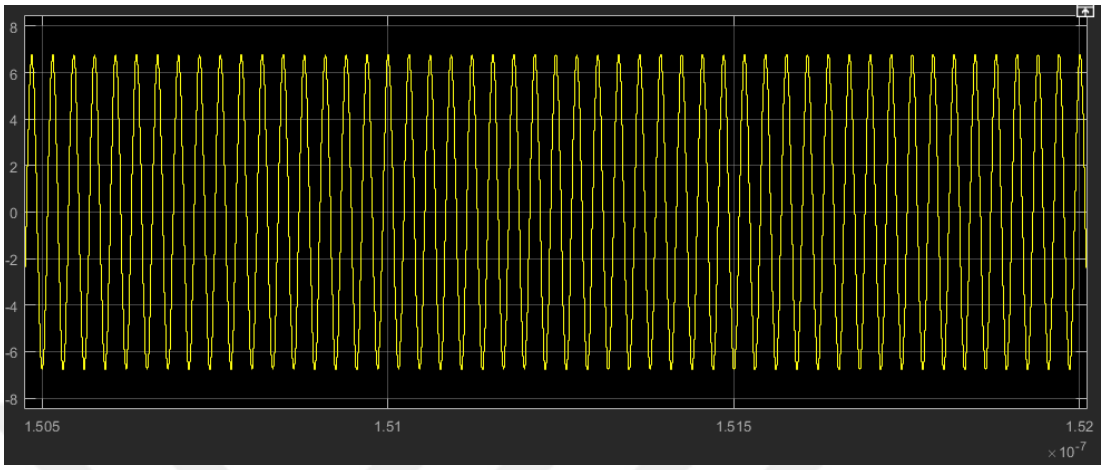

Figure 5.45 33 GHz LO signal in time domain

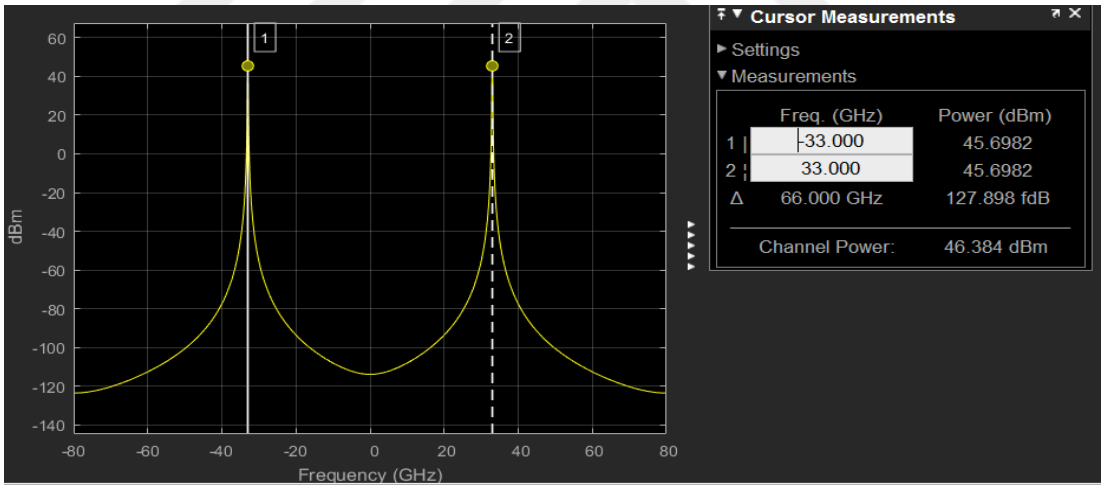

Figure 5. 46 33 GHz LO signal in frequency domain

Using proper frequency doublers and band-pass filters, the 33 GHz LO signal is up-converted to 66 GHz, 132GHz and 264 GHz respectively. For simulating frequency doublers, Mixer block is used. Mixer block input signal is multiplied with itself to obtain double the frequency at the output. Band-pass filter is used for selecting the desired harmonic among others. Figure 5.47 shows the Simulink model for upconverting LO signal to 264 GHz.

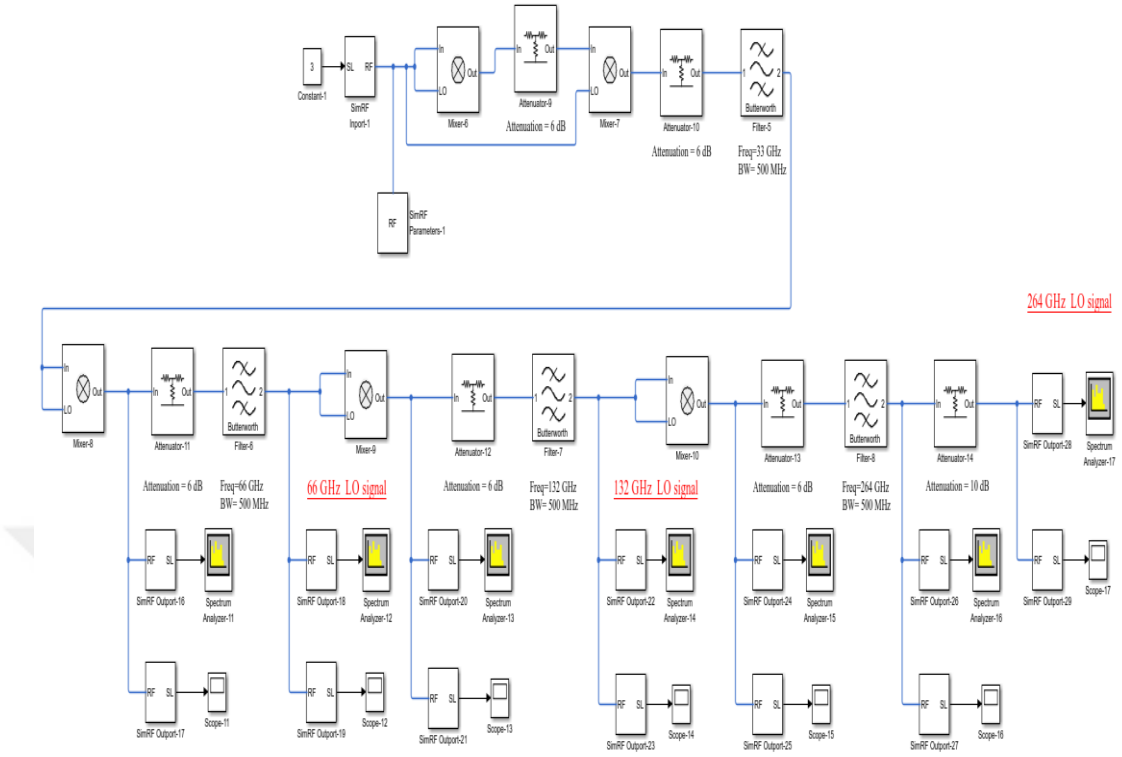

Figure 5.47 Simulink model showing that upconversion from 33 GHz LO signal to 264 GHz LO signal

Observing the modelled system, it can be seen that up-conversion of LO signal from 33 GHz to 264 GHz is realized using the previously designed frequency up-converter blocks. First of all, in the spectrum of Mixer-8 block output, there are two signals; baseband and 66 GHz frequency.

The time and frequency domain plots for Mixer-8 block output are shown in Figure 5.48 and Figure 5.49.

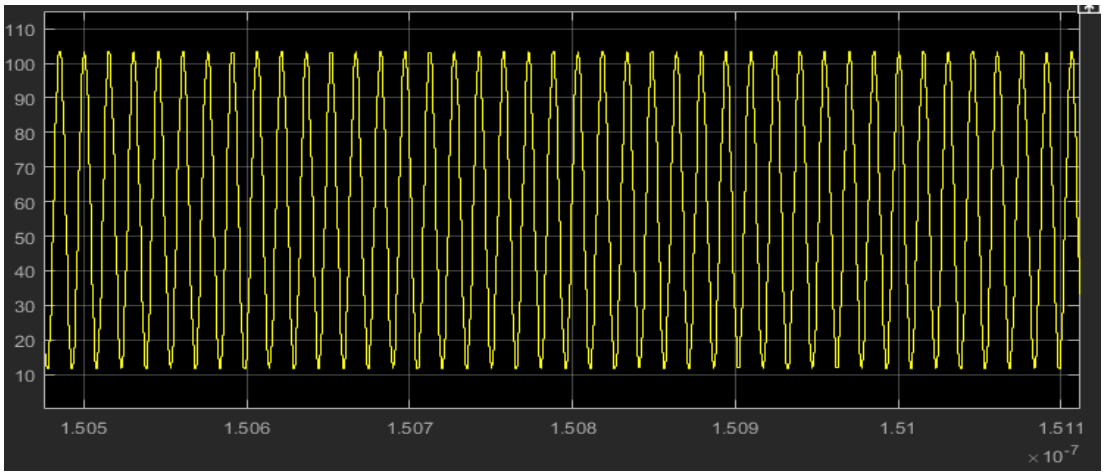

Figure 5.48 Output of Mixer-8 in time domain

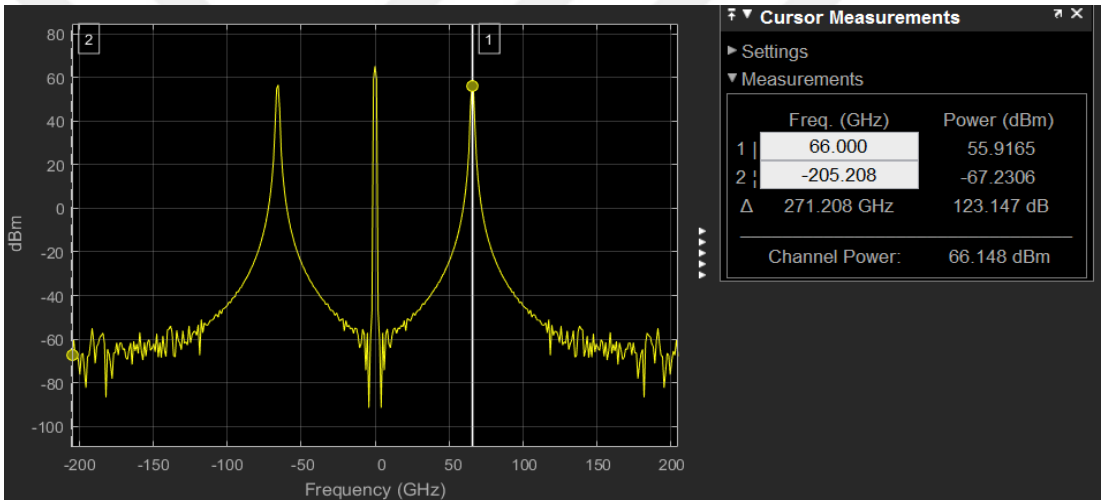

Figure 5.49 Output of Mixer-8 in frequency domain

The amplitude of the Mixer-8 block output signal is halved using Attenuator-11 block with 6 dB attenuation. Filter-6 block with parameters given in Figure 5.50 is used for negating the effects of other harmonics and selecting only 66 GHz signal from the spectrum in Figure 5.49.

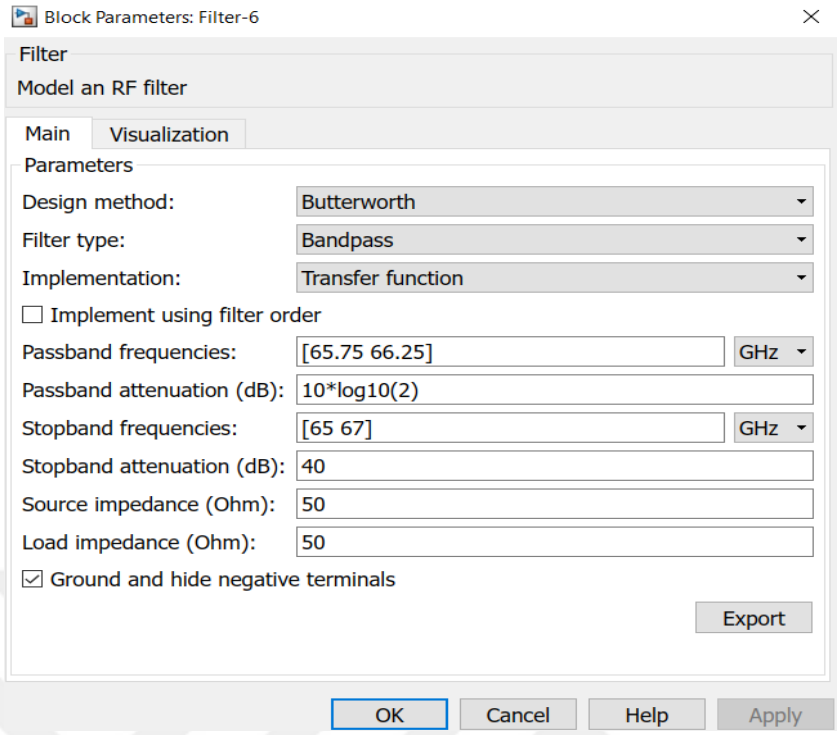

Figure 5.50 Filter-6 block parameters

For Filter-6 block, Butterworth BPF type is selected with passband frequencies; 65.75 GHz, 66.25 GHz and stopband frequencies; 65 GHz, 67 GHz. The LO signal is up-converted to 66 GHz after filtering. The time and frequency domain plots for the Filter-6 block output signal are shown in 5.51 and Figure 5.52.

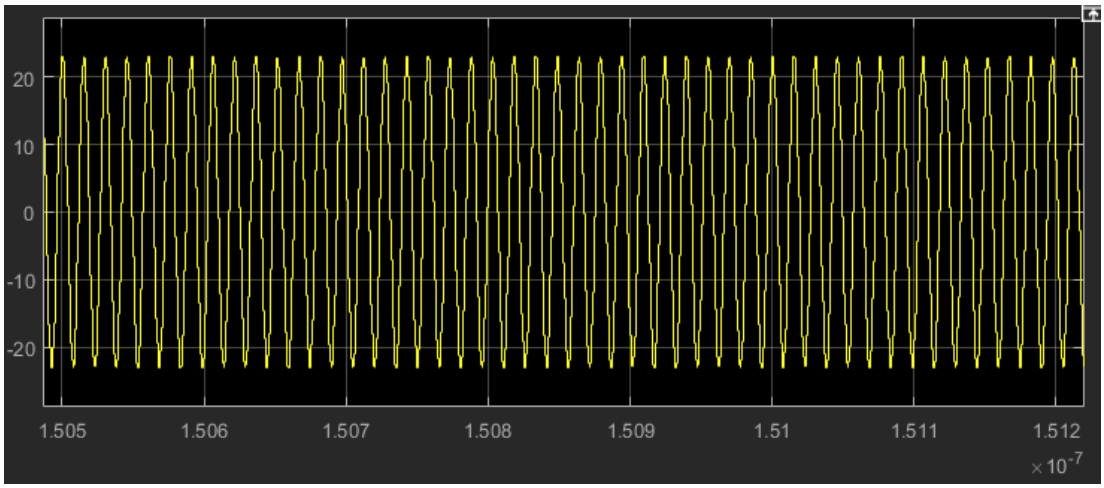

Figure 5.51 66 GHz LO signal in time domain

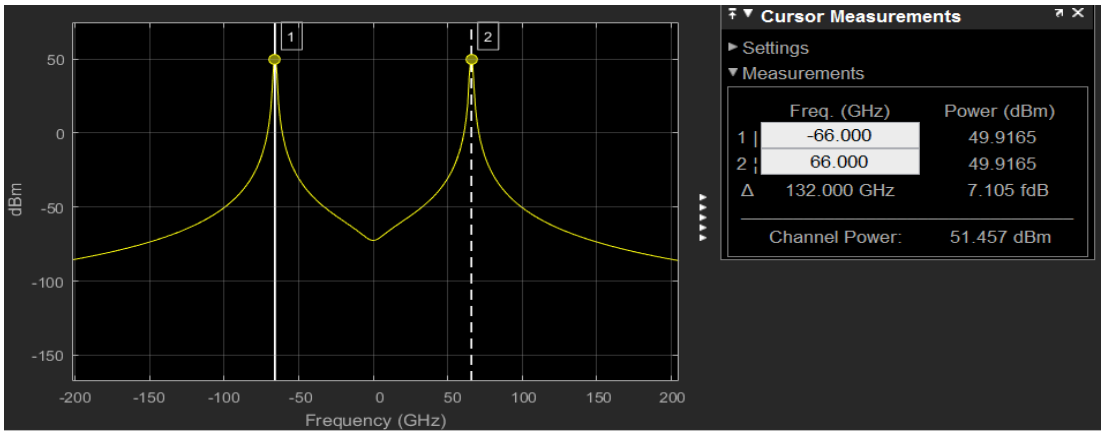

Figure 5.52 66 GHz LO signal in frequency domain

The same steps used in up-converting 33 GHz LO signal into 66GHz are applied for up-conversions from 66 GHz to 132 GHz and from 132 GHz to 264 GHz. Using Mixer-9 block, the 66 GHz LO signal is squared to obtain baseband and 132 GHz output signals. The frequency domain plot for the output signals is given in Figure 5.53.

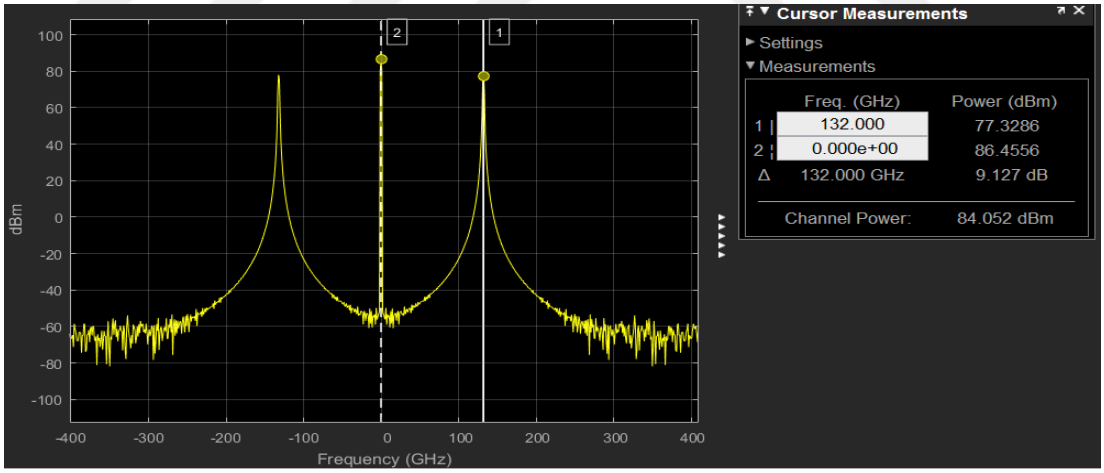

Figure 5.53 Output of Mixer-9 in frequency domain

Amplitude of the Mixer-9 block output signal is halved using Attenuator-12 block with 6 dB attenuation. Filter-7 block with parameters given in Figure 5.54 is used for selecting only the 132 GHz signal from the spectrum in Figure 5.53.

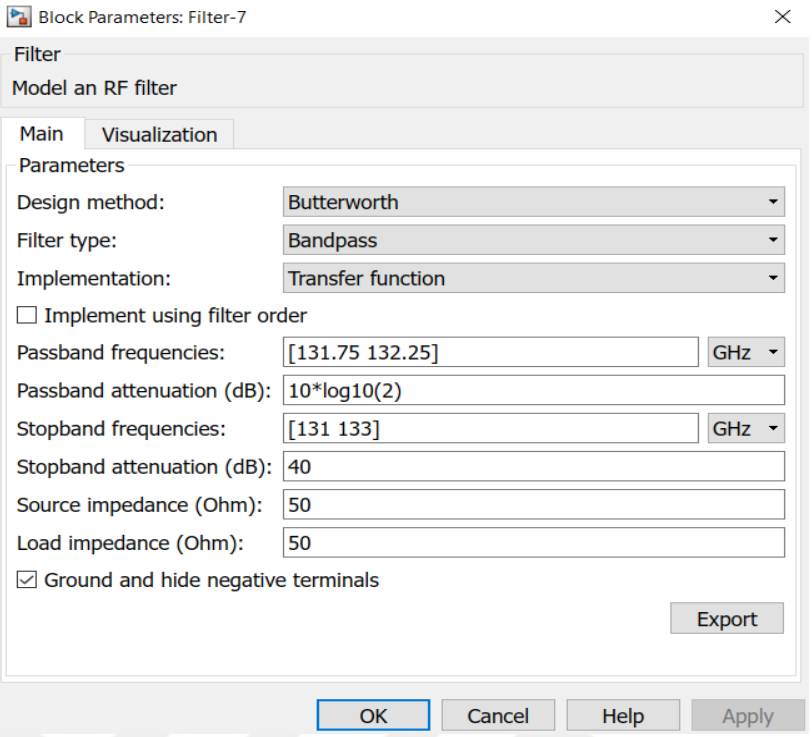

Figure 5.54 Filter-7 block parameters

Filter-7 block is of Butterworth BPF type with passband frequencies; 131.75 GHz, 132.25 GHz and stopband frequencies; 131 GHz, 133 GHz. LO signal is up-converted to 132 GHz after filtering. The time and frequency domain plots for the Filter-7 block output signal are given in Figure 5.55 and Figure 5.56.

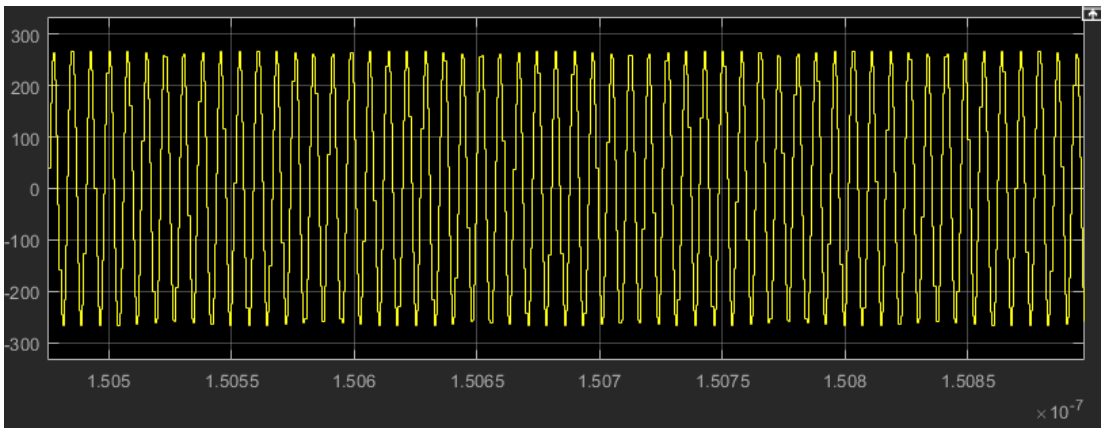

Figure 5.55 132 GHz LO signal in time domain

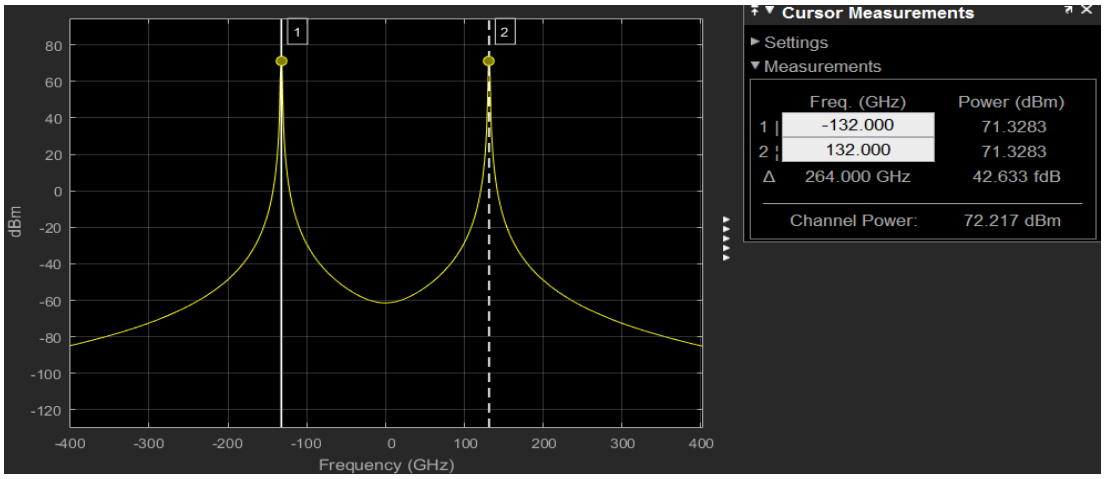

Figure 5.56 132 GHz LO signal in frequency domain

Finally, using Mixer-10 block, 132 GHz LO signal is squared to obtain baseband and 264 GHz frequency signals. The frequency domain plot for the signal is given in Figure 5.57.

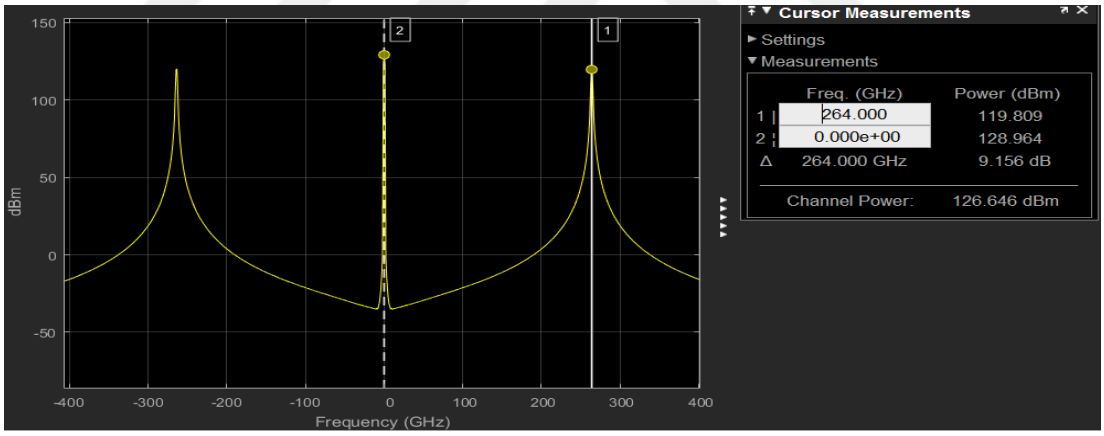

Figure 5.57 Output of Mixer-10 in frequency domain

The amplitude of the Mixer-10 block output signal is halved using Attenuator-13 block with 6 dB attenuation. Filter-8 block with parameters given in Figure-5.58 is used for selecting only the 264 GHz signal from the spectrum in Figure 5.57.

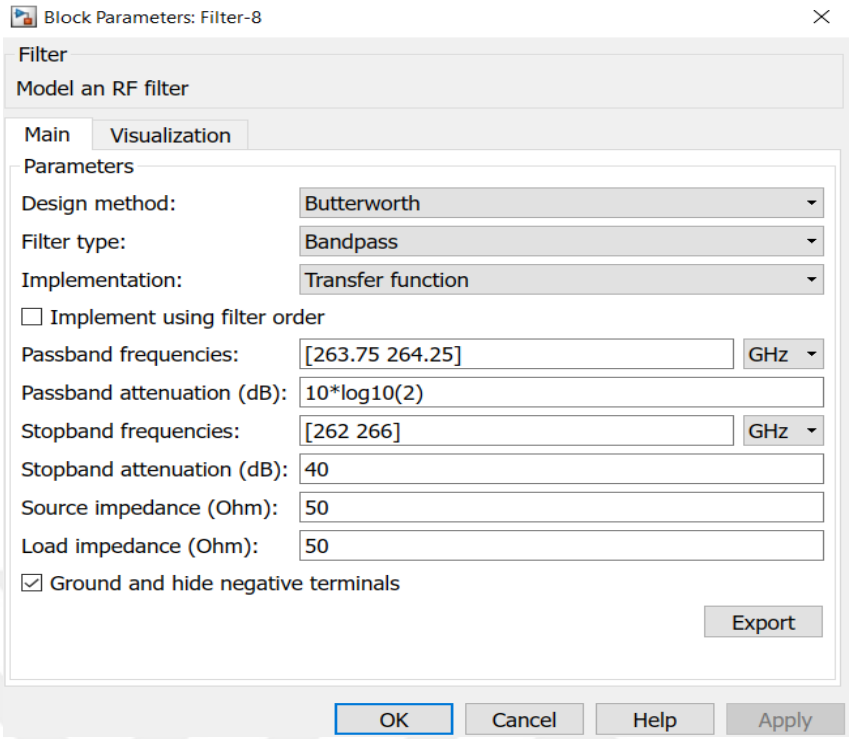

Figure 5.58 Filter-8 block parameters

Filter-8 block filter is of Butterworth BPF type with passband frequencies; 263.75 GHz, 264.25 GHz and stopband frequencies; 262 GHz, 266 GHz. The LO signal is up-converted to 264 GHz after filtering. The time and frequency domain plots for the Filter-8 block output signal are shown in Figure 5.59 and Figure 5.60 respectively.

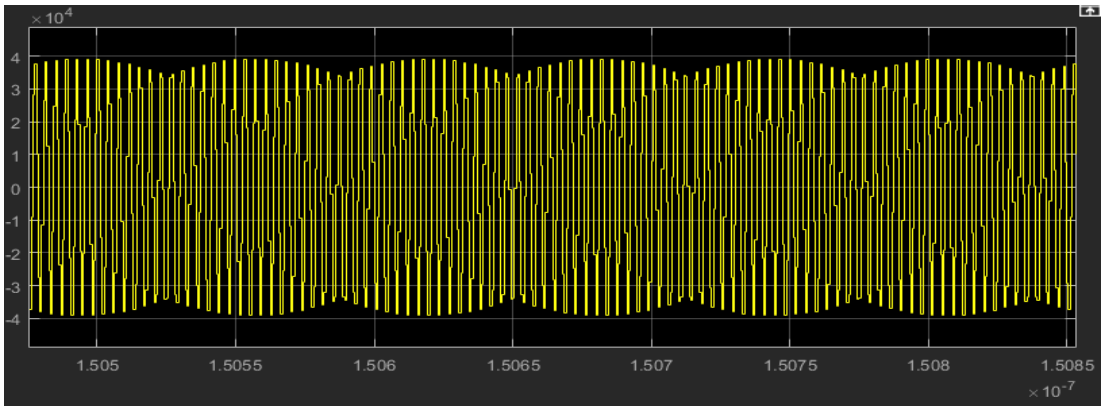

Figure 5.59 264 GHz LO signal in time domain

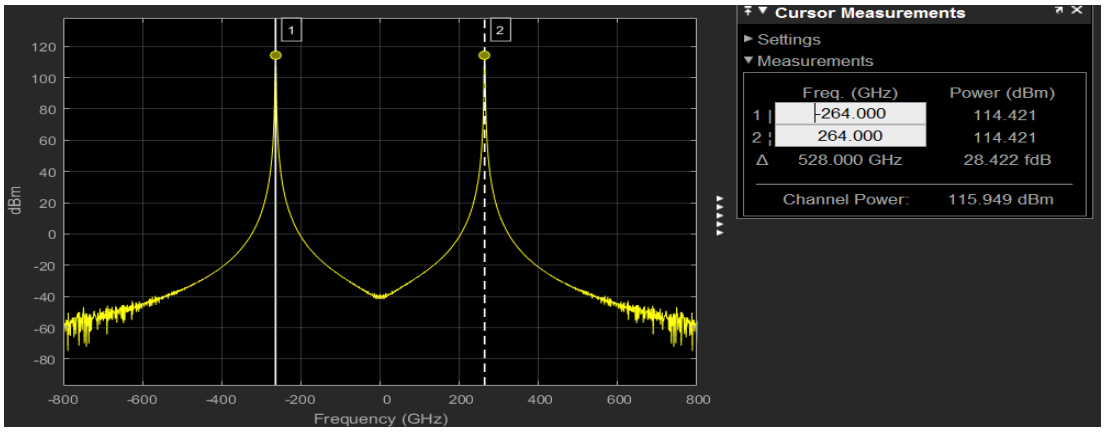

Figure 5.60 264 GHz LO signal in frequency domain

The amplitude of the 264 GHz LO signal is attenuated using Attenuator-14 block. Attenuation is done in order to simulate and model the loss effects of nonlinear Schottky diode based frequency doublers, frequency triplers and mixers that will be used during the experimental process. Attenuation parameter is set as 10 dB for the Attenuator-14 block. The frequency domain plot representation of LO signal at the output of Attenuator-14 block is shown in Figure 5.61.

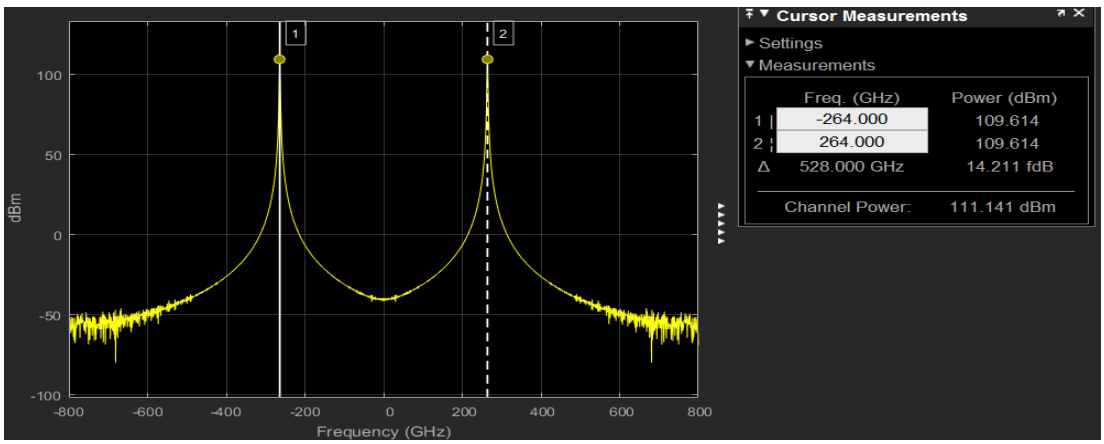

Figure 5.61 Output of Attenuator-14 in frequency domain

Modelling of frequency down-converter blocks will be completed after the 264 GHz LO signal is multiplied with the 240GHz OOK modulated signal obtained in section 5.1.5. Figure 5.62 shows the Simulink model for frequency down-converter blocks.

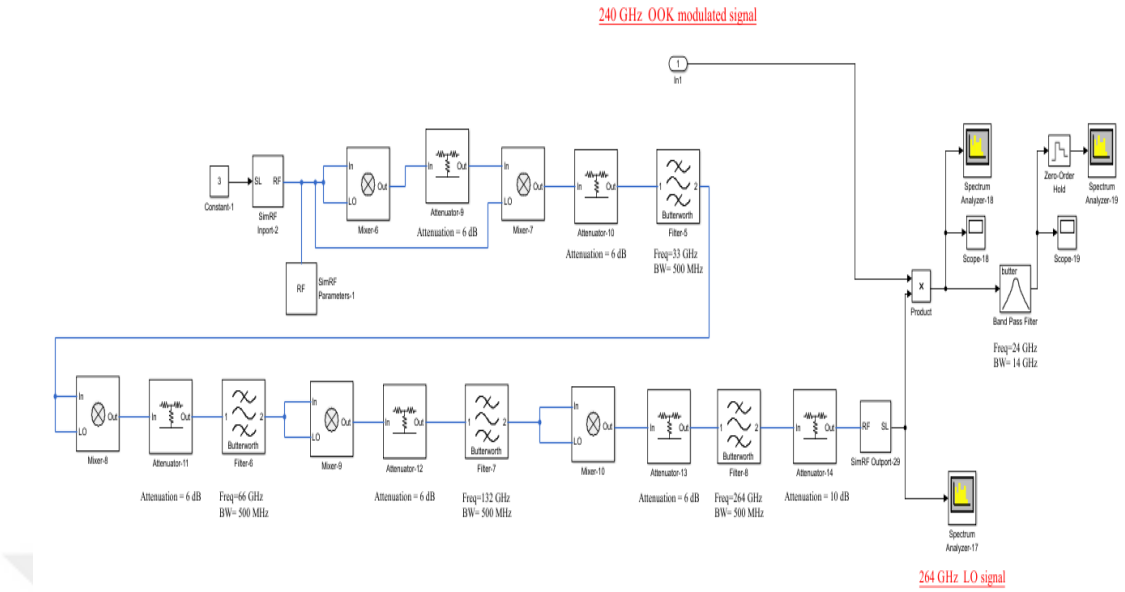

Figure 5.62 Design of frequency downconversion blocks

In this Simulink model, the Product and Analog Filter Design blocks are used for modelling the Schottky based subharmonic mixer structure. The down-converted signal is obtained at the output of Analog Filter Design block with the parameters given in Figure 5.63.

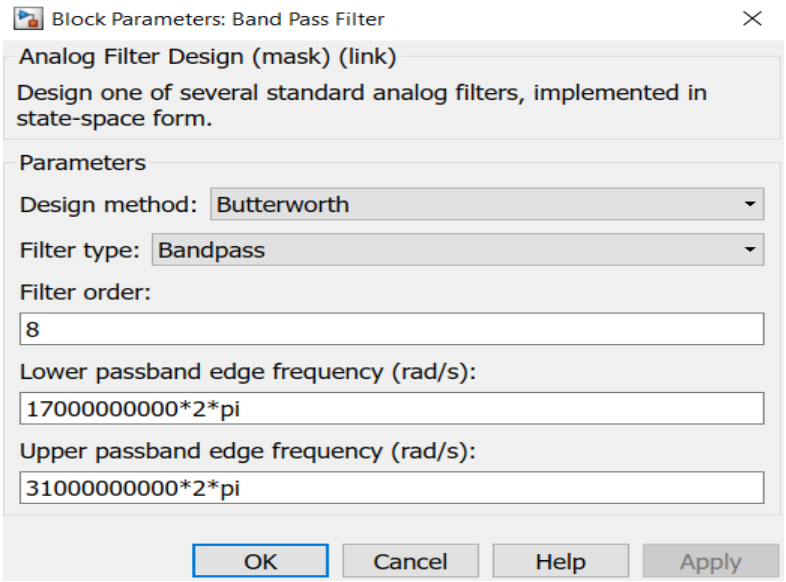

Figure 5.63 Analog Filter Design block parameters

Analog Filter Design block is of Butterworth BPF type with center frequency of 24 GHz, cut-off frequencies; 17 GHz, 31 GHz. The time and frequency domain plots for the OOK modulated signal at the output of frequency down-converter are shown in Figure 5.64 and Figure 5.65.

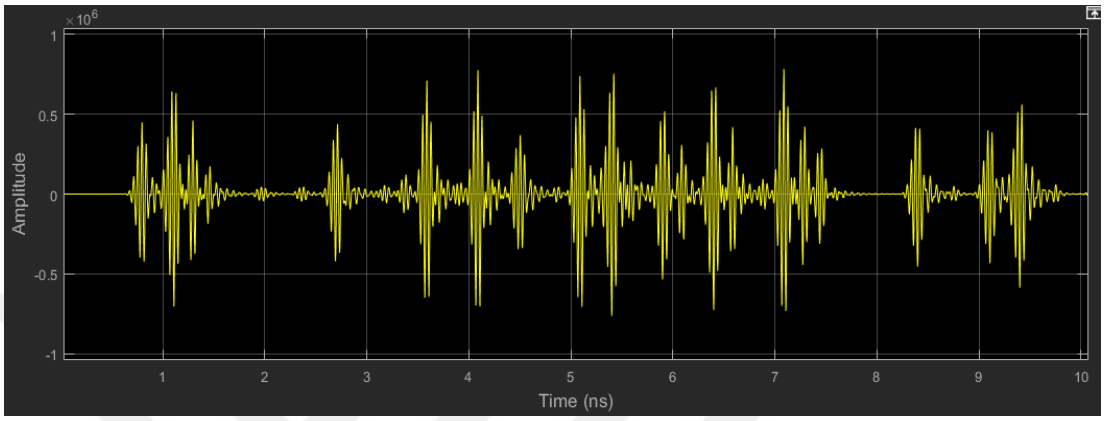

Figure 5.64 Output signal of frequency downconversion blocks in time domain

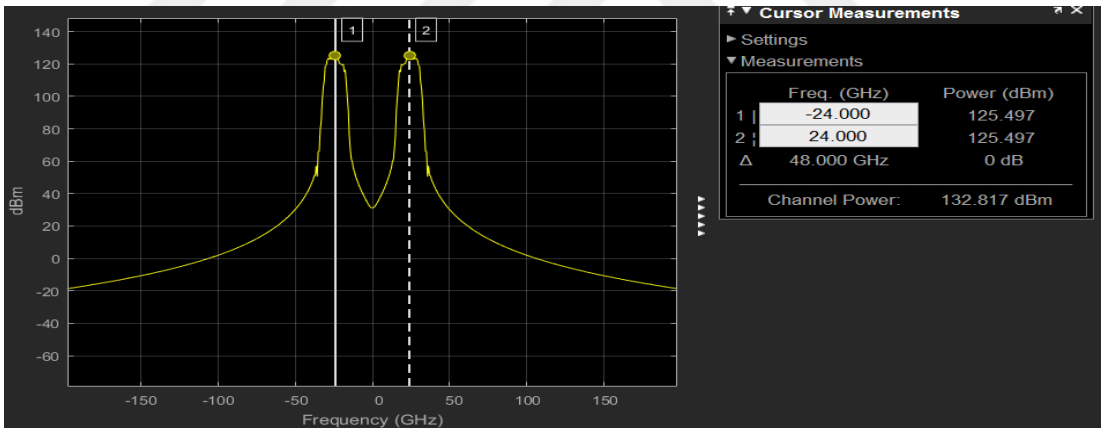

Figure 5.65 Output signal of frequency downconversion blocks in frequency domain

The design and modelling of frequency down-conversion blocks are completed after obtaining the frequency down-converted signal. The design of transmitter/receiver for 240 GHz communication system with OOK modulation will be completed after the OOK demodulator is modelled for demodulation process. Figure 5.66 shows the Simulink model of the OOK transmitter and receiver structures for high data rate communication systems at 240 GHz.

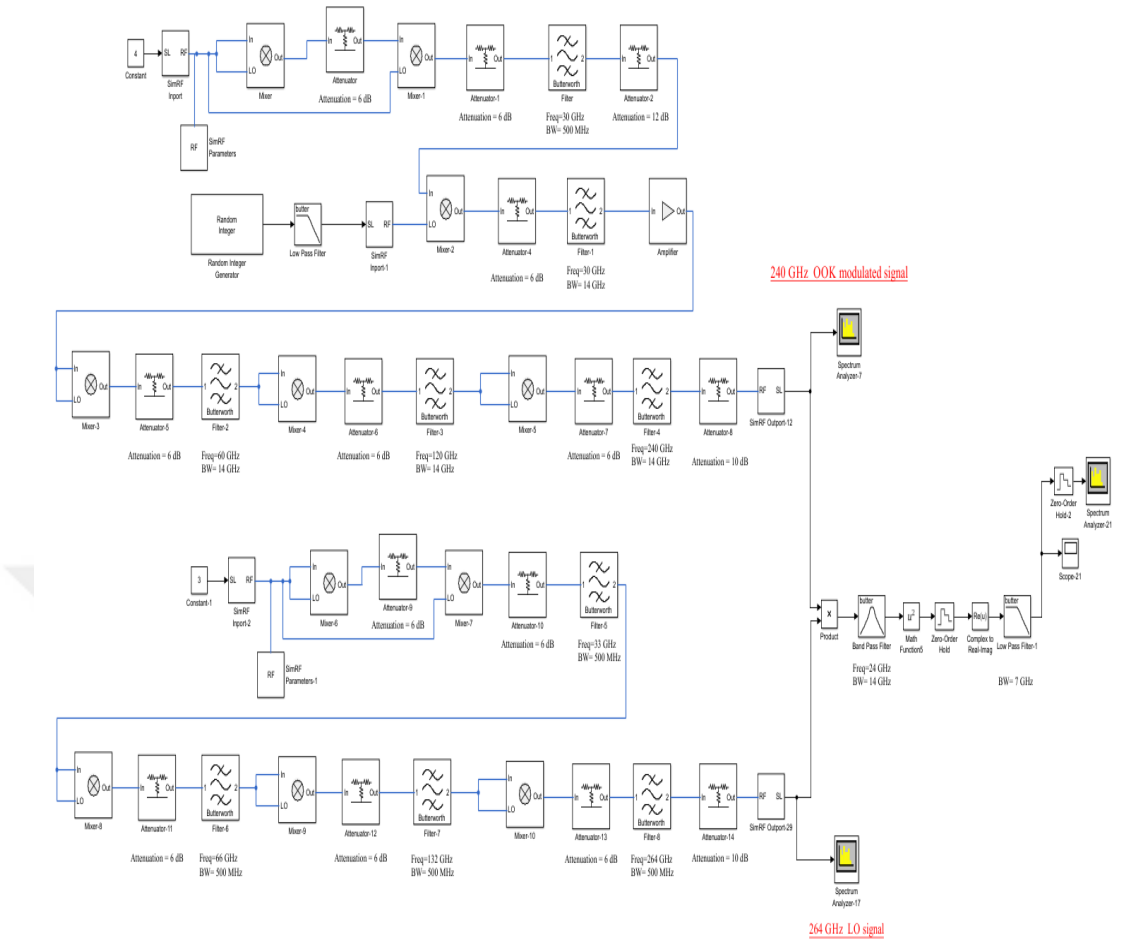

Figure 5.66 Design of OOK transmitter and receiver structures for high data rate communication systems at 240 GHz

OOK demodulation is accomplished using an Envelope detector. Therefore, the OOK modulated 24 GHz down-converted signal is passed through the rectifier and LPF. The Math Function block with square operation in Simulink is used as Rectifier and the output is sent to Analog Filter Design-1 block with parameters given in Figure 5.67. Analog Filter Design-1 block is of Butterworth LPF type with cut-off frequency of 7 GHz. The time and frequency domain plots for LPF output signal are shown in Figure 5.68 and Figure 5.69.

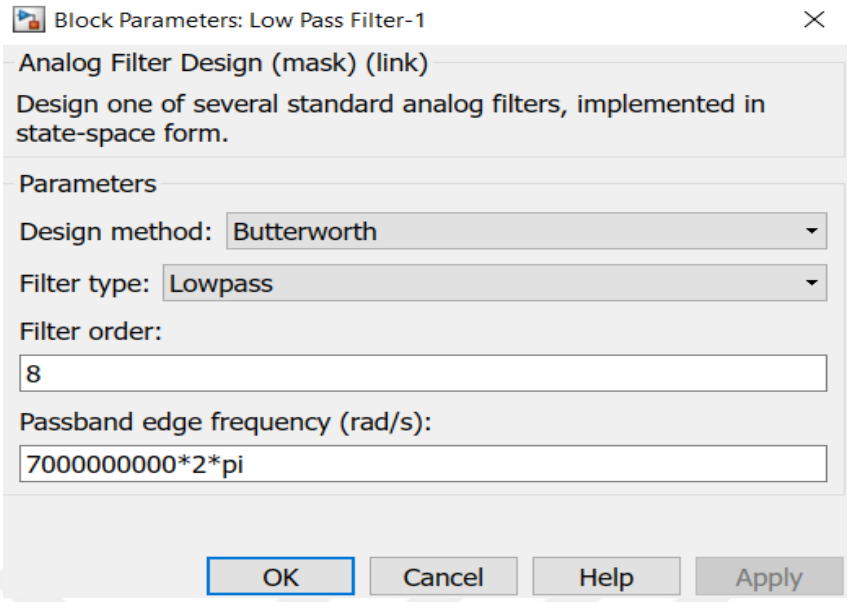

Figure 5.67 Analog Filter Design-1 block parameters

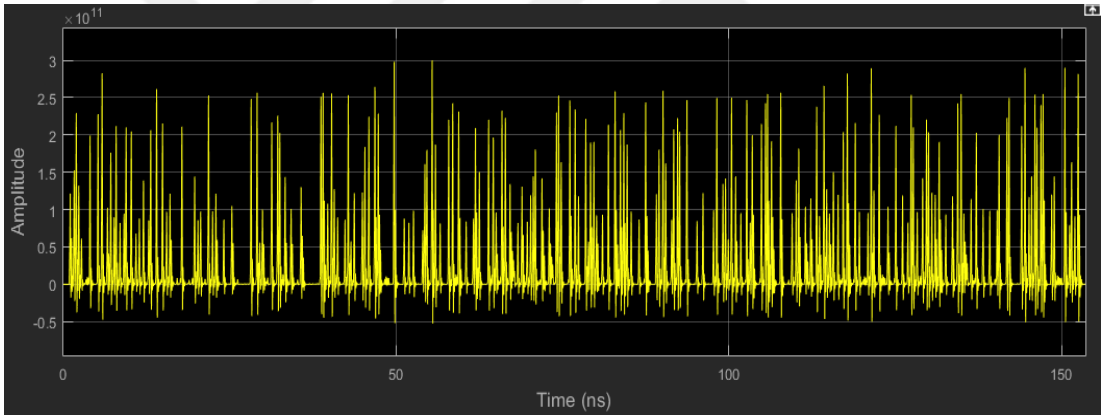

Figure 5.68 Output of Analog Filter Design-1 block in time domain

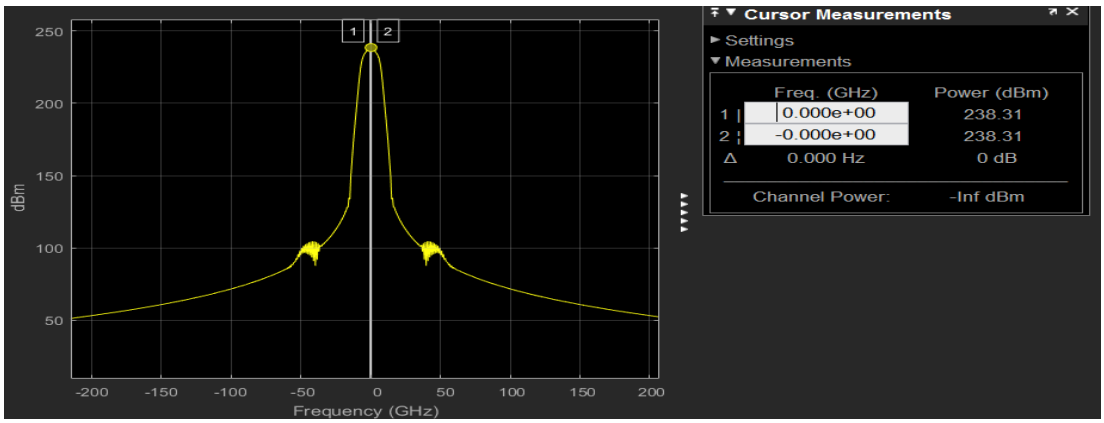

Figure 5.69 Output of Analog Filter Design-1 block in frequency domain

It can be observed that the transmitted data signal can be recovered utilizing proper decision maker circuit at the output of LPF.

5.2 Modelling and Design of BPSK and QPSK Communication Transmitter/Receiver System

In this section, the system implemented by OOK modulation is implemented using BPSK modulation. Figure 5.70 shows the transmitter and receiver model created in Simulink for BPSK modulation.

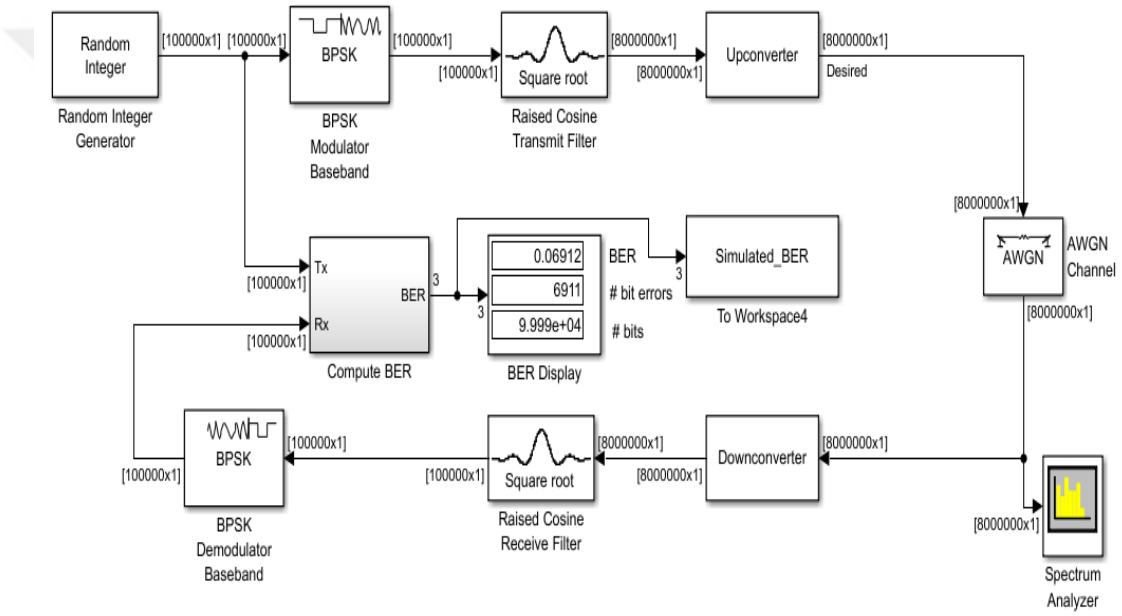

Figure 5.70 Simulink model of BPSK transmitter and receiver structures for high data rate communication systems at different frequencies.

Here, unlike the model created in Simulink for OOK modulation, Raised Cosine Transmit Filter, Raised Cosine Receive Filter, AWGN and Error Rate Calculation blocks are used. Raised cosine transmit filter block is used to upsample and filter the input signal using a normal or square root raised cosine FIR filter, whereas raised cosine receive filter is used to downsample and filter the input signal, using a normal or square root raised cosine FIR filter [1]. By using error rate calculation block received data is compared with the transmitted data and is calculated error rate of the

received data. The block output gives the error rate, the number of detected errors and the total number of symbols compared. The AWGN channel block parameters used for AWGN channel structure are shown in Figure 5.71.

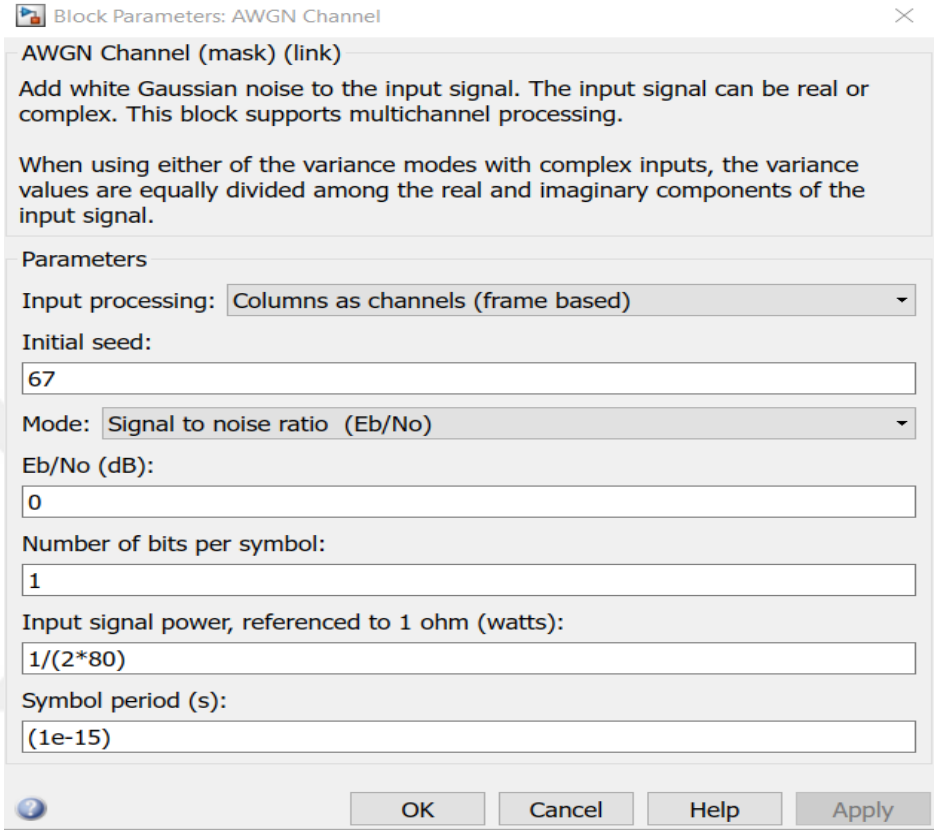

Figure 5.71 AWGN channel block parameters

Simulink model shown in Figure 5.70, firstly, data signal with 1 gbps is produced and is modulated using the binary phase shift keying method in the BPSK modulator block. At the next step, BPSK modulated signal is upconverted with different LO signals generated and upconverted signal is passed through AWGN channel. At the receiver part, received signal is downconverted using LO signal having the same frequency as the LO signal used on the transmitter side and demodulation process is fulfilled. Finally, computation of error rate of the received data is done using error rate calculation block within the compute BER subsystem. BER graph of the system obtained as a result of performance analysis is shown in Figure 5.72.

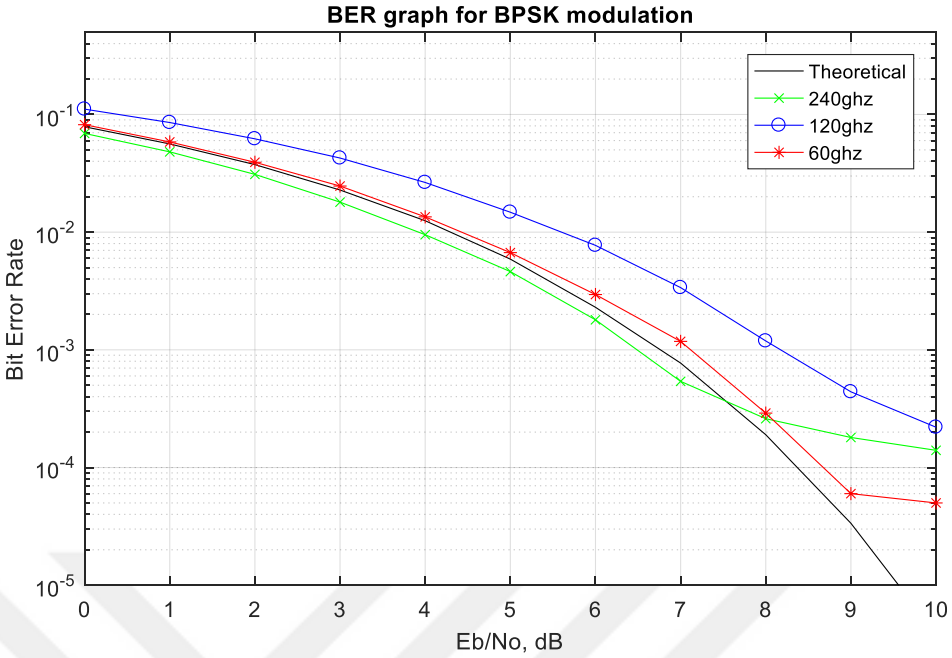

Figure 5.72 Comparison of simulated and theoretical BPSK BER

BER performance analysis for BPSK modulation in four different schemes. These are

- Theoretical BPSK BER analysis at baseband.
- Simulated BPSK Modulation BER analysis at 60 GHz.
- Simulated BPSK Modulation BER analysis at 120 GHz.
- Simulated BPSK Modulation BER analysis at 240 GHz.

In the Simulink model, frequency of LO signal increases, the symbol period parameter of AWGN channel block decreases. Because of this, symbol period of AWGN channel block is determined by trial and error method. Therefore, although the same BER curve as the theoretical curve given in the graph is expected approximately, different BER curves for simulation in different frequency bands of 60 GHz, 120 GHz, and 240 GHz respectively, are observed.

Modelling of QPSK transmitter and receiver structures for communication systems with high data rate in Simulink can only be performed by modifying the BPSK modulator and the BPSK demodulator blocks in Simulink model given in Figure 5.70 with the QPSK modulator and QPSK demodulator blocks as shown in Figure 5.73.

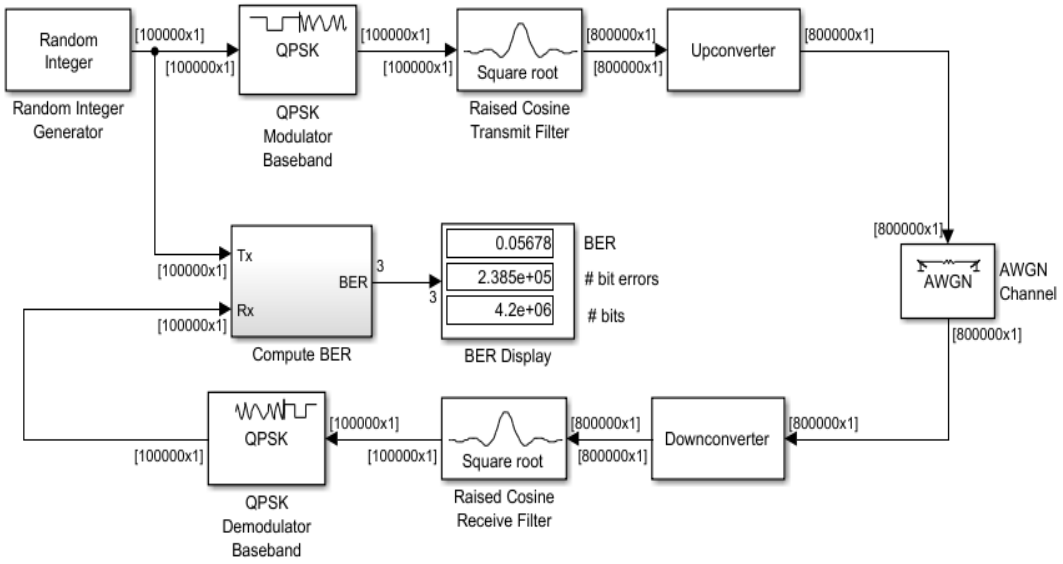

Figure 5.73 Simulink model of QPSK transmitter and receiver structures for high data rate communication systems at 240 GHz.

CHAPTER 6

CONCLUSIONS AND FUTURE WORKS

In this thesis, transmitter and receiver structures for high data rate communication systems at 240 GHz are developed and performance analysis for different modulation techniques are performed in Simulink. To perform this, firstly THz frequency bands and THz communication systems have been investigated. The Schottky diode technology expected to offer a solution for THz applications due to improving efficiency and reliability, and Schottky diode based components such as frequency doubler, frequency tripler and subharmonic mixer have been studied. By using these components, frequency up-converter and frequency down-converter structures have been designed on the basis of frequency multiplication method for THz communication systems and the performance analysis has been performed to achieve the system with bit error rates that are theoretically available. Rather than producing high frequency signals directly with oscillators, generating low frequency signals and carrying signals into the desired frequency band with Schottky diode based frequency multipliers provides significant advantages in terms of lower noise and power consumption. In addition to this, nonlinear effects and losses of Schottky diode based components were tried to take into account, during modelling THz communication systems. By using different modulation techniques, data transmission with high data rates ranging from 1 to 10 gbps has been carried out and results of performance analysis have been obtained in Simulink. The time and frequency domain analysis of Simulink models have been made in theory.

Simulink is quite useful to reuse of model designed in different application and this property provides an important advantage. However, the durations of simulation and adjusting sample time, especially in RF models prevent the simulation from being efficient. Therefore, perform the model simulation in Matlab can be suggested to improve the present model.

Simulink models presented in this thesis, will lead to the experimental implementation of THz communication systems. To extend the study,

- LDPC encoder and decoder,
- MIMO-OFDM wireless communication systems,
- Block coding such as Alamouti codings,
- Fading channels, such as Rayleigh and Ricean,

can be added to Simulink models.

REFERENCES

[1] Wang, J., Venkatesha Prasad, R., Niemegeers, I., "*Analyzing 60 GHz radio links for indoor communications*", IEEE Transactions on Consumer Electronics, vol.55, no.4, pp.1832-1840, November 2009.

[2] Zhang, H., Wang, J., Lu, T., Gulliver, T. A., *"Capacity of 60 GHz wireless communication systems over Ricean fading channels"*, 2011 IEEE Pacific Rim Conference on Communications, Computers and Signal Processing (PacRim), pp. 437-440, Aug. 2011.

[3] Jie, D., Wang, J., Zhang, H., Wang, G., *"Channel Capacity of 60 GHz Wireless Communication Systems over Indoor Line-of-Sight and Non-Line-of-Sight Channels"*, 2010 6th International Conference on Wireless Communications Networking and Mobile Computing (WiCOM), pp.1-4, Sept. 2010.

[4] Marinkovic, M., Piz, M., Choi, C., Panic, G., Ehrig, M., Grass, E., *"Performance evaluation of channel coding for Gbps 60-GHz OFDM-based wireless communications"*, 2010 IEEE 21st International Symposium on Personal Indoor and Mobile Radio Communications (PIMRC), pp.994-998, Sept. 2010.

[5] Daniels, R.C., Heath, R.W., *"60 GHz wireless communications: emerging requirements and design recommendations"*, IEEE Vehicular Technology Magazine, vol.2, no.3, pp.41-50, Sept. 2007.

[6] Park, C., Rappaport, T. S., *"Short-Range Wireless Communications for Next-Generation Networks: UWB, 60 GHz Millimeter-Wave WPAN, And ZigBee"*, Wireless Communications, IEEE , vol.14, no.4, pp.70,78, August 2007.

[7] Maltsev, A., Maslennikov, R., Sevastyanov, A., Khoryaev, A., Lomayev, A., *"Experimental investigations of 60 GHz WLAN systems in office environment"*, Selected Areas in Communications, IEEE Journal on, vol.27, no.8, pp.1488,1499, October 2009.

[8] Martinez-Ingles, M.-T., Sanchis-Borras, C., Molina-Garcia-Pardo, J.-M., Rodriguez, J.-V., Juan-Llacer, L., *"Experimental Evaluation of an Indoor MIMO-OFDM System at 60 GHz Based on the IEEE802.15.3c Standard",* Antennas and Wireless Propagation Letters, IEEE, vol.12, no., pp.1562,1565, 2013.

[9] Katayama, Y., Nakano, D., Valdes-Garcia, A., Beukema, T., Reynolds, S. *"Multi-Gbps wireless systems over 60-GHz SiGe radio link with BW-efficient noncoherent detections",* in Multimedia and Expo, 2008 IEEE International Conference on, pp. 513–516, 2008.

[10] Hirata, A., Takahashi, H., Yamaguchi, R., Kosugi, T., Murata, K., Nagatsuma, T., Kukutsu, N., Kado, Y., *"Transmission characteristics of 120-GHz-band wireless link using radio-on-fiber technologies",* J. Lightwwave Technol., Vol. 26, No. 15, pp. 2338-2344, 2008.

[11] Wang, C., Lin, C., Chen, Q., Deng, X., Zhang, J., *"0.14THz high speed data communication over 1.5 kilometers",* Infrared, Millimeter, and Terahertz Waves (IRMMW-THz), 2012 37th International Conference on, pp.1,2, Sept. 2012.

[12] Takahashi, H., Kosugi, T., Hirata, A., Takeuchi, J., Murata, K., Kukutsu, N., *"120-GHz-Band Fully Integrated Wireless Link Using QSPK for Realtime 10-Gbit/s Transmission",* Microwave Theory and Techniques, IEEE Transactions on, vol.61, no.12, pp.4745,4753, Dec. 2013.

[13] Kallfass, I., Antes, J., Schneider, T., Kurz, F., Lopez-Diaz, D., Diebold, S., Massler, H., Leuther, A., Tessmann, A., *"All Active MMIC-based wireless communication at 220 GHz"*, IEEE Trans. Terahertz Science and Technology, Vol. 1, No.2, pp.477-487, 2011.

[14] Antes, J., Konig, S., Leuther, A., Massler, H., Leuthold, J., Ambacher, O., Kallfass, I., *"220 GHz wireless data transmission experiments up to 30 Gbit/s",* Microwave Symposium Digest (MTT), 2012 IEEE MTT-S International , pp.1-3, June 2012.

[15] Lopez-Diaz, D., Tessmann, A., Leuther, A., Wagner, S., Schlechtweg, M., Ambacher, O., Koenig, S., Antes, J., Boes, F., Kurz, F., Henneberger, R., Kallfass, I., *"A 240 GHz quadrature receiver and transmitter for data transmission up to 40 Gbit/s",* Microwave Conference (EuMC), 2013 European, pp.1411-1414, Oct. 2013.

[16] Song, H.-J., Ajito, K., Hirata, A., Wakatsuki, A., Muramoto, Y., Furuta, T., Kukutsu, N., Nagatsuma, T., Kado, Y., *"8 Gbit/s wireless data transmission at 250 GHz",* IEE Electron. Lett., Vol. 45, No. 22, pp. 1121-1122, 2009.

[17] Jastrow, C., Münter, K., Piesiewicz, R., Kürner, T., Koch, M., Kleine-Ostmann, T., *"300 GHz transmission system",* Electron. Lett., Vol. 44, No. 3. pp. 213-214, 2008.

[18] Wang, C., Lu, B., Lin, C., Chen, Q., Miao, L., Deng, X., Zhang, J., *"0.34-THz Wireless Link Based on High-Order Modulation for Future Wireless Local Area Network Applications",* Terahertz Science and Technology, IEEE Transactions on, vol.4, no.1, pp.75,85, Jan. 2014.

[19] Moeller, L., Federici, J., Su, K., *''THz Wireless Communications: 2.5 Gb/s error-free transmission at 625 GHz using a narrow-bandwidth 1mW THz source",* Tech, Dig. URSI General Assembly and Scientific Symposium, Turkey, August 2011.

[20] Jastrow, C., Priebe, S., Spitschan, B., Hartmann, J., Jacob, M., Kurner, T., Schrader, T., Kleine-Ostmann, T., *"Wireless digital transmission at 300 GHz*", Electron. Lett., vol. 46, no. 9, pp. 661–663, April 2010.

[21] Antes, J., Reichart, J., Lopez-Diaz, D., Tessmann, A., Poprawa, F., Kurz, F., Schneider, T., Massler, H., Kallfass, I., *"System concept and implementation of a mmW wireless link providing data rates up to 25 Gbit/s",* IEEE COMCAS, 2011.

[22] Liu, C., Wang, C., Cao, J-C., *"Performance analysis of LDPC codes on OOK terahertz wireless channels",* Chin. Phys. B Vol. 25, No. 2 (2016) 028702

[23] Faber, M. T., Chramiec, J., Adamski, M. E., *"Microwave and Milimeter-wave Diode Frequency Multipliers"*, Artech House, Boston, 1995.

[24] De Lucia, F. C., *"The submillimeter: Aspectroscopist's view"*, Journal of Molecular Spectroscopy, 261, 1-17, 2010.

[25] Chattopadhyay, G., *"Technology, Capabilities, and Performance of Low Power Terahertz Sources",* IEEE Transactions on Terahertz Science and Technology, vol. 1, no. 1, pp. 33-53, September 2011.

[26] Kollberg, E. L., Tolmunen, T. J., Frerking, M. A., East, J. R., *"Current Saturation in Submillimeter Wave Varactors"*, IEEE Transactions on Microwave Theory and Techniques, vol. 40, no. 5, pp. 831-838, May 1992.

[27] Song, H-J., Nagatsuma, T., *"Handbook of Terahertz Technologies Devices and Applications",* Pan Stanford, CRC Press, 2015.

[28] Jin, C., *"GaN Schottky Diodes for Signal Generation and Control",* Phd. Dissertation, Technical University of Darmstadt, 2015.

[29] Frequency Multipliers, February 13, 2017, from

http://www.qsl.net/va3iul/Frequency_Multipliers/Frequency_Multipliers.pdf

[30] Woolard, D. L., Loerop, W. R., Shur, M. S., *"Terahertz Sensing Technology Volume 1: Electronic Devices and Advanced Systems Technology"*, Word Scientific, Singapore, 2003.

[31] Bozhkov, V. G., *"Semiconductor Detectors, Mixers and Frequency Multipliers for the Terahertz Band"*, Radiophysics and Quantum Electronics, vol. 46, Nos. 8–9, 2003.

[32] VDI Diodes, Inc, *"VDI-732 Broadband Frequency Doubler Operationa Manual",* May 24, 2017, from http://www.vadiodes.com/images/Products/Multipliers/Product_Manuals/VDI-732_Broadband_Doubler_Product_Manual.pdf,

[33] VDI Diodes, Inc, *"VDI-733 Broadband Frequency Tripler Operational Manual",* May 24, 2017, from http://www.vadiodes.com/images/Products/Multipliers/Product_Manuals/VDI-733-Broadband-Tripler-Product-Manual.pdf ,

[34] Hjorth, M., Hvittfeldt, B., *"Modelling an RF Converter in Matlab",* Master's Thesis, Linköping University, 2002.

[35] Maestrini, A., Thomas, B., Wang, H., Jung, C., Treuttel, J., Jin, Y., Chattopadhyay, G., Mehdi, I., Beaudin, G., *"Schottky Diode Based Terahertz Frequency Multipliers and Mixers",* C. R. Physique 11, 480-495, 2010.

[36] VDI Diodes, Inc, *"VDI-735 Subharmonic Mixer Operational Manual",* May 24, 2017, from http://www.vadiodes.com/images/Products/Mixers/VDI-735_SHM_Product_Manual.pdf ,

[37] Goldsmith, A., *"Wireless Communications",* (1st Ed.), Cambridge University Press, USA, 2005.

[38] Rappaport, T. S., *"Wireless Communications Principles and Practice",* (1st Ed.), Prentice-Hall, Upper Saddle River, NJ, 2002.

[39] Haykin, S., Moher, M., *"Introduction to Analog and Digital Communications",* (2nd Ed.), John Wiley and & Sons Inc., New Jersey, 2007.

[40] Viswanathan, Mathuranathan., *"Simulation of Digital Communication Systems Using Matlab",* (2nd Ed.), Mathuranathan Viswanathan at Amazon., 2013.

[41] https://www.mathworks.com [Date of access: 15.05.2017]

CURRICULUM VITAE

Özgün ERSOY was born in Aydın, Turkey in 1989. He received the BSc degree in Kocaeli University, 2012. His department was Electronics and Communications Engineering. He is currently working as reserach assistant in the Department of Electrical and Electronics Engineering in Ankara Yıldırım Beyazıt University. He is still a graduate student in the Department of Electrical and Electronics Engineering in Ankara Yıldırım Beyazıt University. His main areas of research interest are wireless communications and THz communications.